Characterisation of cancer cell vulnerabilities acquired during senescence for cancer cell clearance

Dissertation

der Mathematisch-Naturwissenschaftlichen Fakultät

der Eberhard Karls Universität Tübingen

zur Erlangung des Grades eines

Doktors der Naturwissenschaften

(Dr. rer. nat.)

vorgelegt von

Katharina Böhm

aus Münchberg

Tübingen

2021

Gedruckt mit Genehmigung der Mathematisch-Naturwissenschaftlichen Fakultät der Eberhard Karls Universität Tübingen.

Tag der mündlichen Qualifikation:	19.07.2021
Stellvertretender Dekan:	Prof. Dr. Thilo Stehle
1. Berichterstatter:	Prof. Dr. Hans-Georg Rammensee
2. Berichterstatter:	Prof. Dr. Martin Röcken

Erklärung / Declaration:

Ich erkläre, dass ich die zur Promotion eingereichte Arbeit mit dem Titel: „Characterisation of cancer cell vulnerabilities acquired during senescence for cancer cell clearance" selbständig verfasst, nur die angegebenen Quellen und Hilfsmittel benutzt und wörtlich oder inhaltlich übernommene Stellen als solche gekennzeichnet habe. Ich versichere an Eides statt, dass diese Angaben wahr sind und dass ich nichts verschwiegen habe. Mir ist bekannt, dass die falsche Abgabe einer Versicherung an Eides statt mit Freiheitsstrafe bis zu drei Jahren oder mit Geldstrafe bestraft wird.

I hereby declare that I have produced the work entitled "Characterisation of cancer cell vulnerabilities acquired during senescence for cancer cell clearance", submitted for the award of a doctorate, on my own (without external help), have used only the sources and aids indicated and have marked passages included from other works, whether verbatim or in content, as such. I swear upon oath that these statements are true and that I have not concealed anything. I am aware that making a false declaration under oath is punishable by a term of imprisonment of up to three years or by a fine.

Tübingen, den _____ _____

Datum / Date Unterschrift /Signature

„It is by logic that we prove,
but by intuition that we discover.“
Henri Poincaré

Acknowledgements

Throughout the writing of this dissertation, I have received a great deal of support and assistance.

I would like to thank Prof. Martin Röcken for his guidance through the project. His expertise was greatly appreciated in developing and refining the research question.

Special thanks to Prof. Hans-Georg Rammensee for his supervision and consent to take part of the Integrated Research Training Group (IRTG) SFB685.

Thanks to my labmates Ellen Brenner, Nadine Simon and Britta Bauer for making the time worthwhile. I will fondly look back to the conferences, Spiele- and Grillabende and trips we shared, all the discussions as well as happy distractions to rest my mind outside of my research.

I am also grateful to Susanne Weidemann and Viola Galinat and would like to extend my thanks to all actual and former members of the Röcken group for technical support, great work-environment, and fun social events.

I would like to acknowledge my colleagues from FOR2314 for their wonderful and constructive feedback. Presenting and discussing data with you was always a great joy.

Finally, to my husband Peter. Thank you for encouraging and supporting me during this time on a personal and scientific level. Your insightful feedback pushed me to sharpen my thinking and brought my work to a higher level.

Abstract

Senescence induction is becoming a relevant strategy in tumour treatment. Besides induction with therapeutic compounds (TIS – therapy induced senescence) senescence can be induced in tumor cells *in vitro* and *in vivo* via cytokine (IFN-γ & TNF) or T_H1 cell treatment (CIS – cytokine induced senescence). Here, vulnerabilities acquired by senescence induction in β-cancer cells were investigated. While most CIS cancer cells remain viable, cease proliferation, and show SA-beta Gal activity, the cells also accumulate features associated with early apoptotic events. The cells lose their original membrane composition indicated by an increased surface localization of negatively charged phospholipids. This is accompanied by reduced mitochondrial membrane potential ($\Delta\psi_m$) as well as changes in opening of the mitochondrial permeability transition pore (PTP), without changes in mitochondrial mass. This in turn compromises the retention of cytochrome c, leading to a depletion of overall cytochrome c protein. While caspase 3 activity in CIS cancer cells is enhanced in comparison to non-senescent cancer cells, it was suspected that increased levels of anti-apoptotic protein Bcl-2 in CIS counteracts death induction in favor of senescence. Indeed, treatment of CIS cancer cells with ABT263 (pan-Bcl-2 inhibitor) induced apoptosis preferentially in senescent cancer cells. Furthermore, the changes in cellular status after senescence induction lifted the resistance of cancer cells to TRAIL induced cell death. This thesis shows that CIS and TIS β-cell tumour cells are susceptible to TRAIL induced cell death in comparison to non-senescent β-cell tumour cells. Further analysis showed that apoptosis induction in senescent cancer cells was a prerequisite to render β-cell cancer cells susceptible to phagocytosis by macrophages. Therefore, type I anti-cancer immune response can act as a relay between inducing a stable growth arrest in cancer cells and senescent cancer cell clearance by macrophages exploiting the acquired sensitivity to TRAIL of senescent cancer cells. Overall, introduction of senescence followed by secondary apoptosis induction may prove to be a relevant therapeutic strategy. The findings may be a first step in understanding new mechanisms in cancer immune therapy with the goal to clear senescent tumour cells.

Zusammenfassung

Die Induktion der Seneszenz tritt zunehmend in den Fokus der Forschung an Krebstherapien. Neben der therapeutischen Senezenzinduktion (TIS - therapy induced senescence) kann Seneszenz in Tumorzellen *in vitro* und *in vivo* mittels Zytokin- (IFN-y & TNF) oder T_H1-Zellbehandlung (CIS - cytokine induced senescence) induziert werden. Die hier vorliegende Arbeit beschäftigt sich mit den Veränderungen, die durch die Seneszenz in Zellen von β-Zelltumoren hervorgerufen werden. β-Krebszellen zeigen nach Zytokinbehandlung für die Seneszenz typische Merkmale wie Seneszenz-assoziierte beta-Galactosidase-Aktivität, Wachstumsarrest aber auch Merkmale, die einem frühen apoptotischen Phänotyp ähneln. Seneszente Krebszellen verändern beispielsweise ihren ursprünglichen Aufbau der Zellmembran, gemessen an einer erhöhten Lokalisation von negativ geladenen Phospholipiden an der extrazellulären Membranoberfläche. Weiterhin akkumulieren in seneszenten Insulinomzellen dysfunktionale Mitochondrien. Zusätzlich zur Depolarisation der mitochondrialen Membran und dem veränderten Öffnungsverhalten der mitochondrialen Pore, setzen seneszente Zellen Cytochrome c frei. Dies führt zu einer geringen Aktivierung von Caspase 3 in seneszenten Zellen im Vergleich zu nicht-seneszenten Zellen. Interessanterweise scheinen erhöhte Bcl-2 Proteinlevel für das Überleben seneszenter Zellen maßgeblich zu sein, da der pan-Bcl-2 Inhibitor ABT263 Apoptose präferentiell Ausmaß in seneszenten β-Krebszellen induziert. Darüber hinaus zeigen seneszente Krebszellen gegenüber TRAIL-induzierten Zelltod eine erhöhte Vulnerabilität. In dieser Arbeit wird gezeigt, dass Zelltod spezifisch in seneszenten Krebszellen eingeleitet werden kann und dass dies Voraussetzung ist für die Phagozytose von seneszenten Krebszellen durch Makrophagen. Daher kann eine Typ-I-Immunantwort gegen Tumore als Relais zwischen der Induktion eines stabilen Wachstumsarrests in Krebszellen und der Clearance seneszenter Krebszellen durch Makrophagen gesehen werden. Zusammengefasst könnte sich die Induktion der Seneszenz gefolgt von einer sekundären Apoptose als eine relevante Strategie in der Krebstherapie erweisen, um seneszente Tumorzellen aus dem Organismus zu entfernen.

List of Publications

Peer Reviewed:

Brenner, Ellen; Schörg, Barbara F.; Ahmetlić, Fatima; Wieder, Thomas; Hilke, Franz Joachim; Simon, Nadine; Schroeder, Christopher; Demidov, German; Riedel, Tanja; Fehrenbacher, Birgit; Schaller, Martin; Forschner, Andrea; Eigentler, Thomas; Niessner, Heike; Sinnberg, Tobias; Böhm, Katharina S.; Hömberg, Nadine; Braumüller, Heidi; Dauch, Daniel; Zwirner, Stefan; Zender, Lars; Sonanini, Dominik; Geishauser, Albert; Bauer, Jürgen; Eichner, Martin; Jarick, Katja J.; Beilhack, Andreas; Biskup, Saskia; Döcker, Dennis; Schadendorf, Dirk; Quintanilla-Martinez, Leticia; Pichler, Bernd J.; Kneilling, Manfred; Mocikat, Ralph; Röcken, Martin (2020): Cancer immune control needs senescence induction by interferon-dependent cell cycle regulator pathways in tumours. In: *Nature Communications* 11 (1), S. 1335. DOI: 10.1038/s41467-020-14987-6.

Yazdi, Amir S.; Barlin, Meltem; Böhm, Katharina; Gendrisch, Fabian; Ghorbanalipoor, Saeedeh; Häberle, Stefanie et al. (2017): ADF Winter School—An exciting concept of the Arbeitsgemeinschaft Dermatologische Forschung to connect young scientists and clinician scientists in Dermatology at the top of Germany. In: *Exp Dermatol* 26 (3), S. 292–294. DOI: 10.1111/exd.13241.

Conference Articles & Poster Presentations:

Senescence enhances sensitivity to TRAIL and immune clearance by reinforcing early apoptotic features
Katharina Böhm, Martin Röcken
47. Jahrestagung der Arbeitsgemeinschaft Dermatologische Forschung (2021)

Böhm, Katharina. (2019): 386 Senescence induces pro-apoptotic features in tumor cells enabling targeted senolysis by type I immune-mediators and subsequent phagocytic clearance. In: *The Journal of investigative dermatology* 139 (9, Supplement), S281. DOI: 10.1016/j.jid.2019.07.388.
48th Annual ESDR Meeting (2019)

Killing of Senescent Cancer Cells by Mediators of Type I Immune Reactions is Needed for the Clearance of Senescent Cancer Cells
Katharina Böhm, Martin Röcken
International Cell Senescence Association Conference (2019)

Senolysis is needed for the clearance of senescent tumor cells
Katharina Böhm, Martin Röcken
46. Jahrestagung der Arbeitsgemeinschaft Dermatologische Forschung (2019)

Böhm, Katharina.; Röcken, Martin. (2018): 1444 Senolysis is needed for the clearance of senescent tumor cells. In: The Journal of investigative dermatology 138 (5, Supplement), S245. DOI: 10.1016/j.jid.2018.03.1462.
International Investigative Dermatology (IID) Meeting (2018)

Senolysis triggers clearance of senescent cancer cells
Böhm, Katharina; Röcken, Martin
EMBO Workshop "Perspectives on skin cancer prevention" (2018)

Cytokine-induced senescence (CIS) drives cancer cells to polarize naive macrophages
Katharina Böhm, Martin Röcken
45. Jahrestagung der Arbeitsgemeinschaft Dermatologische Forschung (2018)

Böhm, Katharina.; Röcken, Martin. (2017): 393 Myeloid cells alter their effector status in response to the secretome of senescent cancer cells. In: *The Journal of investigative dermatology* 137 (10, Supplement 2), S259. DOI: 10.1016/j.jid.2017.07.588.
47th Annual ESDR Meeting (2017)

The senescent cancer cell secretome alters the function of myeloid cells
Böhm, Katharina; Röcken, Martin
19th International AEK Cancer Congress (2017)

Cell death and senescent cancer cell clearance
Böhm, Katharina; Braumüller, Heidi; Wieder, Thomas; Röcken, Martin
44. Jahrestagung der Arbeitsgemeinschaft Dermatologische Forschung (2017)

Exogenous induced senescence triggers intrinsic vulnerabilities in pancreatic ß-cell cancer
Böhm, Katharina; Braumüller, Heidi; Wieder, Thomas; Röcken, Martin
43. Jahrestagung der Arbeitsgemeinschaft Dermatologische Forschung (2016)

Exogenous induced senescence triggers intrinsic vulnerabilities in pancreatic ß-cell cancer
Böhm, Katharina; Braumüller, Heidi; Wieder, Thomas; Röcken, Martin
5. ADF Winter School (2016)

Characterization of fluorescent nanoprobes for live cell imaging of cell cycle and actin dynamics
Katharina Böhm, Björn Tränkle, Ulrich Rothbauer, Larisa Yurlova, Kourosh Zolghadr, Christian Schmees
EMBO|EMBL Symposium: Seeing is Believing – Imaging the Processes of Life (2012)

Table of Contents

1 Introduction

1.1 Discovery and evolution of senescence

The first description of senescence on a cellular level was made by Hayflick and Moorhead in 1961. Originally, it was used to describe “age-related” changes in eukaryotic cells *in vitro*. The word senescence itself consequently was derived from the latin word senescere meaning “to become aged, grow old”.

After isolation of primary human fibroblasts for virus production, Hayflick and Moorhead observed degeneration and stop in proliferation in these fibroblasts after a year in cell culture or after about 50 subpopulations, respectively. Hayflick reasoned it is not the number of subpopulations that led to degeneration of these cells in culture but the number of cell population doublings, defining senescence as a loss of proliferative capacity without loss of viability or metabolic activity[1,2]. As suggested later, the reason for the stalled replication was the progressive shortening of telomere strands in successive cell divisions and the insufficient restoration of lagging strands by DNA polymerase[3–5]. Thereby, inadequate telomere length and accompanying disruption of the protective ends of telomeres initiates a DNA damage response (DDR). Successively, these cells express DDR associated proteins, such as γ-H2AX and 53BP1, NBS1 or MDC1 and show activation of DDR kinases like ATM and ATR, all of which proofed to be useful surrogate markers for the identification of senescent cells. These findings led to the classic concept of senescence according to which it was assumed that cells grow old by an internal mechanism, successively leading to accumulation of further shortcomings. This type of senescence is today referred to as replicative senescence (detailed below).

Currently, senescence is defined by the expression of different biomarkers associated with senescence or aging. The wide-ranging definition of senescence today connects the fields of aging research with microbiology to cancer research and more. This broadened classification of senescence now includes cells that are unable to go into replicative senescence, for example cancers cells, but can express these biomarkers after internal or external stimulation.

1.2 Types and markers of senescence

It must be noted that senescence describes a complex biological phenomenon relying on various, partly independent molecular mechanisms. Therefore, it is conceivable that an inclusive definition of senescence, as it is currently used in literature, does not always refer to the same cellular programs but much rather illustrates a collection of similar phenotypes caused by in parts entirely different underlying processes.

In literature senescence is either defined by its symptoms or the underlying mechanism deemed to cause senescence. Commonly agreed on symptoms, and therefore biomarkers of senescence, are the proliferative arrest, pH dependent beta-Galactosidase activity and increased levels of cell cycle regulatory proteins like p16 or p21. These symptoms can be induced by oncogenes (oncogene induced senescence – OIS), telomere shortening (replicative senescence), engineered compounds (therapy induced senescence – TIS) or by cytokines (cytokine induced senescence – CIS) for example (Figure 1). In the following section an overview of senescence mechanisms and biomarkers will be given.

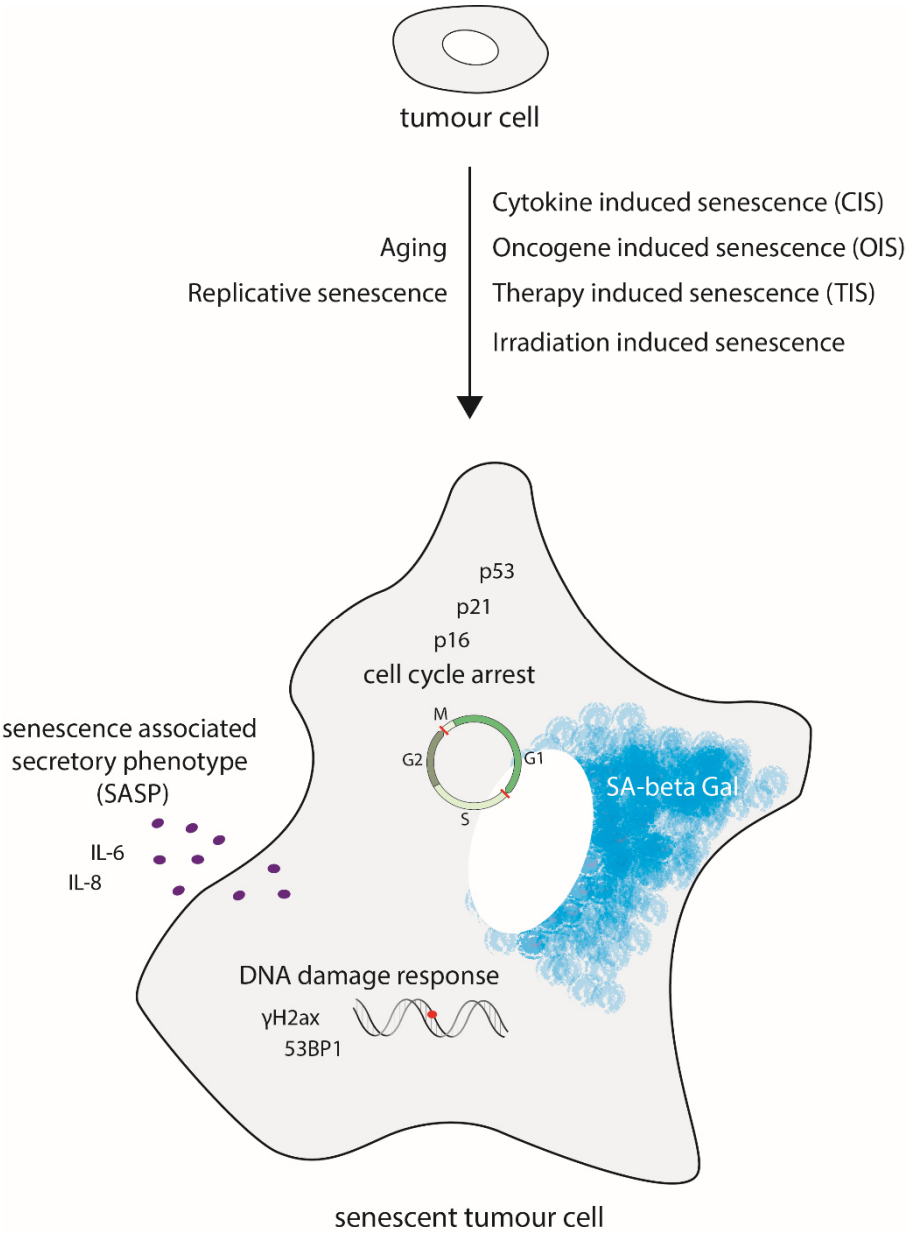

Figure 1: Senescence inductors and evoked biomarkers

Senescence is a phenotype caused by a plethora of different inducers eliciting a similar cellular response. Among these inducers are cytokines (cytokine induced senescence – CIS), oncogene expression (oncogene induced senescence – OIS), therapeutic compounds (therapy-induced senescence – TIS) or external cues like irradiation inducing DNA damage. The elicited cellular response led to the definition of biomarkers to define senescence, like senescence associated beta Galactosidase (SA-beta Gal) activity, changes in DNA damage response and cell cycle regulating proteins as well as emergence of the senescence associated secretory phenotype (SASP)[6].

Replicative senescence, as mentioned above, is the type of senescence most often associated with aging. It was believed that replicative senescence may be the cause of organismal and organ aging as several studies showed an accumulation of senescence associated beta-galactosidase positive cells in organismal aging[7,8]. In human cells, for example, replicative senescence was shown to depend on the phosphorylation of p53 inducing an upregulation of p21[9–11]. Interestingly, similar observations were made in aged baboons, demonstrating a conserved mechanism across species[12–14]. Plausibly, the senescent and the aging phenotype share common features. In hindsight, however, it is barely possible to distinguish whether senescence is the cause or merely a symptom of aging processes. Considering the different pathways described in senescence and the multifactorial phenotype that arises in senescence and aging alike committing to replicative senescence as the only type of senescence associated with aging seems unlikely.

Human fibroblasts respond to expression of oncogenic RAS with a p53 and p16 dependent cell cycle arrest in G1-phase[15]. This finding led to the discovery and definition of **oncogene-induced senescence (OIS)**. The list of oncogenes capable of inducing a senescent phenotype is constantly expanding[16]. However, it has to be kept in mind that loss of tumour suppressors, like PTEN, can also trigger senescence [17,18]. A common feature observed in OIS in human cells is the regulation of p16[19,20]. In murine cells on the other hand functional inactivation of p53 or p19 is enough to bypass Ras induced senescence, indicating a stronger dependency on these proteins for OIS[21]. Importantly, OIS has been found in human[22] and murine lesions[23] possibly acting as a break in early tumourigenesis[24]. Furthermore, OIS can initiate a DNA damage response[25], often caused by irregular DNA replication[19] or ROS stress[26].

The list of drugs inducing senescence in therapeutic settings *in vitro* is long and includes for example doxorubicin or etoposide[27]. This shaped the term **therapy-induced senescence (TIS)**. Most of these agents induce senescence in a dose dependent manner via DNA damage, yet ROS generating drugs[28] or inhibitors of DNA polymerases are also among therapeutic senescence inducers[29,30]. Originally however, senescence induction was not the primary goal in these therapies but rather a subsidiary effect. Nonetheless, bystander senescence has been found in several human tumours *in vivo* after chemotherapy[31,32]. Furthermore, the presence of

senescent cancer cells after chemotherapy was also found in breast cancer cells in response to retinoid treatment[33] or *in vivo* in animal models of lymphoma treated with cyclophosphamide[34] for example. One challenge of inducing senescence with therapeutic compounds was the exclusive targeting of the tumour cell and reduction of their effect on regular stromal cells. As one of the common markers of senescence is the upregulation of proteins like p16 or p21, inhibitors of cell cycle progression, the idea of therapeutically inducing senescence led to the design of compounds mimicking their function. By targeting cyclin dependent kinases (CDK) a stop in proliferation in malignant lesions seemed achievable. Indeed, a prominent example of successful TIS realization in the clinics is the CDK4/6 inhibitor Palbociclib (Figure 2), currently approved in treatment of breast cancer[35,36]. It is one of the first drugs aiming at senescence as the desired outcome without it being merely a bystander effect.

Besides endogenous triggers inducing senescence, exogenous stimulation with cytokines has been shown to establish **cytokine-induced senescence (CIS)** in cancer cells (Figure 2). Combinatorial treatment of mouse β-cell tumour cells with the cytokines IFN-γ and TNF led to growth arrest and SA-beta Gal activity and other features of senescence. *In vivo*, preventive treatment of mice developing β-cell tumours with T-helper 1 cells, expressing IFN-γ and TNF, induced senescence, and arrested cancer development. These findings demonstrate that immune responses can induce senescence[37,38]. Furthermore, therapy of patients with immune checkpoint inhibitors may leave behind residual, not proliferating cancer cells at the original tumour site. The proliferative arrest of the residual cancer cells often depends on p16 or p21 regulation. Interestingly, deletion of p16 or p21, common senescence inducing cell cycle regulators, in tumour cells diminished immune checkpoint blockade efficacy. This shows a dependency of immune therapy with immune checkpoint inhibitors on cell cycle regulators also associated with senescence[39].

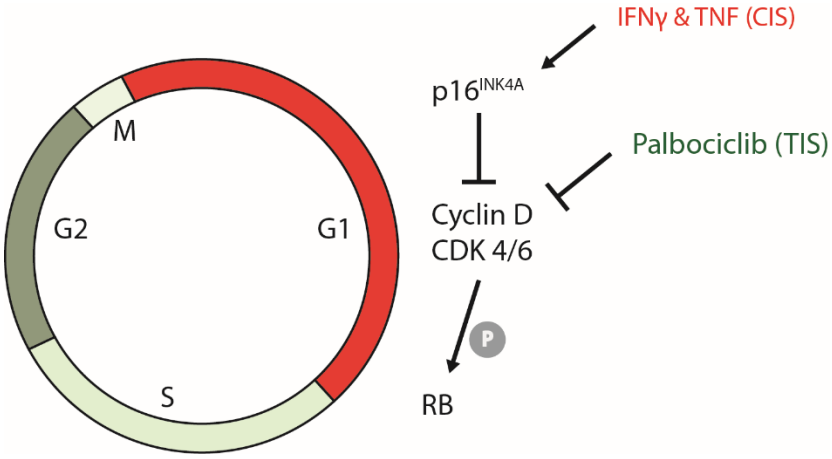

Figure 2: Cell cycle regulation in CIS and TIS

Cytokine- and therapy induced senescence inhibit cell cycle progression via inhibition of CDK4/6. CIS depends on p16 upregulation[37], whereas Palbociclib directly inhibits CDK4/6[40], mimicking the function of p16. Therefore, CIS and TIS induce a cell cycle arrest in G1.

1.3 Biological relevance and features of senescence

As described above senescence has mostly been discovered in the context of cellular damage or stress. This view has been challenged by the discovery of cytokine-induced senescence. While CIS was discovered in the context of tumour therapy, the physiological inducers, IFN-γ and TNF, hint at a function of senescence in normal biological processes.

For a long time, it has been an unchallenged dogma that senescence is the result of aging or pathologies. In recent years however, senescence has been identified in several embryonic structures. In murine embryogenesis senescent cells have been found in the mesonephros and the endolymphatic sac (Figure 3). Mechanistically, **developmental senescence** in these structures was dependent on p21. After macrophage infiltration, clearance of senescent cells and tissue remodeling was needed for correct embryogenesis. Intriguingly, during development, p21-null embryo exhibited a loss of senescence with partial compensation of tissue remodeling by apoptosis, demonstrating the entanglement of these two biological processes. However, a complete compensation of senescence by apoptotic processes was not possible and detectable abnormalities remained[41].

Further proof of senescence as a developmental process in embryogenesis was found in the apical ectodermal ridge (AER) and the neural roof plate. Cells ceased proliferation during normal development and expressed p21, p15 and SASP associated proteins. Mice lacking p21 therefore, displayed deficiencies in senescence induction and apical ectodermal ridge development. Interestingly, the underlying mesenchyme was discovered to be the source of senescence induction in the AER, being a second example for exogenously induced senescence next to CIS. Upon development senescent cells were redistributed to the interdigital mesenchyme where apoptosis was induced and senescent cells ultimately cleared by macrophages[42].

While current evidence is mostly based on studies of murine embryos, developmental senescence has also been observed in human[41], chicken[42] and quail[43] supporting senescence as a conserved physiological mechanism between species.

Next to embryogenesis, senescence has also been found in adult organisms alongside aging. Megakaryocytes, for example, become senescent as part of their maturation program, characterized by SA-beta Gal activity, proliferative arrest and HP1γ accumulation. Interestingly, malignant megakaryocytes from primary myelofibrosis do not express p21 and are unable to initiate senescence indicating its relevance in physiological maturation of megakaryocytes[44].

Other evidence of senescence in physiological function has been found at the maternal-fetal placental barrier. SA-beta Gal activity, as well as p16 and p21 expression was observed in placental syncytiotrophoblasts. Fusion of precursor trophoblasts gives rise to syncytiotrophoblasts resulting in a multinucleated, polyploid cell that expresses senescence markers. Therefore, it was suggested that the fusion induces senescence that might be needed for proper cell function[45].

Developmental senescence

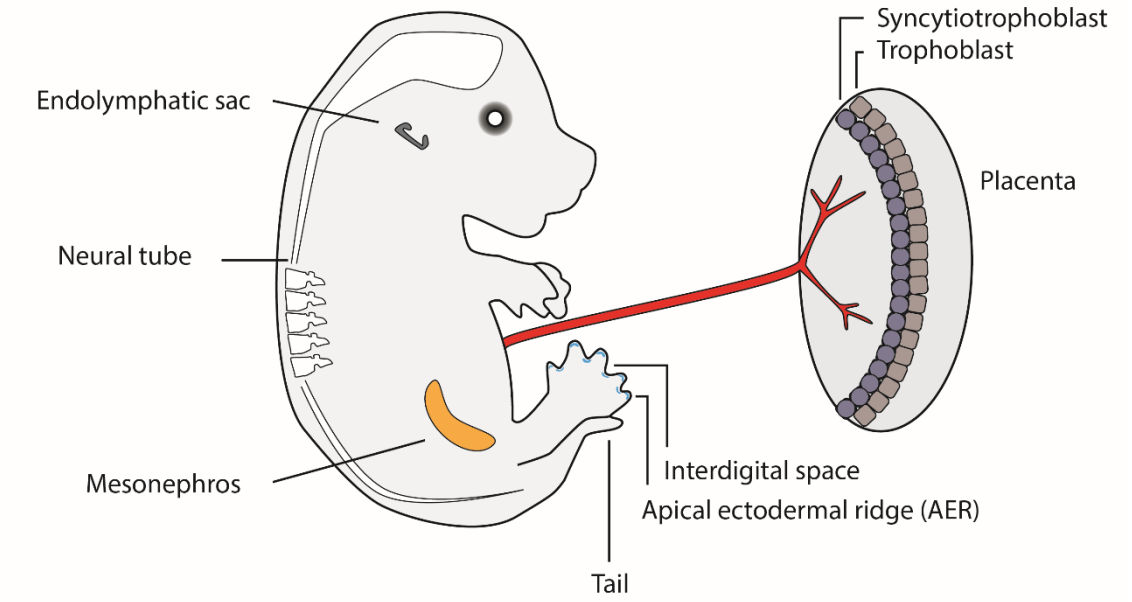

Senescence in adulthood

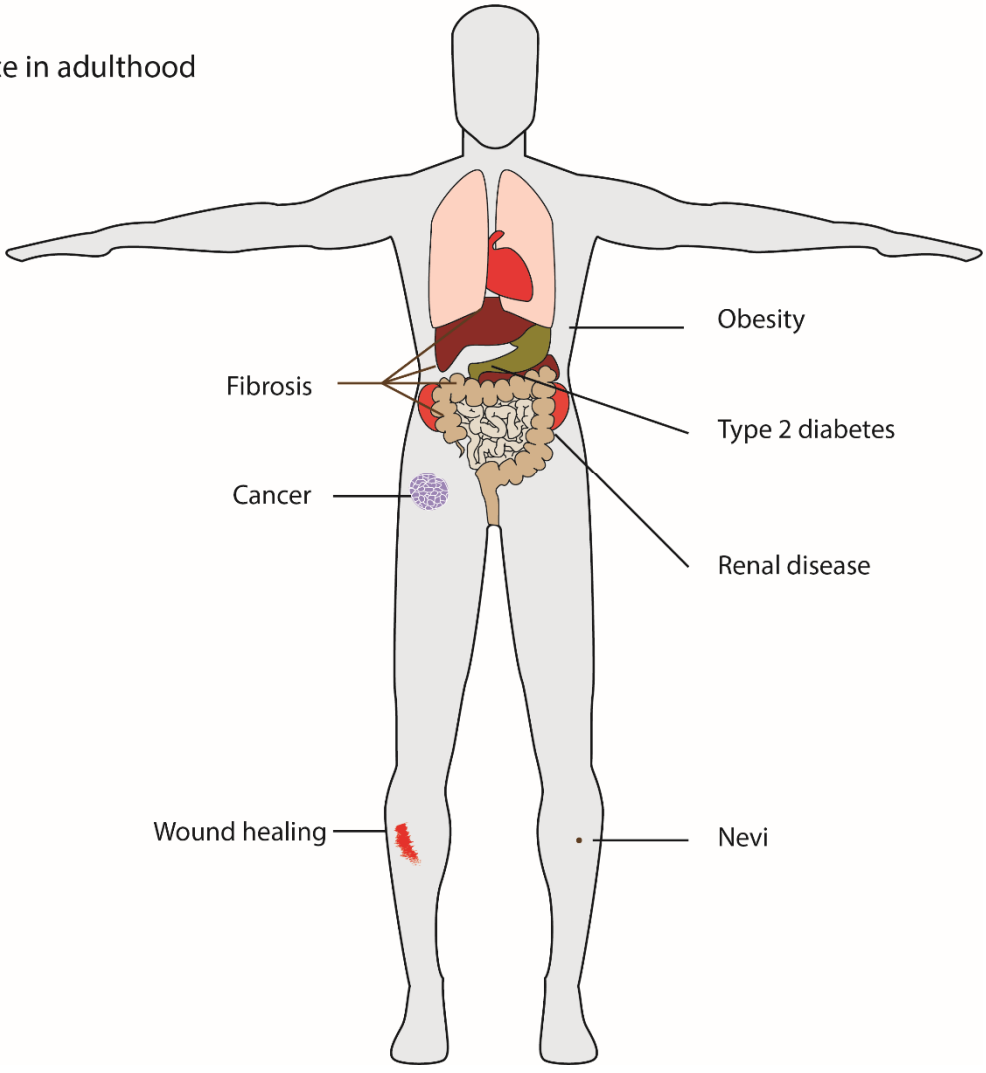

Figure 3: Senescence in development and adulthood

Senescence is associated with developmental and physiological processes. An overview of structures in embryogenesis and disease are depicted in Figure 3, showing the abundance of senescence in functional processes. During embryogenesis, the induction of senescence was necessary for normal embryonic development. Structures like the apical ectodermal ridge (AER) or the mesonephros depend on senescence induction during embryogenesis[41,42]. Further evidence of physiological senescence in adults has been found in nevi[46] and placenta development[45], next to disease associated senescence in cancer or fibrosis[47–49].

1.4 Regulation of survival networks – senescence as a choice

Senescence can arise from genetic damages caused endogenously (telomere shortening[50], ROS overload[51], etc.) or exogenously (UV radiation[52], microenvironment[53], etc.). Physiologically, initiation of a proper DNA damage response requires an arrest in proliferation for damage repair. Usually, if the damage is irreparable the cell undergoes apoptosis. However, the temporary arrest in proliferation initiated by DDR can convert to a permanent senescence associated growth arrest. The mechanisms underlying this cell fate decision are still under investigation. Arguably, the dose of cellular damage or the concentration of damaging agent influences this choice. Consequently, initiation of senescence in low doses and cell death in high doses has been shown for DNA damaging agents like etoposide[54], doxorubicin[55], UV-B[56] and others.

The physiological consequence of this choice – senescence or apoptosis, however, differs immunologically. Apoptosis is an anti-inflammatory event and apoptotic bodies generated by this process are rapidly cleared from the organism by immune cells. This prevents the release of intracellular molecules of the dying cell that would otherwise act as damage-associated molecular patterns (DAMPs) initiating an immune response. The anti-inflammatory nature of phagocytic clearance in apoptosis is furthermore strengthened by the release of anti-inflammatory cytokines like TGF-β and IL-10 by phagocytes[57,58]. Senescence on the contrary is regarded as an immunogenic, pro-inflammatory state recruiting and activating the immune system[59]. The following

sections will give an overview of the regulation of apoptosis pathways in senescence and the interaction between senescent cells and the immune system.

1.4.1 Surviving apoptosis – viability and vulnerability in senescence

Based on intrinsic changes in senescent cells, an increased susceptibility to apoptosis would be expected. Interestingly, some senescent cells were more resistant to apoptotic stimuli than proliferating cells. However, it must be taken into account that most of these studies were done on fibroblasts studying replicative senescence[56,60–62]. These studies observed apoptosis resistance for the following apoptotic stimuli: serum withdrawal/starvation[60], UV damage in keratinocytes[62], oxidative stress[61] and compounds[63]. The underlying pathways responsible for this anti-apoptotic response of senescent cells as well as the mechanisms allowing for their prolonged survival in tissue are currently under investigation as targets for senolytic drugs.

One feature of senescence that may contribute to the increased resistance in apoptosis induction of senescent cells is the cessation in proliferation. Proliferating cells depend on growth molecules and nutrients. Therefore, cancer cells with higher mitotic rates are more reliant on sufficient nutrient delivery – a possible therapeutic target for cytotoxic agents in therapy. These agents are not tumour cell specific though, but rely on the differential toxicity for highly mitotic cells versus slowly or non-dividing cells[64]. Senescence induction of tumour cells therefore may be a potential strategy to ensure survival under stress conditions. In a study investigating the contribution of p21 to the survival of DNA damage induced senescent cells it was shown that knockdown of p21 in senescent fibroblasts and H2199 cells (non-small lung cell carcinoma) *in vitro* led to a caspase and JNK dependent cell death. Moreover, these findings were transferred to an *in vivo* model of liver fibrosis and showed elimination of senescent cells from fibrotic scars in p21 knockout mice[65]. Therefore, p21 plays a role in maintaining viability under DNA damaged induced senescence. This pro-survival effect may, however, not exclusively be attributed to p21 and its role in proliferative arrest. Knockdown of p16 for example did not induce cell death in senescent cells[66]. Interestingly, the function of p21 seems to be determined by p53 status as it was shown that p21 is necessary for the escape of cancer cells from senescence by deregulation of DNA replication machinery in p53-null cancer models[67].

Another way of promoting survival of senescent cancer cells is the SASP. On the one hand, secreted proteins may reinforce growth arrest in an autocrine manner via NFκB signalling and ROS generation[68], on the other hand transcriptional activation of anti-apoptotic Bcl-2 family members can ensure survival. Plausibly, these proteins are often overexpressed in senescent cells[60,62].

A recurrent finding in senescence is reactive oxygen species (ROS) accumulation inflicting endoplasmic reticulum (ER) stress. A cellular countermeasure to chronic ER stress is autophagy, a process involved in protein degradation and removal of oxidized molecules, thereby alleviating accumulation of oxidative stress. Interestingly, impairment in autophagy leads to mitochondrial dysfunction stabilizing oxidative stress-induced senescence[69–71]. While increased autophagy has been examined in senescent fibroblasts[72] and endothelial cells[73], dysregulation of autophagy leads to cell death in senescent keratinocytes[74]. The activation of autophagy may be regulated by Bcl-2 family members by binding to Beclin1 thereby inhibiting autophagosome formation[75]. These findings strengthen the idea of senescence as a response to stress or sub-lethal damage.

1.4.2 Apoptotic signalling and senescence

Deregulation of survival networks is commonly found in senescence. While senescence and apoptosis are alternative cell fates, survival of senescent cells often depends on the regulation of proteins involved in apoptotic signalling. Many studies show an upregulation and a dependency on anti-apoptotic Bcl-2 for survival in senescent cells[62,63,76], however, the opposite was found in IMR90 fibroblasts. Irradiation induced senescence in IMR90 cells led to upregulation of pro-apoptotic proteins PUMA and BIM, but downregulation of Bcl-2 in gene expression analysis[77]. Exploiting dependency on anti-apoptotic Bcl-2 proteins in other types of senescence, led to the development of Bcl-2 inhibitors (e.g., ABT263, ABT737). These compounds pre-dominantly affect viability of senescent cells without inducing apoptosis in regular cells, showing their potential as senolytic drugs[62,63,76,78]. However, Bcl-2 family members can act in a redundant manner to protect senescent cells from apoptosis, therefore possibly limiting the potential of senolytics targeting single proteins of this family.

Extrinsic apoptosis is initiated by signalling transmission of death receptors. Transmembrane proteins of the tumour necrosis factor receptor family transduce extracellular apoptotic signals to intracellular signalling cascades via their cytoplasmic death domain. Among these death receptors are TNF receptor 1 (TNFR1), CD95 (Fas) and the TNF-related apoptosis inducing ligand receptor 1 and 2 (TRAIL-R1, TRAIL-R2 or DR4 and DR5). Upon ligand binding death receptors trimerize and recruit adaptor proteins via the death domain. Fas-associated death domain (FADD) recruits pro-caspase 8 and 10 to form a death-inducing signalling complex (DISC) leading to caspase 8 activation. Caspase 8 either directly signals to caspase 3 or engages the intrinsic apoptosis pathway by proteolytic cleavage of pro-apoptotic Bid to t-Bid, therefore relaying apoptotic signalling (Figure 4). Interestingly, in replicative senescence of human fibroblasts, caspase 3 is downregulated and exhibits decreased activity[56]. cFLIP, as a negative regulator of caspase 8 activation, competes in binding to caspase 8 with FADD, therefore preventing DISC formation. While cFLIP is involved in TRAIL resistance in normal cells, reports showed it is downregulated upon DNA damage or Myc activation in fibroblasts[79,80].

Further possibilities to avoid death induction are decoy receptors (DcRs). These receptors lack the intracellular domain and are therefore incapable of signal transduction. The upregulation of DcR1 (TNFRSF10C) and DcR2 (TNFRSF10D) have been proposed as markers for senescence[81,82]. Feasibly, in human fibroblasts silencing of DcR2 with siRNA or shRNA sensitized those cells for TRAIL mediated apoptosis[49]. Investigations on the susceptibility of senescent cells to TRAIL or immune mediated apoptosis induction are still underway. While upregulation of DcRs increases the resistance to extrinsic apoptosis induction, upregulation of DRs may counteract the upregulation and restore susceptibility. Ionizing radiation and chemotherapy, for example, may induce sensitivity to TRAIL via DR5 upregulation and c-Flip downregulation[79,83].

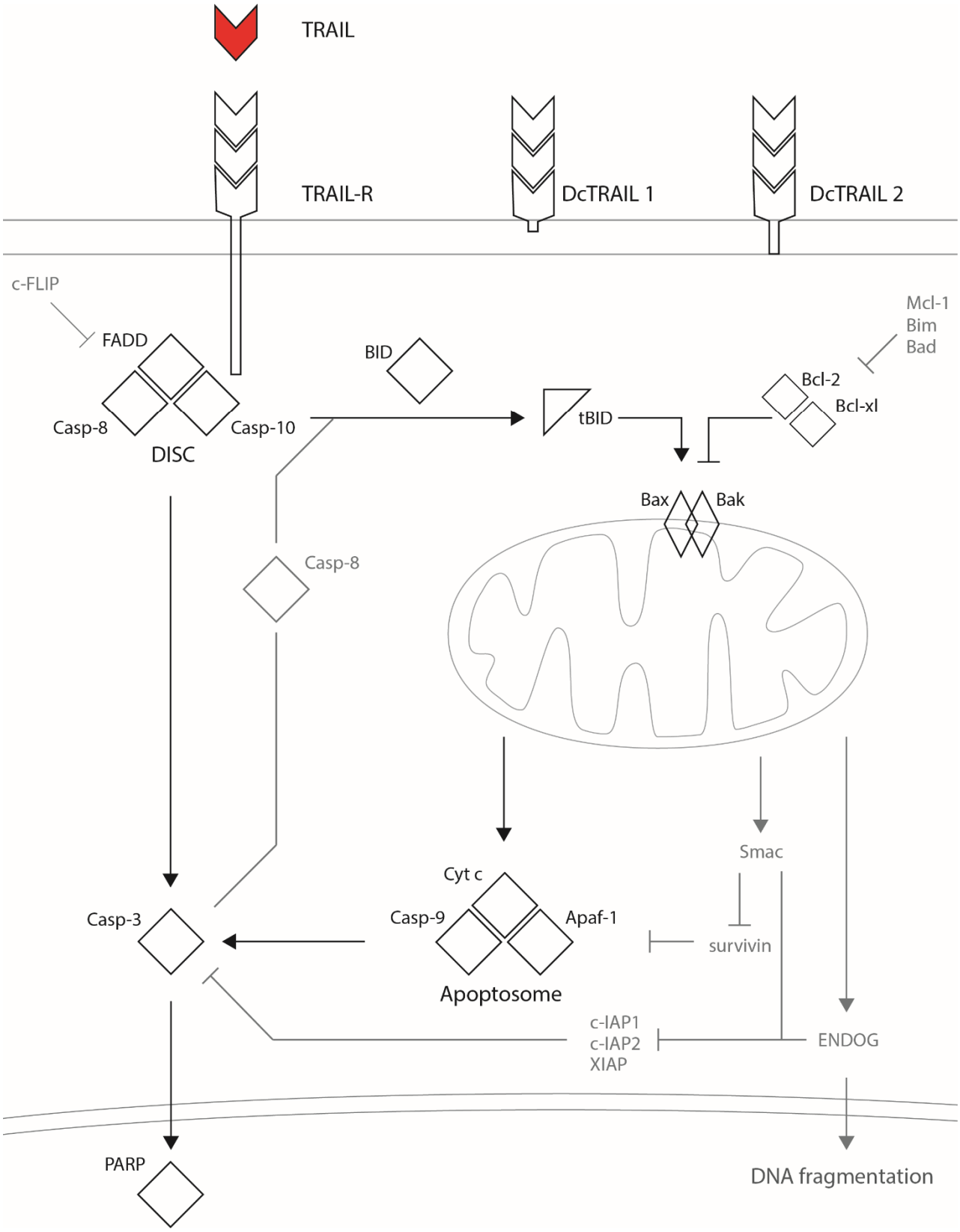

Figure 4: Apoptotic signalling pathways linked to TRAIL mediated apoptosis

Figure 4 shows the extrinsic activation of the apoptosis pathway by the example of TRAIL. TRAIL binds to its receptor TRAIL-R (DR5) as a trimer initiating receptor clustering and FADD recruitment to the intracellular death domain (DISC). DISC formation either directly activates caspase 3 or initiates mitochondrial dependent death induction. Upon DISC formation the pro-apoptotic Bcl-2 family protein BID is cleaved leading to recruitment of additional pro-apoptotic Bcl-2 family members like Bax and Bak to the mitochondria promoting the release of cytochrome c. After release of cytochrome c into the cytosol it constitutes the apoptosome with Apaf-1 and caspase 9, subsequently activating caspase 3.

1.4.3 Immunogenicity of senescent cells

Current strategies in directed elimination of senescent cells are based on their intrinsic changes resulting from senescence. However, therapeutic interventions and senolysis, the cell death of senescent cells, could also be mediated by the immune system. Immune surveillance in senescence has been found in senescent hepatic stellate cells triggering their own elimination mediated by Natural Killer (NK) cells[48]. Interestingly, in a model of hepatocellular carcinoma, senescence induction led to an infiltration of neutrophils, NK cells and macrophages with subsequent tumour regression[84]. Nevertheless, the mechanisms of immune surveillance in senescence are cell type and senescence type dependent. For example, the upregulation of NKG2D, a recognition molecule for NK cells has been shown in several types of senescence[85]. Yet the immune response elicited differs in types of senescence. Induction of senescence in a Nras(G12V) driven model of hepatocarcinogenesis led to initiation of a $CD4^+$ T cell response along with macrophage infiltration and the removal of senescent cells[86]. Recently, evidence of immune mediated senolytic therapy was achieved by generating chimeric antigen (CAR) T cells targeting urokinase-type plasminogen activator receptor (uPAR) selectively expressed on senescent cancer cells as reported in the paper[87]. This study elegantly bypasses the lack of highly selective markers for targeted therapy yet omitted the relevance of the uroginase receptor system in immunology[88]. Lately, dipeptidyl peptidase 4 (DPP4) was suggested as a selective cell surface marker in senescent fibroblasts, allowing for selective NK cell killing in antibody-dependent cell mediated cytotoxicity assays[89].

On cellular level immune cell recognition is mediated by “eat-me” and “don’t eat me” signals. A common “eat-me” signal is the presentation of phosphatidylserine (PS) on

the extracellular membrane. In apoptosis, PS externalization is mediated by enzymes called scramblases, leading to the binding of serum proteins and opsonins, which in turn enhance phagocytosis by macrophages. In physiological, steady-state conditions, exposed PS acts as an anti-inflammatory and immunosuppressive signal. Intriguingly, increased PS exposure in viable tumour cells has been described[90]. Therefore, not all externalized PS is functionally equivalent, as it was demonstrated in mouse lymphoma cell lines with introduced constitutive PS exposure. Phagocytosis of lymphoma cells with constitutive PS exposure needed additional death induction by Fas[91]. Another example of functional differences in PS exposure is the exploitation of PS exposure by viruses, called apoptotic mimicry, to evade the immune system[92,93].

The key “don’t eat me” signal CD47 is expressed on all healthy cells in high density surface clusters, mediating immune evasion. After apoptosis induction cells loose this surface clustering and the successively dispersed CD47 proteins are unable to protect from phagocytosis[94]. Interestingly, in human hepatocellular carcinoma down regulation of CD47 or PD-L1 is required for tumour regression and induction of senescence upon MYC inactivation[95]. While CD47 is an important protein involved in the immune evasion of cells, its role in senescence is still studied.

Overall, studies investigating the immune surveillance of senescent cells require further research. Yet, findings highlight the potential of immune mediated surveillance in senescence and senescent cell clearance.

2 Aims of this study

The aim of this thesis is to characterize vulnerabilities in murine β-cell tumour cells that arise in senescence and to investigate mechanisms of senescent cancer cell clearance by the immune system.

Cellular senescence plays an important role in embryonic development, tissue homeostasis and cancer control. In cancer cells senescence induction changes the cells morphology and growth pattern. These changes, however, are hypothesized to come at a cost. The first part of this work investigates the senescence response in Rip1-Tag2 tumour cells to the cytokines IFN-γ and TNF (cytokine-induced senescence - CIS) and Palbociclib (therapy-induced senescence - TIS). Therefore, growth patterns and senescence-associated β-Galactosidase (SA-beta Gal) were measured. Further, changes in senescent cancer cells were investigated to find vulnerabilities for therapeutic targeting. In this context, assays investigating the outer cell membrane composition and mitochondrial health were conducted, as well as proteins involved in apoptosis studied. To prove dependency of survival on differentially regulated proteins inhibitors were used to measure cell death in senescent cancer cells, a process known as senolysis. CIS induction relies on physiological triggers, therefore the efficacy of a physiological death inducing protein TNF-related apoptosis inducing ligand (TRAIL) was examined.

The second part of this thesis aims to investigate if murine macrophages can phagocytose senescent cancer cells or if senolysis induction is necessary for senescent cancer cell clearance. Therefore, primary murine macrophages were challenged with viable or senolytic cancer cells and phagocytosis was measured. Understanding the mode of action in senescent or senolytic cancer cell clearance may give insight into the process of cancer immune surveillance and mechanism involved in efficient cancer immune therapy.

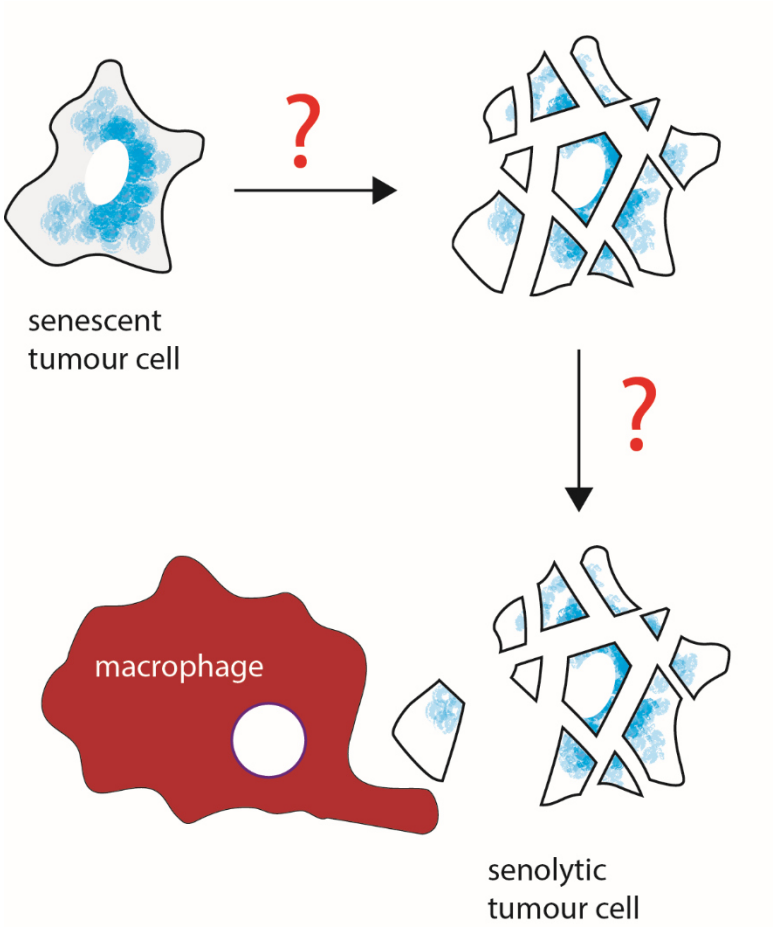

Figure 5: Aims of this thesis

This thesis seeks to understand possible vulnerabilities in β-cell tumour cells that may be acquired in senescence. Further, it investigated if senolysis is sufficient for senescent cancer cell clearance by macrophages.

3 Material and methods

3.1 Materials

3.1.1 Antibodies

Table 1: Producer and identifier of antibodies

Reagent or Resource	Source	Identifier
anti-beta actin [C4]	Merck KGaA / Millipore	MAB150R1
anti-mouse Bcl2 [BCL/10C4] Alexa Fluor 488	BioLegend	633505
anti-BID	Cell Signaling Technology, Inc.	2003S
anti-cleaved Caspase 3 [Asp175]	Cell Signaling Technology, Inc.	9661S
anti-mouse CD16/32 [93]	BioLegend	101320
anti-mouse CD47 [miap301] APC	BioLegend	127513
anti-CD47 [H-100]	Santa Cruz Biotechnology, Inc.	sc-25773
anti-mouse CD253 (TRAIL) [N2B2] APC	BioLegend	109309
anti-mouse CD262 (DR5, TRAIL-R2) [MD5-1] PE	BioLegend	119905
anti-mouse Cytochrome c [6H2.B4] Alexa Fluor 647	BioLegend	612310
anti-mouse DcTRAIL-R1 [mDcR1-3] PE	BioLegend	133804
anti-F4/80	Novus Biologicals	NB600-404
anti-mouse F4/80 [BM08] APC	BioLegend	123155
anti-mouse F4/80 [BM08] PE	BioLegend	123110
anti-iNOS [EPR16635]	Abcam plc.	ab178945
anti-Insulin	Agilent Technologies, Inc.	A0564
anti-Insulin	Abcam plc.	ab63820
anti-Ki67	Abcam plc.	ab15580
anti-Synaptophysin	Novus Biologicals	NB300-653
armenian hamster IgG [HTK888] PE	BioLegend	400908
mouse IgG1, k [MOPC-21] Alexa Fluor 488	BioLegend	400132
mouse IgG1, k [MOPC-21] Alexa Fluor 647	BioLegend	400155
rat IgG2a, k [RTK2758] APC	BioLegend	400512
rat IgG2a, k [RTK2758] PE	BioLegend	400507
goat-anti-rabbit Fluor Alexa 488	Thermo Fisher Scientific Inc. / Invitrogen	A11008
goat-anti-mouse (igG H&L) DyLight488	Abcam plc.	ab96871
goat-anti-rabbit (IgG H&l) DyLight 594	Abcam plc.	ab96885
goat IgG anti-Rat IgG (F(ab')2)-Rhod. Red-X	DIANOVA GmbH	112-225-006
goat IgG anti-Rat IgG (F(ab')2)-Cy3	DIANOVA GmbH	112-165-006
goat-anti-mouse IgG IRDye 680RD	LI-COR Biosciences GmbH	926-68070
goat-anti-mouse IgG IRDye 800 CW	LI-COR Biosciences GmbH	926-32210
goat-anti-rabbit IgG IRDye 680RD	LI-COR Biosciences GmbH	926-68071
goat-anti-rabbit IgG IRDye 800 CW	LI-COR Biosciences GmbH	926-32211

Table 2: Concentration and method of antibodies used

Antibody	Dilution/Concentration	Method
anti-beta actin [C4]	1:5000	WB
anti-mouse Bcl2 [BCL/10C4] Alexa Fluor 488	0,5 ug/ml	FACS
anti-BID	1:500	WB
anti-cleaved Caspase 3 [Asp175]	1:500	IF
anti-mouse CD16/32 [93]	0,2 µg/ml	FACS
anti mouse CD47 [miap301] APC	1:500	FACS
anti-CD47 [H-100]	1:1000	WB
anti-mouse CD253 (TRAIL) [N2B2] APC	0,2 µg/ml	FACS
anti-mouse CD262 (DR5, TRAIL-R2) [MD5-1] PE	0,2 µg/ml	FACS
anti-mouse Cytochrome c [6H2.B4] Alexa Fluor 647	0,5 ug/ml	FACS
anti-mouse DcTRAIL-R1 [mDcR1-3] PE	0,2 µg/ml	FACS
anti-F4/80	1:500	IF
anti-mouse F4/80 [BM08] APC	0,2 µg/ml	FACS
anti-mouse F4/80 [BM08] PE	0,2 µg/ml	FACS
anti-iNOS [EPR16635]	1:500	IF
anti-Insulin	1:500	IF
anti-Insulin	1:500	IF
anti-Ki67	1:500	IF
anti-Synaptophysin	1:500	IF
armenian hamster IgG [HTK888] PE	concentration used equivalent to respective antigen specific antibody	FACS
mouse IgG1, k [MOPC-21] Alexa Fluor 488		FACS
mouse IgG1, k [MOPC-21] Alexa Fluor 647		FACS
rat IgG2a, k [RTK2758] APC		FACS
rat IgG2a, k [RTK2758] PE		FACS
goat-anti-rabbit Fluor Alexa 488	1:1000	IF
goat-anti-mouse (igG H&L) DyLight488	1:1000	IF
goat-anti-rabbit (IgG H&l) DyLight 594	1:1000	IF
goat IgG anti-Rat IgG (F(ab')2)-Rhod. Red-X	1:200	IF
goat IgG anti-Rat IgG (F(ab')2)-Cy3	1:200	IF
goat-anti-mouse IgG IRDye 680RD	1:10000	WB
goat-anti-mouse IgG IRDye 800 CW	1:10000	WB
goat-anti-rabbit IgG IRDye 680RD	1:10000	WB
goat-anti-rabbit IgG IRDye 800 CW	1:10000	WB

3.1.1 Chemicals, Peptides, and recombinant protein

Table 3: Chemicals, Peptides, and recombinant protein

Reagent or Resource	Source	Identifier
2-log DNA ladder	New England Biolabs	N3200L
2-Propanol	VWR International, LLC.	20842.330
7-AAD	BD Biosciences	559925
ABT263 (Navitoclax)	Selleck Chemicals	s1001
Aceton	AppliChem GmbH	1.310.071.212
Agarose	Carl Roth GmbH + Co. KG	2267.4
Albumin Fraktion V	Carl Roth GmbH + Co. KG	8076.4
Ammonium persulfate	Merck KGaA / Sigma-Aldrich	A3678-100G
AnnexinV APC	BioLegend	640945
AnnexinV FITC	BioLegend	640920
Carbonyl cyanide 3-chlorophenylhydrazone	Merck KGaA / Sigma-Aldrich	C2759-100mg
CM-H2DCFDA	Thermo Fisher Scientific Inc. / Invitrogen	C6827
Collagenase NB8, 250mg	SERVA Electrophoresis GmbH	17456
D-(+)-Glucose	Merck KGaA / Sigma-Aldrich	G6152-500G
DAPI (4',6-diamidino-2-phenylindole, dihydrochloride)	Thermo Fisher Scientific Inc. / Thermo Scientific	62247
DirectPCR Lyse Reagenz	7BioScience GmbH	402-E
DMSO	CarlCarl Roth GmbH + Co. KG	A994.1
EDTA Dinatriumsalz Dihydrat (Titrierkomnplex III)	Carl Roth GmbH + Co. KG	8043.1
Ethanol	VWR International, LLC.	20821330
Formaldehyde	Merck KGaA / Sigma-Aldrich	252549-500ml
Glycerin	Carl Roth GmbH + Co. KG	3783.1
Glycin	Carl Roth GmbH + Co. KG	3908.2
Hydrogen peroxide solution	Merck KGaA / Sigma-Aldrich	216763-500ML
Ionomycin	Thermo Fisher Scientific Inc. / Invitrogen	I24222
JC-1 Dye	Thermo Fisher Scientific Inc. / Invitrogen	T3168
Kaliumchlorid	Merck KGaA / Millipore	1049361000
Kaliumhexacyanoferrat (II)	AppliChem GmbH	131505.1210
Kaliumhexacyanoferrat (III)	AppliChem GmbH	131503.1210
Lipopolysaccharides from Escherichia coli O55:B5	Merck KGaA / Sigma-Aldrich	L4524
Lithiumchlorid	Carl Roth GmbH + Co. KG	3739.1
Magnesiumchloride-Hexahydrat	AppliChem GmbH	141396.1211
Methanol	VWR International, LLC.	20847.307
Milk Powder	Carl Roth GmbH + Co. KG	T145.2
Mitotracker Green FM	Thermo Fisher Scientific Inc. / Invitrogen	M7514
Natriumazid	Carl Roth GmbH + Co. KG	K305.1

Natriumchlorid (NaCl)	Carl Roth GmbH + Co. KG	3957.1
Natriumhydrogencarbonat	Carl Roth GmbH + Co. KG	6885.2
NOC-18 - CAS 146724-94-9 - Calbiochem	Merck KGaA / Calbiochem	487957
Nonident P40 Substitute	Merck KGaA / Sigma-Aldrich	74385
Orange G (C.I.16230)	Carl Roth GmbH + Co. KG	0318.1
Palbociclib (PD-0332991) HCl	Selleck Chemicals	s1116
Propidium Iodide Staining Solution	BD Biosciences	556463
Proteinase K Pulver	Genaxxon bioscience GmbH	E-003269-00-0005
recombinant murine IFN-γ	R&D Systems, Inc.	485-MI-100
recombinant murine IL-4	PeproTech, Inc.	214-14
recombinant murine mCSF	PeproTech, Inc.	315-02
recombinant murine TNF	R&D Systems, Inc.	410-MT-050
recombinant murine TRAIL	PeproTech, Inc.	315-19
SDS / Natriumlaurylsulfat	Carl Roth GmbH + Co. KG	5136.1
Sodium deoxycholate	Merck KGaA / Sigma-Aldrich	D6750-10G
Sodium hydroxide	Merck KGaA / Sigma-Aldrich	S8045-500G
Staurosporine	Selleck Chemicals	s1421
Tris ultrapure	AppliChem GmbH	A1086.1000
X-Gal (5-Brom-4-chlor-3-indolyl-ß-D-galactopyranosid)	VWR International, LLC. International, LLC.	730-1498
Zombie Violet Fix Kit	BioLegend	423114
z-VAD-FMK	Selleck Chemicals	s7023

3.1.2 Commercial Assays

Table 4: Commercial Assays

Reagent or Resource	**Source**	**Identifier**
beta-Galactosidase Staining Kit	Biomol GmbH	G1041-76.1
DCFDA Cellular ROS Detection Assay Kit	Abcam plc.	ab113851
DuoSet Ancillary Reagent Kit 2	R&D Systems, Inc., Inc	DY008
Mitoprobe Transition Pore Assay Kit	Thermo Fisher Scientific Inc. / Invitrogen	M34153
Mouse CXCL10/IP-10/CRG-2 DuoSet ELISA	R&D Systems, Inc.	DY466
Mouse CXCL9/MIG DuoSet ELISA	R&D Systems, Inc.	DY492
Multi.Analyte ELISArray Kit	Thermo Fisher Scientific Inc. / Qiagen	MEM-009A
murine JE-MCP1 Mini ABTS ELISA	PeproTech, Inc.	500-p113b
murine RANTES (CCL5) Mini ABTS ELISA Development Kit	PeproTech, Inc.	900-124
Pierce BCA Protein Assay Kit	Thermo Fisher Scientific Inc. / Thermo Scientific	23225

PKH67 Fluorescent Cell Linker Kit	Merck KGaA / Sigma-Aldrich	PKH67GL-1KT

3.1.3 Consumables & Compounds

Table 5: Consumables

Reagent or Resource	Source	Identifier
10 µl Graduated Tip	STARLAB GmbH	S1111-3800
1000 µl Blue Graduated Tip,	STARLAB GmbH	S1111-6801
200 µl Yellow Bevelled Tip	STARLAB GmbH	S1111-1806
6 well plates	FAUST Lab Science GmbH	TPP92006
96 well plates	FAUST Lab Science GmbH	TPP92007
96 well plates	FAUST Lab Science GmbH	TPP92096
96 well, TC, µclear, schwarz	Greiner Bio One International GmbH	655090
Accu-Check Aviva blood glucose test strip	Roche Diagnostics Deutschland GmbH	6453970003
ACK Lysing Buffer	Lonza Group Ltd.	10-548E
Biosphere Filter Tips, 0.1 - 20 µl	Sarstedt AG & Co. KG	701.186.210
Biosphere Filter Tips, 2 - 100 µl	Sarstedt AG & Co. KG	70.760.212
Biosphere Filter Tips, 50 - 1.250 µl	Sarstedt AG & Co. KG	70.1186.210
Cell lifter	Merck KGaA / Corning	3002554
Chamber Culture Slides	BD Falcon	354108
cOmplete Tablets, Mini, EDTA-free, EASYpack	Roche Diagnostics Deutschland GmbH	46931590001
Corning Transwell polycarbonate membrane cell culture inserts	Merck KGaA / Sigma-Aldrich	CLS-3421-48EA
DMEM	Bio&SELL GmbH	F 0455
Dulbeccos Phosphate Buffered Saline	Merck KGaA / Sigma-Aldrich	D8537-500ML
Eppendorf Safe-Lock Tubes, 0.5 mL	Eppendorf AG	30121023
Eppendorf Safe-Lock Tubes, 1.5 mL	Eppendorf AG	30120086
Eppendorf Safe-Lock Tubes, 2 mL	Eppendorf AG	30120094
Falcon Round-Bottom Polystyrene Tubes	Thermo Fisher Scientific Inc. / Fisher Scientific	352058
Falcon Round-Bottom Polystyrene Tubes	Thermo Fisher Scientific Inc. / Fisher Scientific	352008
Fetal calf serum	Merck KGaA / Sigma-Aldrich	F7524-500ml
Fluorescent Mounting Medium	Agilent Technologies, Inc. / DAKO	s3023

Hanks	Merck KGaA / Millipore	L2035
Hepes, 50x	Biochrom GmbH	L1613
Immobilon-FL Transfer Membran PVDF für LI-COR Biosciences GmbH	Merck KGaA / Millipore	IPFL000-10
Magic Marker XP Western Standard	Thermo Fisher Scientific Inc. / Invitrogen	LC-5602
MEM Amino Acids, 50x	Biochrom GmbH	K0363
Needle 24G x1" 0,55mm x 25 mm	BD Biosciences	304100
Needle 30G x ½" 0,3mm x 13 mm	BD Biosciences	304000
Odyssey Nitrocellulose Membrane, 0.22 um	LI-COR Biosciences GmbH	926-31090
PageRuler Plus Prestained Protein Ladder	Thermo Fisher Scientific Inc. / Thermo Scientific	26620
Pasteurpipettes Steril	Carl Roth GmbH + Co. KG	EA66.1
PCR 8er_SoftStrips,farblich gemischt, 5 Btl. á 25 Strips	Biozym Scientific GmbH	711038
Penicillin/Streptomycin	Biochrom GmbH	A2213
Petri dishes 94/16 mm	Greiner Bio One International GmbH	633161
PhosSTOP EASYpack	Roche Diagnostics Deutschland GmbH	490683700 1
Protein Block, Serum-free, 110 ml	Agilent Technologies, Inc. / DAKO	X0909-30
Protein-Block serum free	Agilent Technologies, Inc. / DAKO	X090930-2
Sodium Pyruvat, 100 mM	Biochrom GmbH	L0473
Syringe 10 ml	B. Braun Melsungen AG	4606108V
Syringe 20 ml	B. Braun Melsungen AG	4606205V
Syringe 5 ml	B. Braun Melsungen AG	4606051V
TC-Flask T175	Sarstedt AG & Co. KG	833.912.00 2
TC-Flask T25	Sarstedt AG & Co. KG	833.910.00 2
TC-Flask T75	Sarstedt AG & Co. KG	833.911.00 2
Trypan Blue Stain 0,4%	Thermo Fisher Scientific Inc. / Gibco	15250-061
Trypsin-EDTA	Thermo Fisher Scientific Inc. / Life Technologies	25300096
Tween 20	Carl Roth GmbH + Co. KG	9127.1
UV transparent disposable cuvettes	Sarstedt AG & Co. KG	67.758.001
Whatman	GE Healthcare GmbH	3017-915

3.1.4 Labware

Table 6: Labware

Instrument	Type	Company
Binocular	Binokular S6 E	Leica Microsystems
Centrifuge	Heraeus Biofuge Pico	Thermo Fisher Scientific Inc. / Thermo Scientific
Centrifuge	Heraeus Biofuge Presco	Thermo Fisher Scientific Inc. / Thermo Scientific
Centrifuge	Heraeus Multifuge 3 S-R	Thermo Fisher Scientific Inc. / Thermo Scientific
Counting Chamber	Neubauer improved counting chamber	Glaswarenfabrik Karl Hecht GmbH & CoKG
ELISA Reader	Multiskan EX	Thermo Fisher Scientific Inc. / Thermo Scientific
FACS	LSR II	BD Biosciences
Fume Hood	Airflow Controller AC2	Waldner AG
Gel electrophoresis	Protean II	Bio-Rad Laboratories, Inc.
Gel electrophoresis	SUB Cell GT	Bio-Rad Laboratories, Inc.
Heating block	Thermomixer Model Comfort	Eppendorf AG
Heating block	HB-LS2	VLM Korrosions-Prüftechnik, Labortechnik & Dienstleistungen GmbH
Imaging System	Odyssey Sa Infrared Imaging System	LI-COR Biosciences GmbH
Incubator	Hera Cell 240	Thermo Fisher Scientific Inc. / Thermo Scientific
Laminarflow Hood	Herasafe KS18	Thermo Fisher Scientific Inc. / Thermo Scientific
Light source	KL 1500 LCD	Schott AG
Light source	HBO100	OSRAM GmbH
Microscopes	Axiovert 25	Carl Zeiss AG
Microscopes	Axiovert 200	Carl Zeiss AG
PCR machine	Primus 96 advanced	MWG Biotech, Inc.
PCR machine	Primus 96 plus	MWG Biotech, Inc.
pH meter	CG 842	Schott AG
Pipette	PIPETBOY acu 2	INTEGRA Biosciences
Pipette	Reference	Eppendorf AG
Pipette	Research	Eppendorf AG
Power supply	Power Pac 300	Bio-Rad Laboratories, Inc.
Power supply	Power Pac basic	Bio-Rad Laboratories, Inc.
Protein transfer	Trans-Blot Turbo	Bio-Rad Laboratories, Inc.
Rocker	STR8 Rocking Platform	Stuart Scientific
Rocker	DRS-12	ELMI
Scale	CP224S	Sartorius AG
Scale	EW1500-2M	KERN & SOHN GmbH

UV transilluminator	RH-5.1 darkroom hood with easy 442K camera	Herolab GmbH
Vortex	Reax Top	Heidolph Instruments GmbH & CO. KG
Water Bath	Type 1003	GFL Gesellschaft für Labortechnik mbH

3.1.1 Software

Table 7: Software

Software	**Company**
Adobe Illustrator CS6 v16.0.3	Adobe Systems
Ascent v2.6	Thermo Fisher Scientific Inc. / Thermo Scientific
Axiovision v4.9.1	Carl Zeiss AG
BD FACSDiva v8.0.1	BD Biosciences
FlowJo v10.5.3	FlowJo, LLC.
GraphPad Prism v8.1.0	GraphPad Software, Inc.
Image Studio Light v3.1.4	LI-COR Biosciences GmbH
Image Studio v1.1.7	LI-COR Biosciences GmbH
ImageJ v1.47	W. Rasband, NIH
Microsoft Office Professional Plus 10	Microsoft Corporation
VisiView	Visitron Systems GmbH

3.2 Methods

3.2.1 Cell culture methods

3.2.1.1 Primary cell culture of tumourigenic pancreatic islet cells

In this work only primary cells were used. The islet tumour cells were isolated from female C3HeB/FeJ-Tg(RIP1-TAg)2/DH (short: Rip1-Tag2) age 12 to 14 weeks. Briefly, mice were euthanized with CO_2 and the peritoneum opened. After ligation of the Ductus choledochus and ligation of the duodenum proximal to the Papilla Vateri, 5 ml Collagenase Solution (5 mg Collagenase in 5 ml 2,8 mM Glucose/Hanks) was injected into the Ductus pancreaticus using a 30G syringe. The inflated pancreas was excised, and collagenase digestion continued for 10 minutes at 37 °C. Collagenase digestion was stopped by adding 10 ml Stop Solution (2,8 mM Glucose & 0,5 % BSA/Hanks) to the excised pancreas. The probe was spun down for 2 minutes at 800 g and supernatant discarded. Tumours were isolated and cleared from surrounding tissue under a binocular. Tumours were collected and washed once in PBS before addition of 500 µl trypsin. Tumours were cut into pieces with a scissor for 5 minutes followed by a 5-minute incubation at 37°C. Trypsin digestion was stopped with 500 µl cell culture media and cells were spun down for 5 minutes at 2000 g. Cells were resuspended in cell culture media and counted before seeding. Tumour cells were used for experiments once a cell culture free from other cells (e.g. fibroblasts) was established. The purity of cell culture was determined by immunofluorescence staining for insulin and synaptophysin. The cells were cultured in Dulbeccos's modified Eagle medium (DMEM) with stable L-Glutamine and 4.5 g/L glucose supplemented with 10% fetal calf serum, 1x HEPES, 1 mM Sodium Pyruvate, 1x MEM Amino Acids and 50 µM 2-Mercaptoethanol at 37 °C and 7.5 % CO_2. The FCS was inactivated prior to supplementation for 60 minutes at 57 degree Celsius. In early passages 100 U/ml Penicillin and 100 µg/ml Streptomycin was added to the media but removed once a stable culture was established.

3.2.1.2 Senescence induction in primary tumour cell culture

Senescence was induced using recombinant cytokines or compounds. For cytokine induced senescence cells were incubated with 100 ng/ml IFN-γ and 10 ng/ml TNF for 96 hours. Therapy induced senescence was established by incubation with 5 µM Palbociclib/DMSO for 96 hours.

3.2.1.3 Primary cell culture of immune cells

Primary macrophages were derived from murine bone marrow isolated from the femur and tibia of mice. Bone marrow from mice sacrificed for tumour isolation or from female wildtype C3HeB/FeJ (short: C3H) was used. In short, the limbs were detached, and muscle tissue removed from bones. The bone was cut on both sides before the epiphysis and the marrow cavity was flushed with PBS using a 30 G syringe. The bone marrow was passed through a 200 µm filter and spun down for 5 minutes at 2000 g. The supernatant was removed, and red blood cells lysed with 500 µl ACK Lysis Buffer for 2.5 minutes. The buffer was diluted in 5 ml PBS and the suspension was spun down before the bone marrow derived stem cells were seeded into 10 cm plates with 20 ng/ml mCSF in cell culture media. On day 3 of culture 5 ml freshly prepared media with 20 ng/ml mCSF was added. Cells were cultured at 7.5 % CO_2 and 37 °C. Differentiation of stem cells into macrophages was completed at day 6 of culture. Macrophages were harvested for experiments on day 6. Culture media was replaced by 8 ml ice-cold PBS. The plates were left at 4 °C for 20 minutes and macrophages were collected using a cell scraper.

3.2.1.4 Immune cell polarization

Primary bone marrow derived macrophages were polarized towards an M1 phenotype by adding 100 ng/ml LPS and 20 ng/ml IFN-γ for 24 hours. Polarization towards an M2 phenotype was achieved by incubation of primary bone marrow derived macrophages with 10 ng/ml recombinant IL-4.

3.2.1.5 Transwell Assay

To determine attraction of SASP to macrophages a transwell assays (24 well format) was done. Transwells with a polycarbonate membrane and 5 µm pore size were used.

The transwell membrane was equilibrated with 100 culture media for 5 minutes before 4 x 10^5 macrophages were added in 200 µl media and left to adhere for 30 minutes in the cell culture incubator (37 °C, 7,5 % CO2). The transwells were transferred to a new plate with 750 µl supernatant of senescent cells or control cells in the bottom chamber. It was ensured that no air bubbles were between the transwell bottom and the supernatant. Supernatant was previously collected from 2.5 x 10^4 senescent or non-senescent tumour cells cultured in a 24 well plate. The assay was done for 4 hours. Afterwards transwells were washed with PBS and fixed in ice-cold methanol:aceton (1:1, v/v) for 5 minutes at -20 °C. Membranes were air-dried for 60 minutes or overnight. Membranes were moisturized in PBS before the top part of the membrane was cleared of macrophages with a Q-tip. Membranes were stained in 300 nM DAPI in the dark for 5 minutes at room temperature and washed in PBS afterwards. For quantification of migrated cells the transwell was placed on a glass slide and images were taken with Zeiss Axiovert 200.

3.2.1.6 ELISA

Supernatant of senescent and non-senescent cells was examined. Cells were seeded at the same cell number and senescence was induced for 96 hours. The supernatant was collected and is referred to as “early-SASP”. After senescence induction or control incubation cells were washed, trypsinized and reseeded at the same cell number as used for induction. The cells were left in culture for an additional 96 hours and supernatant collected was termed “late-SASP”. To determine Chemokine secretion the assay “Multi.Analyte ELISArray Kit” was performed according to manufacturers (Thermo Fisher) protocol.

3.2.1.7 Death assays

Cells were trypsinized and resupended at a defined volume. Trypan Blue was added at a dilution of 1:10 and cells were counted under a microscope using a Neubauer Chamber. To induce cell death different compounds were used. If not indicated otherwise TRAIL was used at a concentration of 5µg/ml, ABT263 at 0.1 µM, NOC-18 at 250 µM and staurosporine at 0.1 µM.

3.2.1.8 PKH67 stain of tumour cells

To assess uptake of tumour cells by macrophages tumour cells were stained using the membrane linker PKH67. Senescent and non-senescent tumour cells were trypsinized and washed twice in serum free media and counted. The following solutions were scaled according to cell count. A cell pellet of 1 x 10^6 primary tumour cells was dissolved in 100 µl Diluent C. 100 µl 2x Staining Solution was added to the dissolved tumour cells to a final concentration of 20 µM PKH67 and incubated for 15 minutes at room temperature. Cell suspension was dispersed by pipetting every 2,5 minutes. Remaining dye was blocked by incubation with 200 µl FCS for 1 minute. Cells were spun down, transferred to a new tube and washed with media containing FCS twice. Viability was controlled by Trypan Blue count before and after staining.

3.2.1.9 Macrophage feeding assay

Primary bone marrow derived macrophages were coincubated with senescenct and non-senescent PKH67 stained tumour cells at a ratio of 5:1 for 24 hours. Subsequently cells were fixed and F4/80 positive cells with PKH67 spots counted. If applicable caspase inhibitors or senolytic compounds were used as described in results part.

3.2.2 FACS

For FACS analysis cells were trypsinized, counted and cell number adjusted before staining. For intracellular FACS analysis cells were fixed in 1,5 % Formaldehyde/PBS for 15 minutes protected from light. Cells were spun down and fixation solution was removed before the cell membrane was disrupted using 0,5 % Saponin/PBS (w/v) for 30 minutes at room temperature protected from light. Cells were washed twice with PBS before Blocking Solution (5 % FCS/PBS) was added for 45 minutes. After washing antibody and respective isotype controls were added. Concentrations of antibody, incubation time and fixation are described in Table 2.

Extracellular staining of antigens was either done in live or fixed cells. In fixed cells the protocol was done as described above without the permeabilization step. For live cell staining the cells were incubated for 20 minutes at 4°C or on ice in 100 µl HBSS or PBS with antibody or isotype and fluorescence minus one (FMO) controls respectively.

If not otherwise indicated Live/Dead exclusion was done using PI (200 ng/ml) or 7-AAD (100 ng/ml) during antibody staining step.

3.2.2.1 Flow Cytometry Kits

To characterize cells and treatment condition the following commercially available kits were used according to manufacturers protocol. Following is a brief description of respective protocol.

3.2.2.2 Mitotracker

To assess mitochondrial mass cells were trypsinized, washed once with PBS before 1 x 10^6 cells were stained with 2 µM Mitotracker in HBSS for 30 minutes at 37°C in 1 ml HBSS according to manufacturers protocol before FACS analysis.

3.2.2.3 Mitopore

The opening of the mitochondrial permeability transition pore can be measured. Calcein-AM, a colorless esterase substrate, diffuses through the membrane and accumulates in cellular compartments including the mitochondria. Inside the cell the acetoxymethyl (AM) ester is cleaved by esterases and fluorescent calcein is liberated. Subsequently fluorescence from cytosolic calcein is quenched using Cobalt(II)-Chloride. Cells were trypsinized, washed once with PBS before 1 x 10^6 cells were loaded with 2 µM Calcein-AM in HBSS/Ca for 15 minutes at 37 °C. To ensure equal cleavage of the AM moiety by esterases cells were spun down and resuspended in HBSS/Ca without Calcein-AM and incubated for an additional 10 minutes. 160 µM $CoCl_2$ was added for quenching and cells incubated for additional 5 minutes. Cells were washed in HBSS/Ca to remove excess quenching reagents and resuspended in 200 µl HBSS/Ca for FACS analysis.

3.2.2.4 Mitoprobe JC-1

The cationic JC-1 accumulates potential dependent in mitochondria. This is indicated by a shift in fluorescence emission. Cells were trypsinized, washed once with PBS before resuspension in HBSS/Ca at a concentration of 1 x 10^6 cells/ml. Cells were labelled with 2 µM JC-1 for 20 minutes at 37 °C, 7.5% CO_2. Cells were pelleted by

centrifugation and resuspended in HBSS/Ca before FACS analysis. CCCP, depolarizes the mitochondrial membrane and is used as a control at a concentration of 50 µM. It was added simultaneously with JC-1.

3.2.2.5 Annexin V

Cells were trypsinized and washed in AnnexinV Binding Buffer (10mM Hepes/NaOH pH7.4; 140mM NaCl; 5mM $CaCl_2$). 1 x 10^6 cells were incubated with 1.5 µg AnnexinV and 20 ng Propidium Iodide in 1 ml AnnexinV Binding Buffer for 20 minutes at room temperature in the dark. Before FACS analysis, cells were washed with Annexin Binding Buffer and resuspended in 250 µl AnnexinV Binding Buffer.

3.2.3 Molecular methods

3.2.3.1 Western Blot

For the generation of Western Blot probes cells were seeded and treated according to text. Before addition of lysis buffer cells were washed twice with PBS. Cell lysis buffer (1 mM EDTA, 0.05 % Triton-X, 20 mM Tris pH8, 137 mM NaCl add to 500 ml H_2O) was supplemented with complete and phospho-stop and probes were left on ice for 20 minutes before they were spun down (13000 rpm, 5 min) and supernatant transferred into a new cup. Protein concentration was determined using BCA-Assay, according to manufacturers protocol. The SDS-Page Gel consists of a lower 10 % separating gel (3.9 ml H_20, 3.3 ml 30 % Polyacrylamide, 0.1 ml 10 % SDS (w/v), 0.1 ml 10 % APS (w/v), 20 µl TEMED, Tris lower pH 8.8 (0.5 M Tris, 0.4 % SDS (w/v)), and an upper 5 % loading gel (3.4 ml H_20, 0.85 ml 30 % Polyacrylamide, 0.05 ml 10 % SDS (w/v), 0.05 ml 10 % APS (w/v), 10 µl TEMED, Tris upper pH 6.8 (1.5 M Tris, 0.4 % SDS (w/v)). Before loading the samples 2x Lämmli (0.125 M Tris HCl pH 6.8, 4 % SDS (w/v), 20 % glycerol (v/v), 10% 2-mercaptoethanol (v/v), 0.004% bromphenol blue(w/v)) was added and samples denatured at 95 °C for 5 minutes. Per gel lane equal protein concentration was loaded onto polymerized SDS-PAGE gel. To determine protein molecular weight one lane was loaded with PageRuler Plus Pre Stained Protein Ladder. The gel was run for 1-2 hours at 100 V. Once the dye reached the lower parts of the gel the PAGE was ended and the protein transferred from gel to Immobilon FL-Transfer Membrane using a semi-dry approach. Whatman was drenched in Semi Dry

Buffer (48 mM Tris, 29 mM Glycin, 0.0388 % SDS (w/v), 20% MeOH (v/v), adjusted to pH 8.5), on top the gel was placed, followed by methanol-activated PVDF membrane and another filter paper. To ensure transfer of proteins on membrane the gel is closer to the cathode and the membrane closer to the anode. The transfer was done for 10 minutes at 1,3 A, 25 Volts in Semi Dry Buffer. This was followed by blocking step for 30 minutes at room temperature dependent on the antibody used. Afterwards membrane was washed in TBST if blocking was done with 5 % milk/TBST, no washing step was done if blocking solution was 5 % BSA/TBST. This was followed by primary antibody incubation at 4 °C overnight. Membrane was washed with TBST twice and incubated with secondary antibody at room temperature for 1 hour. For detailed antibody concentration, blocking used and secondary antibody see table Table 2. Protein was detected using Odyssey Sa Infrared Imaging System and quantified using Odyssey Sa Application Software.

3.2.3.2 SA-β-Galactosidase assay

SA-β-Galactosidase assay was done using a commercially available kit or using self-made solutions. If SA-β-Galactosidase assay kit was used the assay done according to manufacturers instruction. The protocol of the self-made SA-β-Galactosidase assay is equivalent to the manufacturers instructions but pH assay controls were added. In short cells were washed with PBS and fixed in glutaraldehyde solution (2 % formaldehyde, 0,2 % glutaraldehyde) for 15 minutes at room temperature. After washing the cells with PBS the pH 6 staining solution (1 mg/ml 5-Brom-4-chlor-3-indolyl-ß-D-galactopyranosid in 40 mM citric acid/sodium phosphate pH6 / 5 mM potassium ferrocyanide / 5 mM potassium ferricyanide / 150 mM NaCl/ 2 mM $MgCl_2$) was added and cells were incubated at 37 °C overnight. Galactosidase substrate turnover was checked under a microscope the next day. If staining was visible the solution was removed, cells washed with PBS and stained with 300 nM DAPI/PBS for 5 minutes in the dark. DAPI staining solution was removed and cells covered in PBS before imaging.

3.2.3.3 Immunofluorescence

For immunofluorescence staining cells were seeded in a 96 well black chimney or on chamber slides and cultivated for at least 24 hours depending on assay. The cells were washed with PBS before fixation. Cells were fixed in ice-cold acetone:methanol (1:1, v/v) for 5 minutes at -20°C. Fixation solution was discarded and cells were left at room temperature to air dry. Blocking solution was applied for 45 minutes at room temperature. Blocking solution was aspirated and primary antibody incubation was done in PBST at 4 °C overnight. The following day wells were washed twice with PBST and secondary antibody added for 1 hour at room temperature in the dark. After two washing steps 300 nM DAPI/PBST was added for 5 minutes. After incubation cells were washed twice with PBST followed by PBS. 96 well plates were covered with 100 ul PBS. Chamber slides were embedded with mounting medium and set at 4 °C in the dark for curing overnight. Images were taken on a Zeiss microscope (AxioVert200).

3.2.4 Statistics

Graphs were designed using GraphPad Prism 8 and illustrated using Adobe Illustrator CS6. Statistics were calculated using GraphPad Prism 8. The test used is indicated in the figure legend of the experiment, respectively. P-values $p \leq 0.05$ (*), $p \leq 0.01$ (**), $p \leq 0.001$ (***), $p \leq 0.0001$ (****), not significant (ns). Error bars always depict standard deviation.

4 Results

The main aim of this thesis was to identify vulnerabilities in cancer cells acquired by senescence to find new therapeutic targets for secondary cancer cell clearance. Therefore, the first hypothesis was that senescence induces changes in tumour cells (acquired vulnerability). The second hypothesis was that this acquired vulnerability can be targeted to induce cell death (senolysis) in senescent tumour cell, therefore allowing for phagocytosis of senescent cancer cells.

4.1 Primary β-cell tumour cells are responsive to CIS and TIS

4.1.1 Stable β-cell marker expression of primary β-cell tumour cells *in vitro*

In this study primary β-cell tumour cells were isolated from C3HeB/FeJ-Tg(RIP1-Tag)2/DH (short: RIP1-Tag2) mice. The RIP1-Tag2 mice express the SV40 Large T-antigen (Tag2) under regulation of the Rat Insulin Promoter (RIP) (Figure 6A). The viral oncogene SV40 Large T-antigen perturbs p53 and retinoblastoma (Rb) tumour suppressor pathways inducing tumours in pancreatic β-cells. At 5-6 weeks of age RIP1-Tag2 mice start to develop hyperplastic islets that are vascularized at 8-10 weeks of age. Upon 10 weeks of age the vascularized islet progress into small, encapsulated adenomas. At 12 weeks of age the tumours show an increased size with the majority of tumours developed into well differentiated adenomas[96–98] (Figure 6B).

Primary tumour cells were isolated from mice at 12-14 weeks of age and tested for suitability. To test the purity of primary tumour cell culture, cells were stained for neuroendocrine marker synaptophysin and β-cell marker insulin, as well as proliferation marker Ki67 (Figure 6C). Cell cultures positive for synaptophysin and insulin (> 80 %) were used for experiments. The mean percentage of synaptophysin positive cells was 89,73 %, of insulin positive cells 83,43 % and of Ki67 positive cells 59,35 %. Eleven of 14 primary cell cultures were above 95 % positive for synaptophysin, and ten out of 14 were above 90 % positive for Insulin. The amount of Ki67 positive cells varied between cell lines, ranging from 17.45 % positive to 95.35 % positive (Figure 6D). While β-cell marker expression of insulin and synaptophysin was transferable from *in vivo*[98] to *in vitro* settings, Ki67 expression varies profusely. This

heterogeneity may at least in part be due to isolation of highly prolific, poorly differentiated invasive carcinomas[98] in combination with differentiated β-cell tumours from RIP1-Tag2 mice.

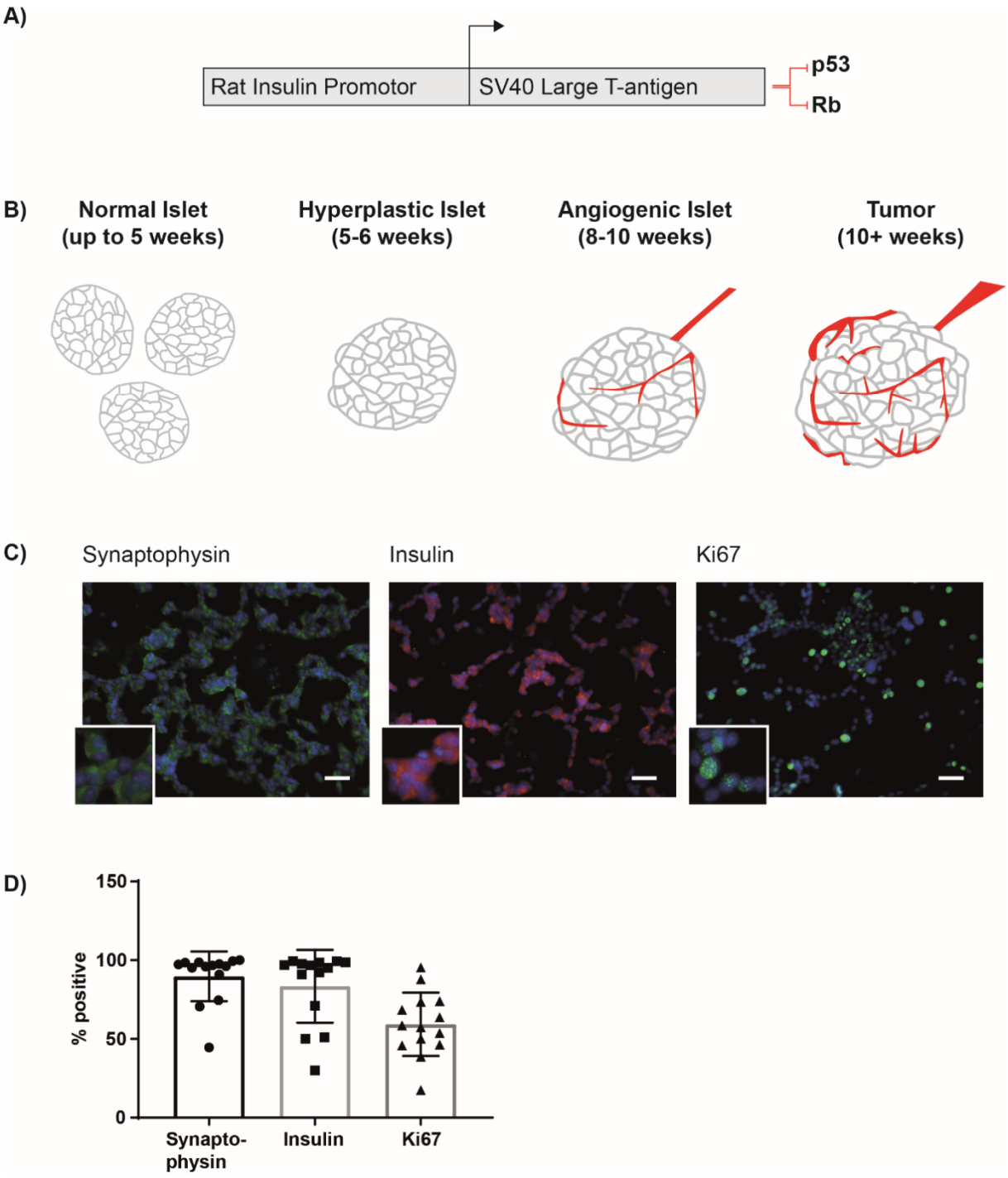

Figure 6: Characterisation of primary β-cell tumour cell cultures

RIP1-Tag2 mice develop β-cell tumours due to expression of the oncogene SV40 Large T-antigen under the Rat Insulin Promotor (A). Islets progress into hyperplasia to vascularized tumour within 10 weeks

(B); modified from [97]. Tumour cells were isolated from 12-week-old mice and tested for β-cell marker expression (synaptophysin, insulin) as well as proliferation (Ki67). C) shows an exemplary immunofluorescent staining of one primary cell culture. Synaptophysin: 96.74 %; Insulin: 97.68 %; KI67: 45.87 %; Scale bar: 50 µm. Isolated β-cell tumour cell culture shows robust marker expression (D). Mean ± SD of 14 cell lines.

4.1.2 Primary β-cell tumour cells are susceptible to senescence induction

Senescence was induced either by treatment of cancer cells with the cytokines IFN-γ and TNF for 96 hours (cytokine induced senescence – CIS), as described previously[37], or by addition of Palbocilib for 96 hours (therapy induced senescence – TIS). To ensure appropriate senescence induction, tumour cell culture was tested for senescence-associated β-Galactosidase (SA-beta Gal) activity and senescence induced growth arrest. Increased SA-beta Gal activity was detected in β-cell tumour cells after senescence induction in comparison to non-senescent cancer cells (Figure 7). While cytokine treatment induced SA-beta Gal activity in primary β-cancer cells, a variable response between primary cell cultures was observed, with some cultures not responding above control level (Figure 7A,C). To ensure quality in senescence response to cytokines cell cultures with at least a 4-fold induction in SA-beta Gal activity were used for further experiments.

In addition to SA-beta Gal activity, proliferation after senescence induction was monitored. To assess cell status directly after induction the recovery rate was calculated. The recovery rate is a calculated readout of the proliferative index in senescence. It describes the cell number after senescence induction, i.e. 1070 cells, divided by the cell number seeded, i.e. 1000 cells, calculating a recovery rate of 1,07 in the exemplary case. After inducing senescence with cytokines for 96 hours the mean recovery rate was 0,86 in contrast to 3,4 in non-senescent tumour cells (Figure 7B). The recovery rate is an indirect measure of cell proliferation. Interestingly, the recovery rate in non-senescent cancer cells spans from 1,17 to 6,76 possibly mirroring the different levels in Ki67 expression in Figure 6D. The dispersion of cells recovered in cytokine induced senescence however, ranges from 0,23 to 2,02. This reveals a differential response to cytokines between primary cell cultures. Thus, not all primary cell cultures seem to respond with thorough growth arrest upon cytokine treatment, indicated by the divergence upwards from 1. Notably, the mean recovery rate after

cytokine treatment is below 1, with the lowest recovery rate measured as 0,23 as mentioned above. Arguably, cytokine treatment induces cell death in a subpopulation of β-tumour cells, likely by sensitization of tumour cells via IFN-γ to TNF-mediated cell death.

Therapy induced senescence using Palbociclib on the other hand initiated a robust SA-beta Gal response (Figure 7D,F) and also showed reduced recovery rates in comparison to control (Figure 7E). Interestingly, as observed in CIS, primary TIS cancer cell cultures show dispersion in total cell number recovered.

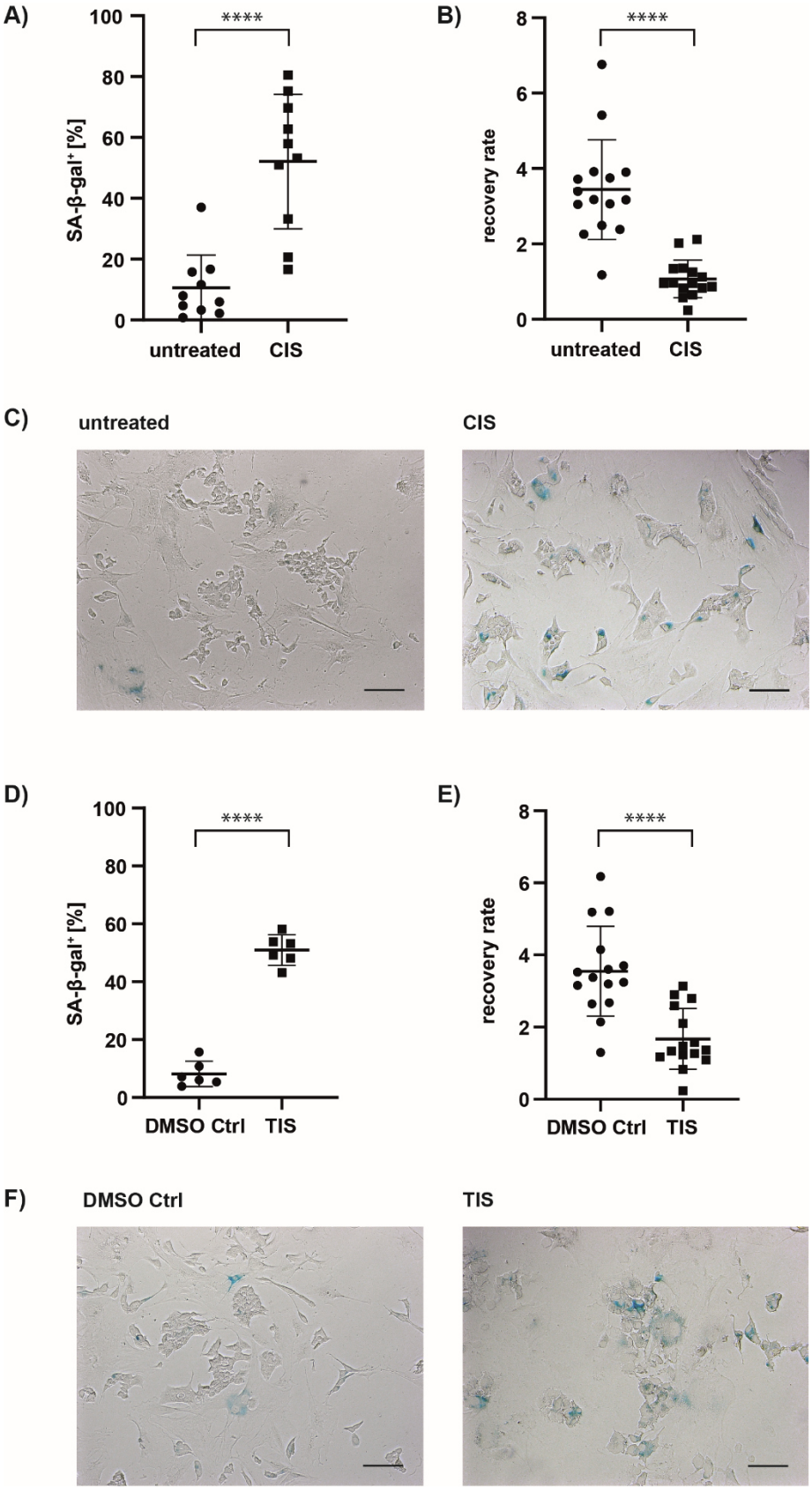

Figure 7: Classification of senescence induction in primary β-cancer cell culture

CIS (A,C) and TIS (D,F) cause SA-beta Gal activity in primary β-cell tumour cell culture. In CIS non-senescent cancer cells showed SA-beta Gal activity in 10.51 % of all cells, cytokine treated cell lines on average in 52.08 % of cells (A). The average recovery rate of untreated cells is 3.44 in comparison to 1.07 in cytokine treated cells (B). Mean ± SD of 15 cell lines. Unpaired t-test, two-tailed, $p < 0.0001$; Scale bar: 100 µm; DMSO control treated cell lines showed SA-beta Gal activity in 9.10 % of all cells, Palbociclib treated cell lines on average in 49.55 % of cells. Mean ± SD of 4 cell lines. (D). E shows the normalized recovery of cells after senescence induction and control. The average recovery rate of DMSO treated cells is 3.55 in comparison to 1.67 % in Palbociclib treated cells. Mean ± SD of 15 cell lines. Unpaired t-test, two-tailed, $p < 0.0001$; Scale bar: 50 µm

To ensure the highest possible stability of senescence upon growth arrest, senescent and non-senescent cancer cells were reseeded, and growth monitored for an additional period of 96 hours (Figure 8). If no proliferation was observed once cytokines were removed the cell culture was defined as responsive to senescence induction.

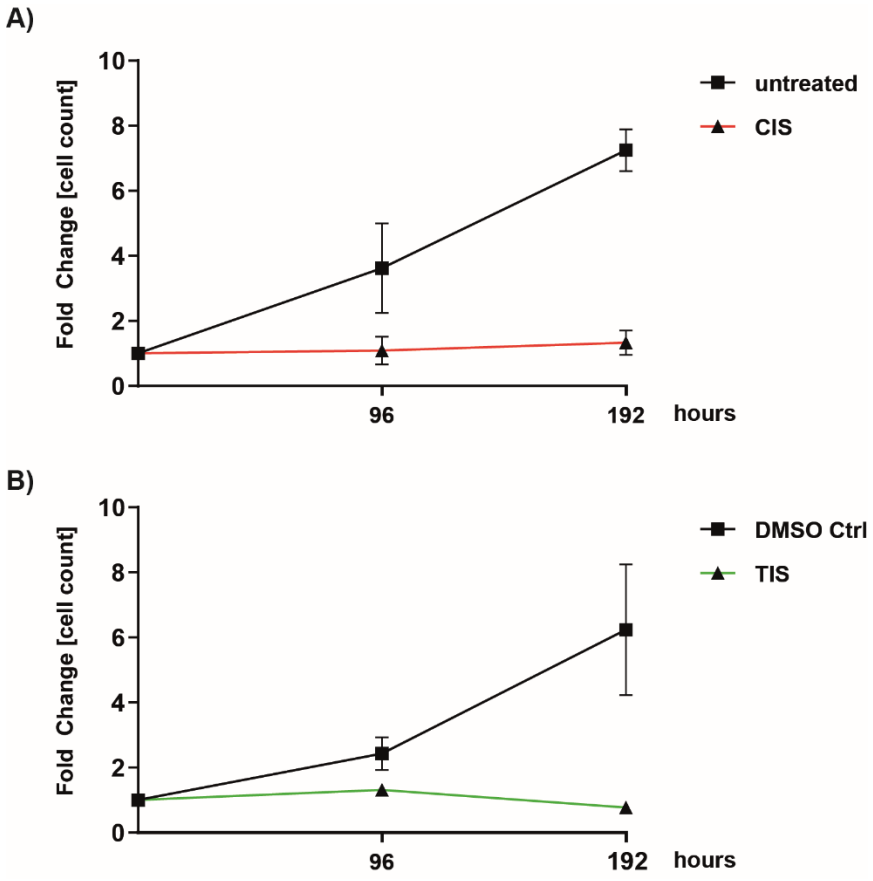

Figure 8: Senescence induces growth arrest in β-cell tumour cells

Exemplary growth arrest of 4 primary cell line per control or treatment condition. After senescence induction for 96 hours, the inductor was removed. Cell numbers did not increase after an additional cultivation period of 96 hours without senescence inductor ((A) CIS – red line; (B) TIS – green line). Control cells proliferated (untreated – black line; 0.1 % DMSO treated – grey line).

Another feature of senescence is the change in secreted factors (i.e., the senescence associated secretory phenotype (SASP)). These secreted proteins consist of inflammatory cytokines and chemokines. Though, no consensus has been reached in

the scientific field on which proteins are specific for the SASP. Examining the change of secreted chemokines revealed an increased secretion of RANTES, SDF-1, IP-10 and MIG in three primary β-cell tumour cell cultures. Interestingly, MCP-1, MIP1α, MIP1β, Eotaxin as well as MDC, KC and 6Ckine are differently secreted. This may be due to possible differences in the underlying senescence response pathways in primary cell cultures in CIS (Figure 9A). Due to their chemotactic nature on immune cells the secreted concentrations of RANTES and CCL2 were determined. RANTES was detected at 0.02 ng/ml on average in the supernatant of proliferating tumour cells in comparison to 2,1 ng/ml in senescent tumour cell supernatant (Figure 9B). The protein levels for secreted CCL2 changed from 5,13 ng/ml in non-senescent tumour cell supernatant to 8,57 ng/ml in SASP (Figure 9C). To certify responsiveness to IFN-γ of primary cell cultures, the chemokines CXCL9 and CXCL10 were measured. Both proteins are normally secreted upon IFN-γ stimulation (Figure 9D,E).

Taken together cytokines can induce a senescence response in primary β-tumour cell culture, characterized by classical markers of senescence, like SA-beta Gal activity, growth arrest and SASP. However, stability varies between isolated primary cultures and requires careful monitoring. Furthermore, primary β-cancer cells are responsive to therapy induced senescence, measured by the markers SA-beta Gal activity and growth arrest.

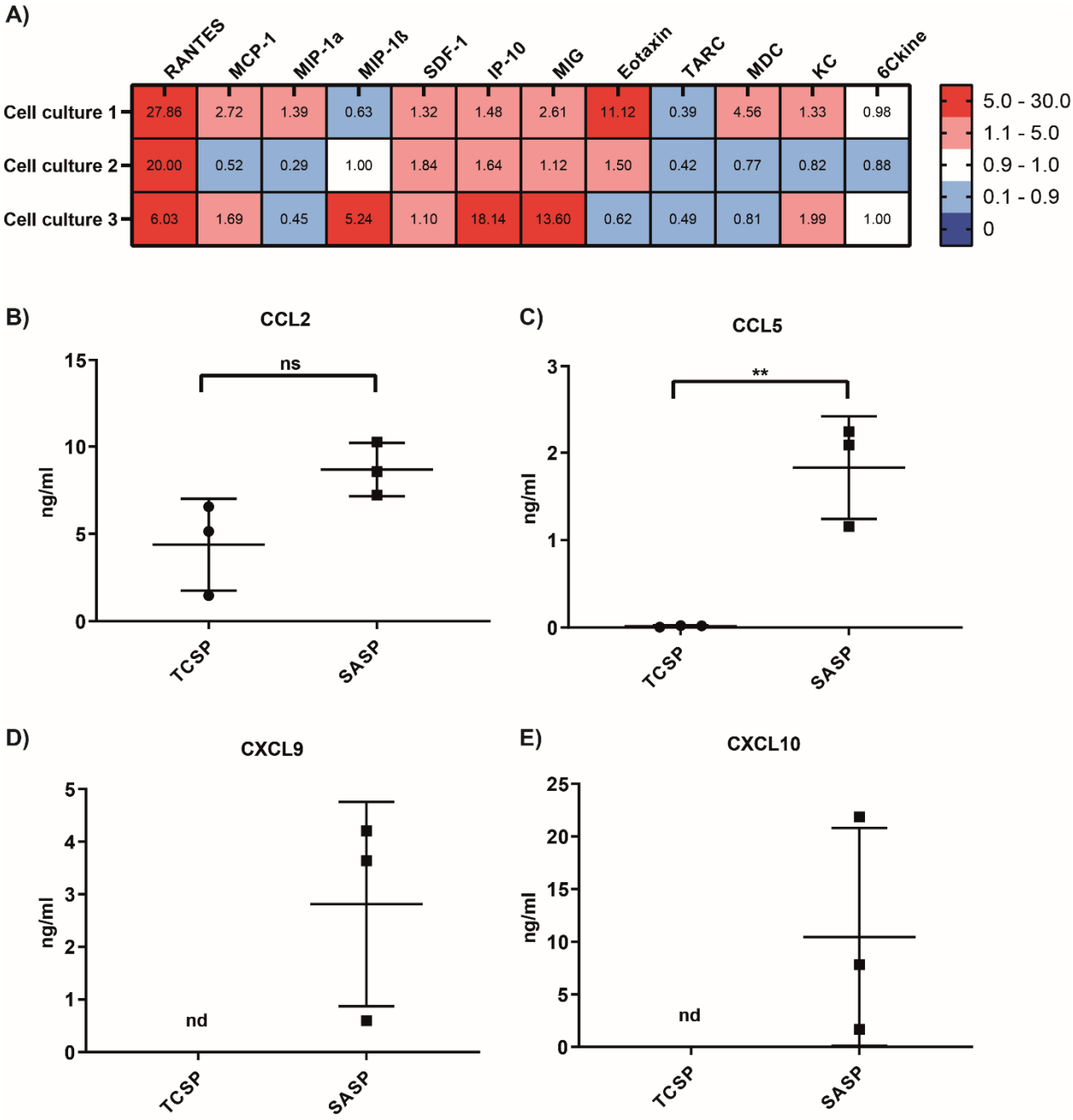

Figure 9: Changes in secretome upon cytokine induced senescence

The secretome of CIS cancer cells differs from the secretome of non-senescent cancer cells (A). B,C) Concentration of chemokines CCL2 (MCP-1) and CCL5 (RANTES) were determined in the supernatant of non-senescent tumour cells (TCSP) and tumour cells after CIS (SASP). The mean detected concentration of CCL2 in TCSP was 5,13 ng/ml in comparison to 8,57 ng/ml in SASP (B). The mean detected concentration of CCL5 was 2,1 ng/ml in SASP in comparison to 0.02 ng/ml in TCSP (C). Unpaired t-test, two tailed CCL5; p=0.0059; Unpaired t-test, two tailed CCL2; p=0.0705; Mean ± SD of 3 cell lines. The concentration of cytokines CXCL9 (MIG) and CXCL10 (IP10) were determined in the supernatant of non-senescent tumour cells (TCSP) and CIS tumour cells (SASP). In TCSP these chemokines were

not detected. The mean detected concentration of CXCL9 in SASP was 2.81 ng/ml (D). The mean detected concentration of CXCL10 was in SASP was 10.46 ng/ml (E). Mean ± SD of 3 cell lines.

4.2 Senescence induces features associated with early apoptosis

Induction of senescence in β-cell tumour cells leads to extensive changes in cell morphology, proliferative capacity, secreted proteins, and SA-beta Gal activity. Therefore, it was hypothesized that additional fundamental changes in various cellular programs are likely to occur. Due to these wide-ranging alterations that are undergone in a relatively short time frame, stress and apoptosis related pathways were investigated.

4.2.1 Membrane based immune modulators in senescence

4.2.1.1 Senescence induces phospholipid asymmetry

The cell membrane separates the interior of cells from the extracellular space and consists of a lipid bilayer with embedded transmembrane proteins. Next to its function as a physical barrier, it is involved in a plethora of physiological processes. The composition of the membrane provides information about the health status of the cell as well as signalling sensitivity towards extracellular stimuli, for instance by regulation of receptor presentation. Upon induction of senescence tumour cell size increases, thereby conceivably inducing changes in outer membrane composition. Such changes in the outer membrane composition can be determined by biochemical assays or by investigating cellular components by FACS. Annexins are a family of membrane binding proteins, able to reversibly bind to negatively charged phospholipids, predominately phosphatidylserine (PS), in the presence of Ca^{2+} [99]. As PS is externalized during apoptosis[100], AnnexinV binding to PS became a widely used assay for detection of apoptotic cells. However, while annexins primarily reside in the cytosol, the protein has been found on the cell surface as well as plasma[101,102], suggesting a release in extracellular space and other physiological functions next to its association with apoptotic cells. Plausibly, living cells have been found to express PS on the cell surface independent of cell death. This has been proven in physiological conditions

during monocyte differentiation[103] or T-cell function[104], as well as myotube formation[105]. Additionally, reports of PS externalization have been found in tumour vasculature[106] and cancer cells[107,108]. Therefore, the differences in PS exposure between non-senescent and senescent β-cell tumour cell culture were investigated (Figure 10).

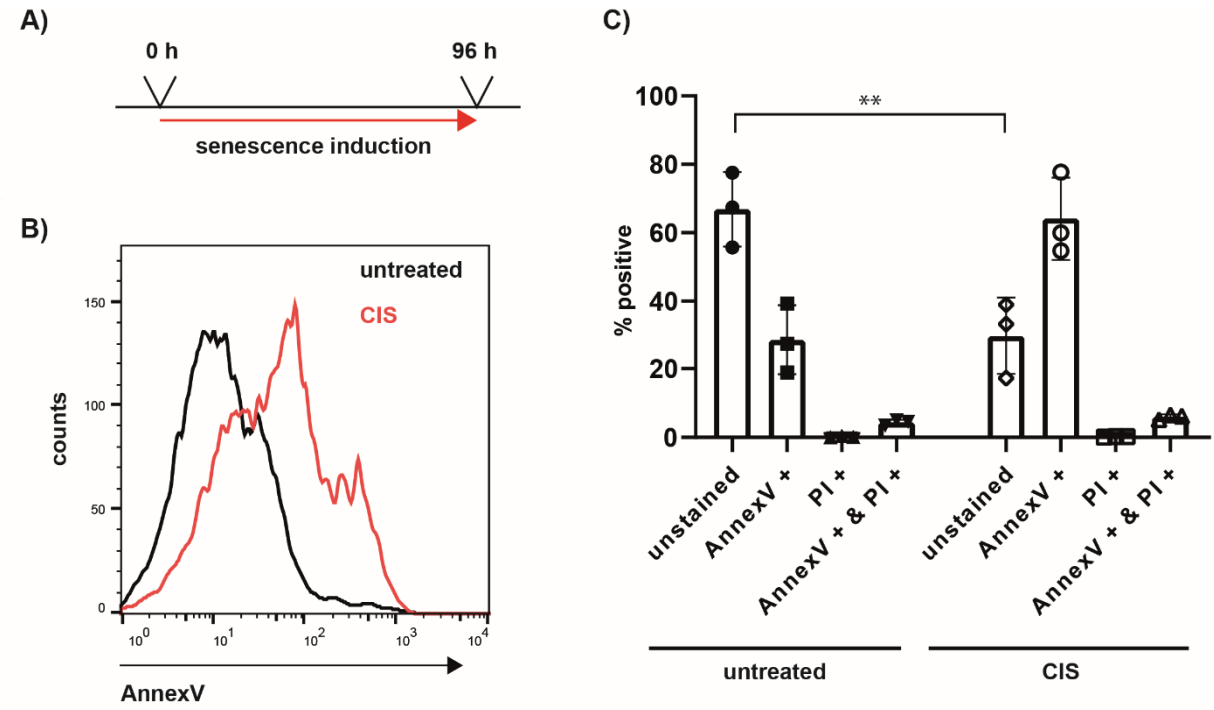

Figure 10: Alterations in negatively charged phospholipids on senescent cells

FACS analysis of untreated β-cell cancer cells and cytokine treated β-cell cancer cells (CIS). Cells were subjected to senescence inducers for 96 hours, washed and cultivated for an additional 48 hours. Unstained cell population is decreased in CIS to 29.79 % in comparison to 66.87 % in control condition. Exemplary histogram showing AnnexV positive population after CIS and in control conditions. Two-way ANOVA; p= 0.0018; Mean ± SD of 3 cell lines.

Intriguingly, senescent β-cell cancer cells show increased binding of AnnexinV on PI negative cells in comparison to untreated β-cell cancer cells (Figure 10A) 48 hours after senescence induction. The percentage of viable AnnexinV positive cells increased from 28,6 ± 10,2 % in non- senescent cells to 64,1 ± 12,0 % in cells after CIS, without significant changes in PI positive (untreated: 0.20 %; CIS: 0.15 %) and AnnexinV & PI (untreated: 4.43 %; CIS: 5.96 %) double positive population.

Interestingly, the PS externalisation persists once cytokines are removed raising the questioning whether its exposure is due to changes associated with apoptosis or of non-apoptotic function.

4.2.1.2 "Don't-find me" protein CD47 is downregulated in senescence

Due to the observation of increased PS levels on the surface of the plasma membrane Cluster of Differentiation 47 (CD47), an immune-evasion protein expressed in all cell types, was investigated. CD47 functions as an inhibitor of phagocytosis through ligation with SIRP1α on phagocytes[109]. Senescent β-cell cancer cells showed reduced protein levels of CD47 in comparison to untreated β-cell cancer cells. Nevertheless, the cluster was detectable on non-senescent and senescent cancer cells (Figure 11). However, CD47 clustering is necessary for phagocyte evasion[94]. To investigate if downregulation of CD47 is of functional relevance in cytokine induced senescence dispersion or clustering of the protein should be investigated.

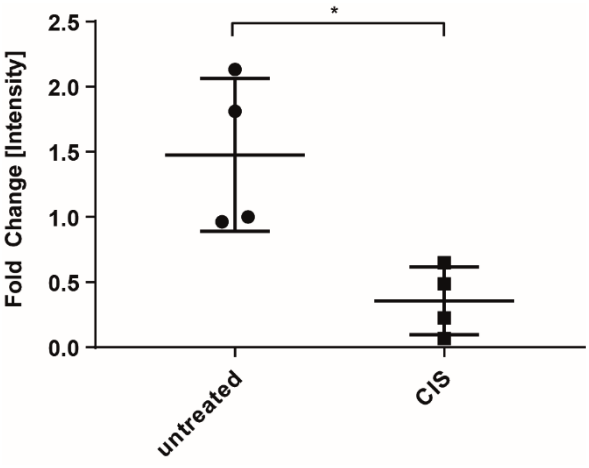

Figure 11: Protein levels of immune-evasion CD47 are downregulated in CIS

β-cell cancer cells were treated with senescence inducing cytokines for 96 hours or left untreated before protein was extracted. Western Blot and immunostaining were performed and CD47 levels set in relation to β-actin before the fold change was calculated. Mean untreated: 1.48, Mean CIS: 0.36; Unpaired t-test, two-tailed, p= 0.0130; Mean ± SD of 4 cell lines.

Interestingly, induction of senescence changed presentation of PS (Figure 10) and CD47 (Figure 11) on the cell surface. PS exposure, on one hand, needed for phagocytic recognition and cancer cell clearance is increasingly presented on senescent cancer cells. Furthermore, CD47, an immune-evasion protein is downregulated in

senescence, arguably indicating increased immune monitoring of senescent cancer cells.

4.2.2 Mitochondrial status is altered in senescent cancer cells

Observing the changes undergone in senescence on the cell surface, the question arose if internal, stress-related deviations occur. Changes in membrane composition and phosphatidylserine presentation are known to arise during apoptosis as well as changes in intracellular calcium levels. Mitochondria play a key role in apoptotic signalling and are vital to regulation of changes in intracellular calcium homeostasis. Therefore, changes in mitochondrial status and health were investigated.

4.2.2.1 Mitochondrial membrane potential depolarization occurs in senescence

For proper mitochondrial function, maintenance of the mitochondrial membrane potential (ΔΨm) is crucial. Preserving ΔΨm is critical in generating an electrochemical gradient potential by serial reduction of electrons through the respiratory chain. This provides the energy to transport protons against their concentration gradient out of the mitochondrial cytoplasm. By gradient dependent reflow of the protons back into the mitochondrial cytoplasm via F1/F0 ATP-synthase, ATP is generated[110]. Therefore, ΔΨm is an important indicator of cellular health, correlating to the cells capacity to generate ATP.

While ΔΨm fluctuates and changes upon cellular function, strong deviations indicate compromised cellular health. The cationic carbocyanide dye JC-1 accumulates in energized mitochondria and forms “red”-fluorescent (emission at 590 nm) aggregates at high concentrations. At low dye concentrations, as a monomer, it emits “green” fluorescence at 530 nm. Thus, a decrease in red aggregates indicates ΔΨm depolarization (less dye accumulation) in mitochondria. In non-senescent cancer cells, the dye accumulated in mitochondria and formed red aggregates. In cytokine-induced senescent cells, however, less accumulation was observed indicating depolarized mitochondria. In TIS depolarization of mitochondria was observed albeit to a weaker extend than in CIS (Figure 12).

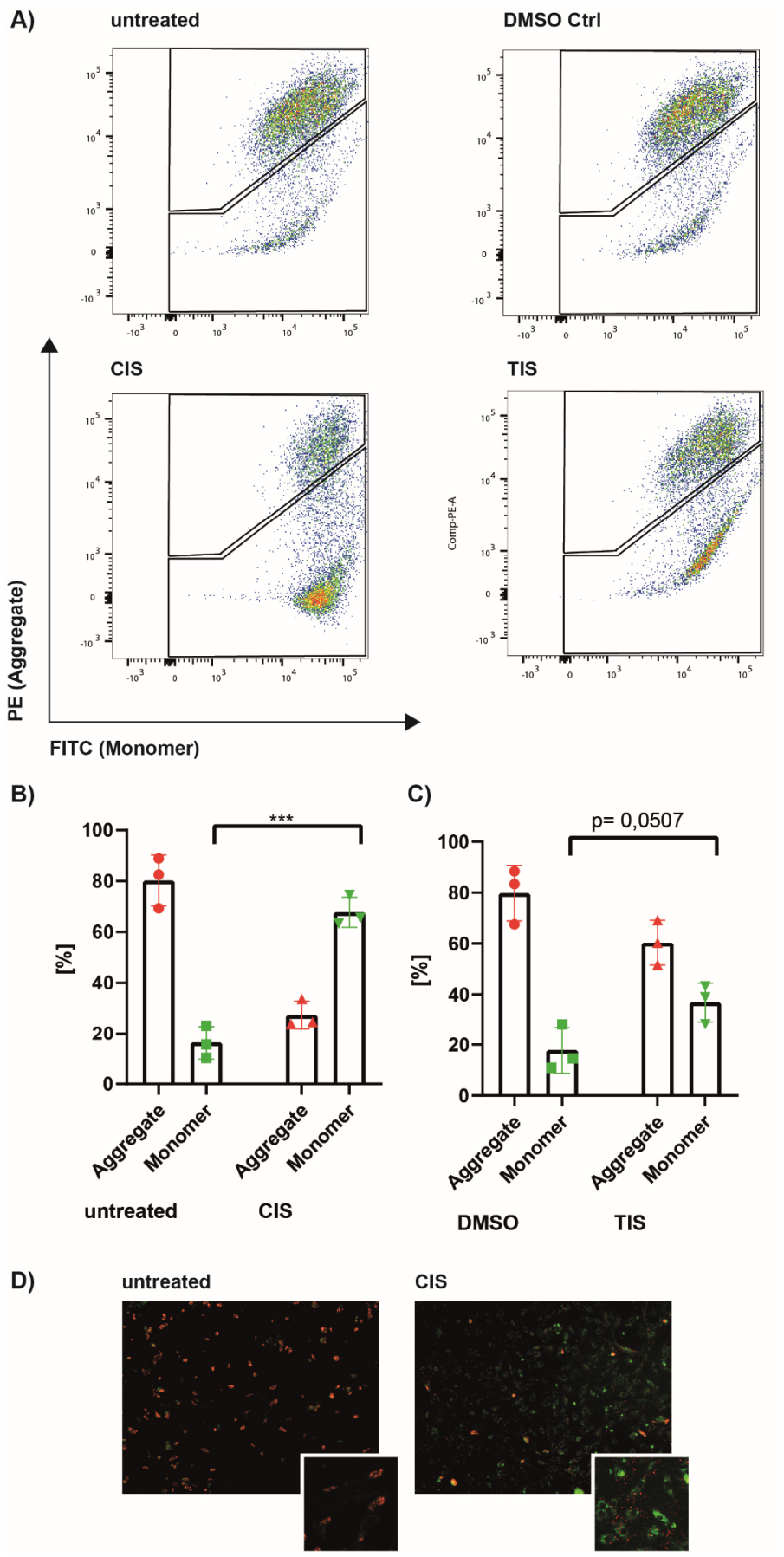
A)
untreated
DMSO Ctrl
CIS
TIS
PE (Aggregate)
FITC (Monomer)
Comp-PE-A
B)
***
[%]
Aggregate
Monomer
Aggregate
Monomer
untreated
CIS
C)
p= 0,0507
[%]
Aggregate
Monomer
Aggregate
Monomer
DMSO
TIS
D)
untreated
CIS

Figure 12: Mitochondrial membrane potential is reduced upon senescence induction

A) shows a scatterplot of exemplary FACS of one of the primary cell culture analysed in B). Non-senescent cells are displayed in the upper panel, senescent cells in the lower panel. Control treated cells show high numbers of JC-1 aggregates that are decreased in senescent cells (B). Unpaired t-test, two-tailed, p=0.0005; Mean ± SD of 3 cell lines. Microscopy image of untreated and cytokine treated cancer cells. Higher numbers of red aggregates are seen in non-senescent cancer cells than in cancer cells after CIS (C).

4.2.2.2 Mitochondrial mass is not distinctively regulated in senescence

Notably, the accumulation of JC-1 is independent of mitochondrial size, shape, or density. As depicted in Figure 12 senescent cancer cells show fewer JC-1 aggregates indicating depolarization of mitochondrial membrane potential. Since depolarized mitochondria lack function, they might be cleared from the cell – a process known as mitophagy. The fluorescent probe Mitotracker stains mitochondria independent of ΔΨm and has been used to indirectly asses mitophagy[111,112]. However, it must be noted that the Mitotracker Dye stain is a measure of mitochondrial mass, as it cannot distinguish between increased numbers or increased size (mitochondrial swelling) of mitochondria. Due to variation in fluorescence intensity in a subset of primary cell lines, data were normalized to untreated tumour cells, therefore set to the value 1. In contrast to untreated tumour cells, CIS cancer cells show a mean normalized fluorescence intensity of 1.11, in comparison to 0.94 of DMSO control cells and 0.76 in TIS (Figure 13). Overall mitochondrial mass is not regulated after senescence induction in a similar manner.

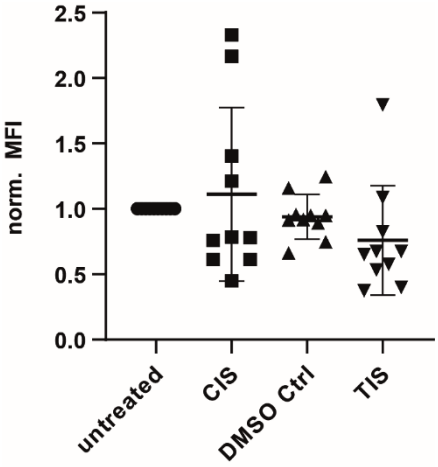

Figure 13: Regulation of mitochondrial mass in senescence

After senescence induction for 96 hours, cells were harvested and stained with Mitotracker-Green. CIS & TIS cancer cells show a differential staining for mitochondrial mass. Data were normalized to media control, due to high differences in dye staining intensity. Mean ± SD of 10 cell lines.

4.2.2.3 Mitochondrial permeability transition pore regulation in senescence

No uniform changes in mitochondrial mass were observed, possibly indicating a replenishment of healthy mitochondria allowing normal function. Instead, the depolarized mitochondrial membrane potential in senescence is likely of physiological relevance in senescent cancer cells. Healthy mitochondrial function depends on controlled ΔΨm, for example initiation of the mitochondrial permeability transition pore (mPTP). The mPTP is a nonspecific channel of the mitochondrial membrane, permeable to molecules of less than 1500 Dalton in size. While mPTP flickering is normal in healthy cells, continuous opening of mPTP induces ΔΨm depolarization[113,114]. Therefore, changes in mitochondrial transition pore formation were investigated.

To investigate mPTP formation senescent and non-senescent cells were loaded with a fluorophore that permeates the cell and mitochondria. Subsequent application of a quencher diminishes the cytosolic fluorescent allowing for time dependent measurement of remaining mitochondrial fluorescence with quencher permeating into mitochondria through the mPTP. Diminished fluorescent signal therefore indicates an increased flickering or prolonged opening of the mPTP.

Interestingly, in CIS and TIS mean fluorescent intensity is lower than in control groups, suggesting differences in mPTP function. The MFI in untreated control cells averages at 2355, while it is lowered to 1195 in CIS. After induction of TIS the MFI is 1710 in comparison to DMSO Control at 2350 (Figure 14).

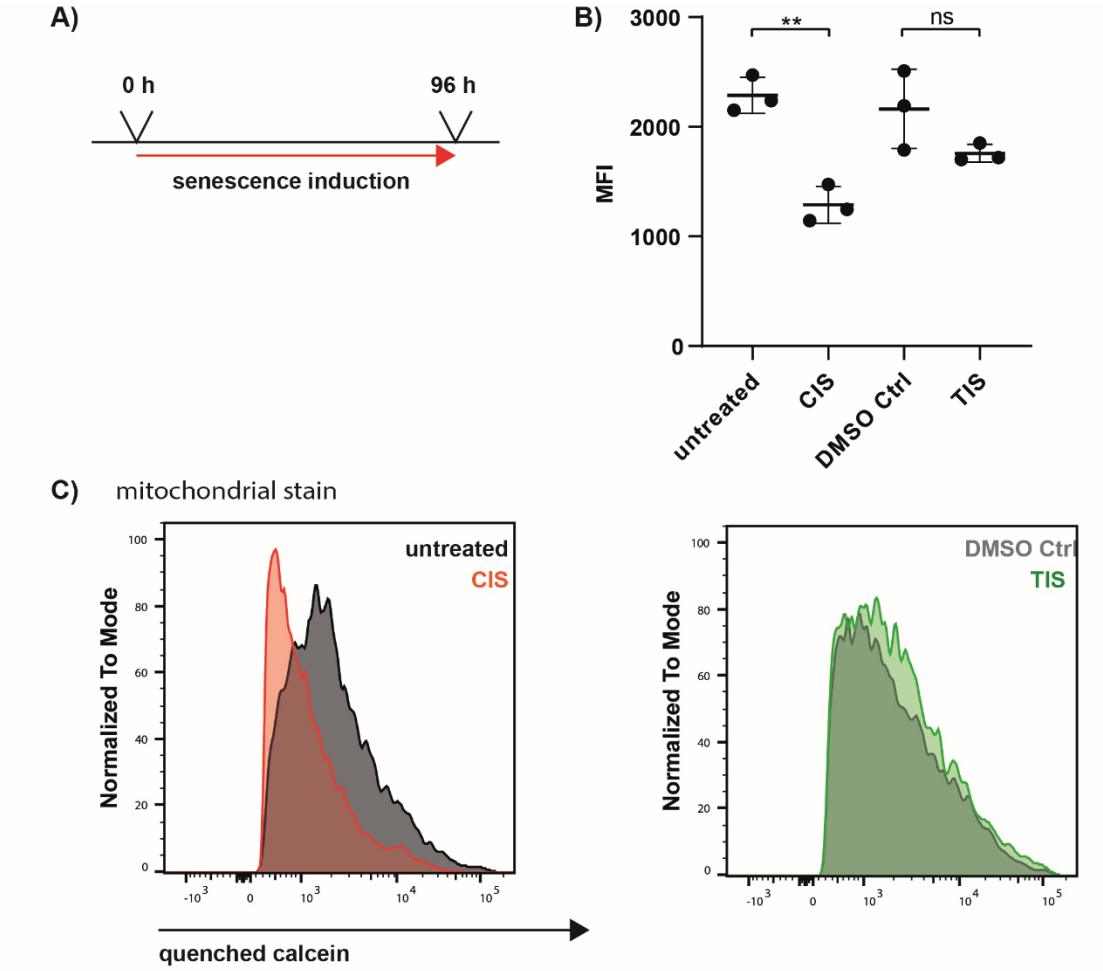

Figure 14: Upon senescence induction mitochondrial pore flickering increases

β-cell cancer cells were treated with IFN-γ and TNF for 96 hours before loading with fluorophore (A). Reduced MFI indicates increased or prolonged flickering of the mitochondrial transition pore. CIS and TIS show increased flickering of the mPTP (B). Unpaired t-test, two-tailed, p= 0.0130 p= 0,0018, ns p= 0,1310; Mean ± SD of 3 cell lines.

In sum, mitochondrial function and status are impaired upon senescence induction. Interestingly, depolarized mitochondria (Figure 12) are more prevalent in senescent cells additionally to dysregulation of mitochondrial permeability transition pore formation (Figure 14). At this point of investigation, however, no definite answer can be given to the question which event causes the other. Precisely, whether the opening of the mPTP causes the depolarization of the mitochondrial membrane or is due to the depolarization of ΔΨm. Cause and effect could be separated by inhibition of pore opening, also shedding light on the influence of these physiological changes in senescence induction itself. While independency of pore opening and depolarized

membrane potential are unlikely, the depolarization could also be explained by deficiencies in the respiratory chain complexes or deficiencies in mitophagy in senescent cells and therefore accumulation of uncleared, defective mitochondria.

4.2.3 Pro- and anti-apoptotic changes in senescence

The decreased mitochondrial membrane potential in senescent β-cell cancer cells, as well as the increase in opening of the mitochondrial permeability transition pore suggests a change in proteins released from mitochondria. mPTP opening is necessary for cytochrome c release from mitochondria into the cytosol - an early feature of apoptosis. The release of cytochrome c subsequently activates caspases possibly initiating programmed cell death. Measuring cytochrome c levels revealed a decrease in CIS (mean MFI: 20165) to DMSO control (mean MFI: 41805). Interestingly, TIS did not alter cytochrome c levels in β-cell cancer cells (mean MFI: 43681) (Figure 15).

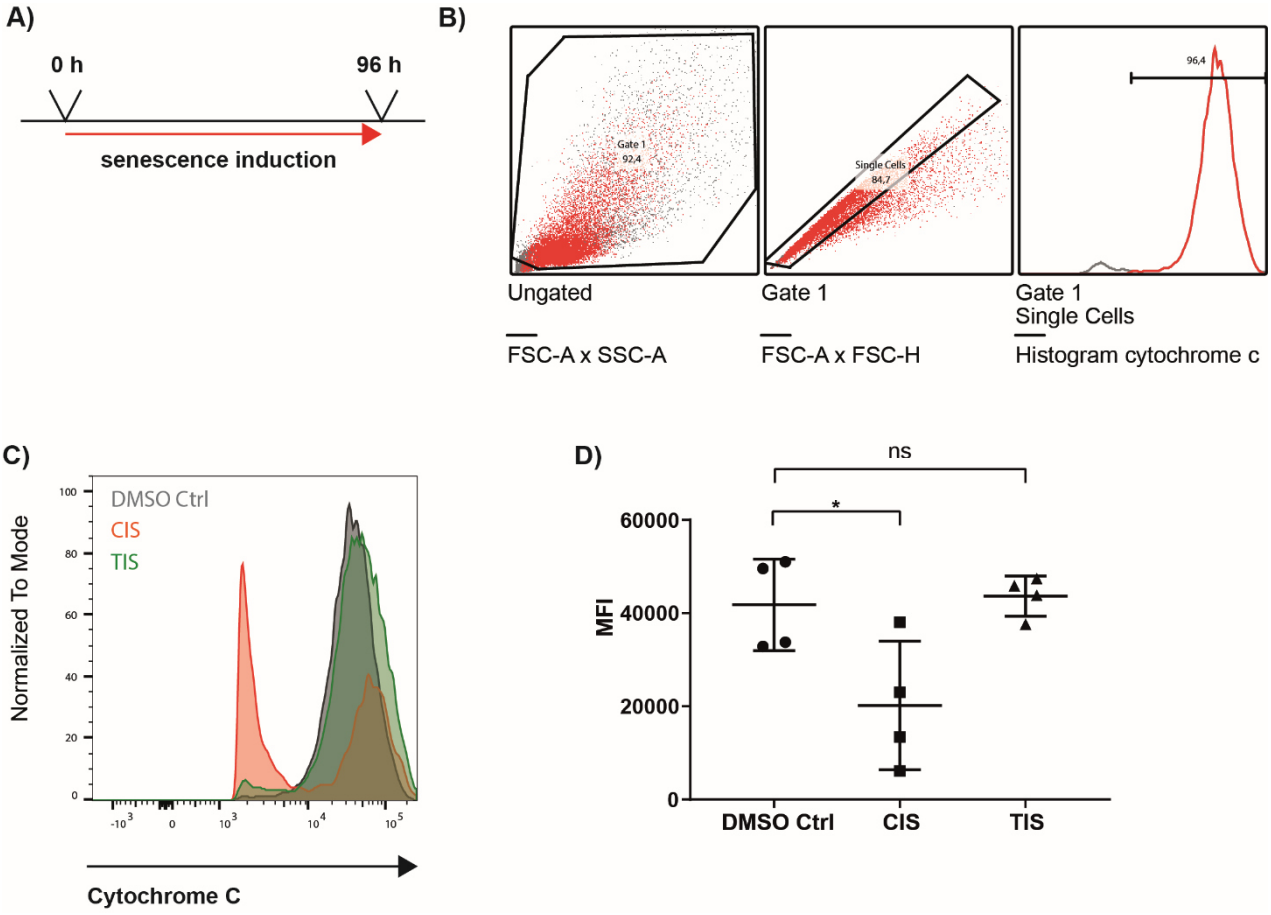

Figure 15: Cytochrome c is released after CIS, but retained after TIS

After senescence induction (A) cytochrome c levels were investigated using FACS. TIS cancer cells did not differ from DMSO treated control cells. After CIS a reduction of cytochrome c levels was observed (C,D). One-way ANOVA, p=0.0344; Mean ± SD of 3 cell lines.

Cytochrome c release into the cytoplasm triggers apoptosome formation and downstream activation of effector caspase 3. To assess whether this signalling pathways is active, caspase 3 levels were determined. Coherently, immunofluorescent staining for active caspase 3 revealed an increase from 2.36 % positive cells in non-senescent cancer cells to 8.54 % in CIS cancer cells (Figure 16). Interestingly, activation of caspase 3 as an effect of cytochrome c release happens in primary cell lines to varying extend, underlining the differences in primary cell culture as well as suggesting the existence of regulatory coping mechanisms. It further shows that caspase 3 can be activated in senescent tumour cells despite the proposed resistance of senescent cells to apoptotic cell death.

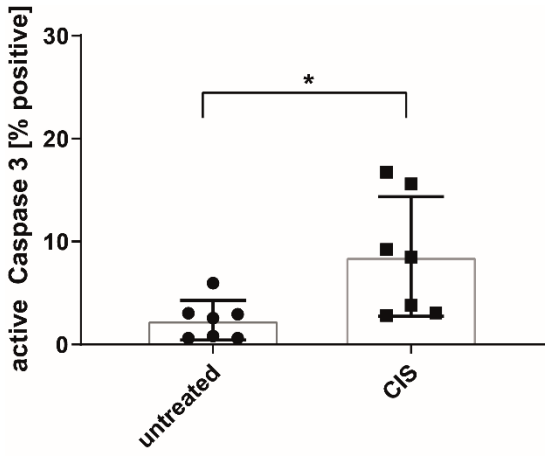

Figure 16: Caspase 3 activity following CIS

Mean cell number of cells positive for active caspase 3 in CIS is 8.54 % in comparison to 2.36 % in control cells. Immunofluorescent staining for active caspase 3 after 96 hours of cytokine treatment or control treatment. Unpaired t-test, two-tailed, p= 0.0205; Mean ± SD of 7 cell lines.

While cells accumulate features associated with early apoptosis as well as activation of effector caspase 3, the cell population surviving senescence induction remains viable for at least an additional 96 hours, suggesting changes in the expression of survival factors in response to CIS. The Bcl-2 protein family includes proteins acting in a pro-apoptotic as well as in an anti-apoptotic manner. Bcl-2 itself is an anti-apoptotic protein localized at the outer mitochondrial membrane inhibiting pro-apoptotic Bcl-2 protein family members, like Bax or Bak[115]. Bcl-2 protein levels were measured using FACS analysis after senescence induction for 96 hours. Following CIS (mean MFI: 1221) as well as TIS (mean MFI: 1071) higher Bcl-2 protein levels were detected than in control group (mean MFI untreated: 814.8; mean MFI DMSO Ctrl: 813.3), indicating a dependency of senescent cancer cell survival on Bcl-2 (Figure 17).

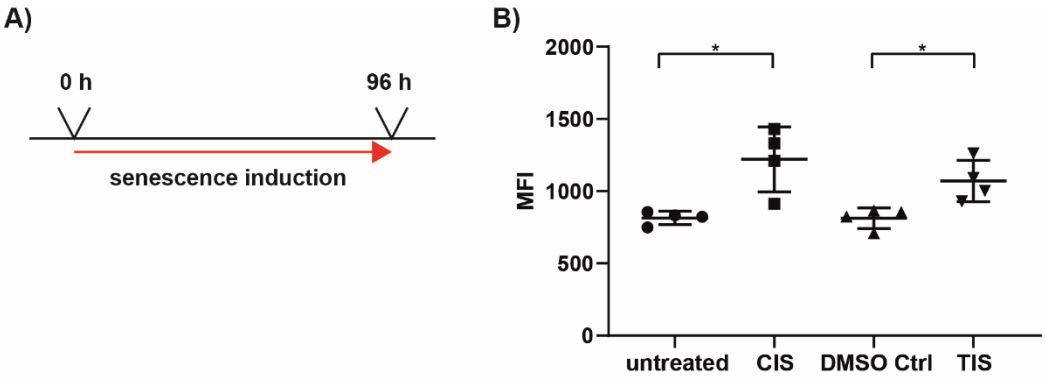

Figure 17: Bcl-2 levels in senescence

Anti-apoptotic protein Bcl-2 is upregulated upon senescence induction in CIS and TIS in comparison to controls (B). FACS analysis for Bcl-2 after 96 hours of cytokine treatment, treatment with palbociclib or control treatment. Unpaired t-test, two-tailed; untreated vs. CIS p=0.0122, DMSO Ctrl vs. TIS p=0.0227; Mean ± SD of 4 cell lines.

By binding to Bax or Bad, Bcl-2 negatively regulates the opening of the mitochondrial permeability transition pore, inhibiting the opening of the pore and reducing cytochrome c release. It must be kept in mind that the assays performed here provide an overview of the cellular state at one specific time point. The situation at this time point suggests an imbalance in apoptotic and survival signalling. On the one hand mitochondrial membrane is depolarized (Figure 12) following senescence induction in accordance with opening of the mitochondrial permeability transition pore (Figure 14) and cytochrome c release (Figure 15). On the other hand, cells that survive senescence induction remain viable. The upregulation of Bcl-2 (Figure 17) may be a way to counteract cell death by the tumour cell, specifically by trying to reduce mitochondrial membrane permeability. These findings suggest a sensitive balance between pro-apoptotic and pro-survival signals.

4.3 CIS renders cells susceptible to TRAIL mediated clearance

The changes undergone in senescence induction thus pose the possibility to be exploited for specific clearance of senescent cancer cells. As shown in Figure 17 senescent β-cell tumour cells have higher protein levels of Bcl-2. To test the dependency of senescent cancer cells on Bcl-2 for survival, senescent and non-senescent cancer cells were incubated with ABT263, a pan-Bcl-2 inhibitor (Figure 18).

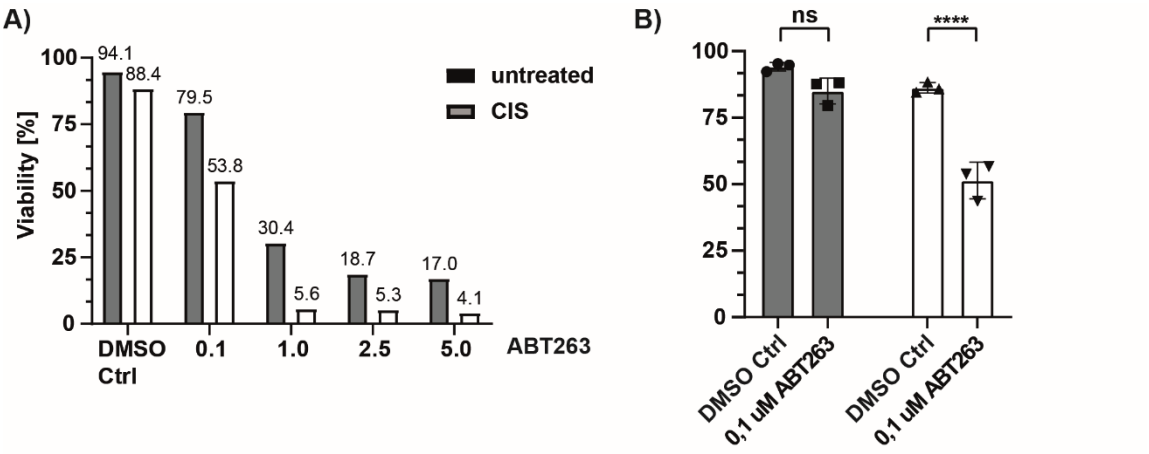

Figure 18: CIS renders cells vulnerable towards ABT263

Titration of ABT263 in one primary cell line (A). Senescent cells, following CIS and non-senescent cells were treated with varying concentrations of ABT264 for 48 hours and viability measured by trypan blue exclusion assay. B) shows a response titration of 3 primary cell lines to ABT263 treatment as in A). Ordinary one-way ANOVA, $p<0.0001$, Mean ± SD of 3 cell lines.

Senescent and non-senescent cancer cells respond to ABT263 in a dose dependent manner, albeit a stronger response is observed in cytokine induced senescent cancer cells (Figure 18A). Treatment of cancer cells with ABT263 decreased total number of viable senescent cancer cells to 51.33 % in comparison to 85.07 % viability in non-senescent cancer cells (Figure 18B). This strengthens the hypothesis of Bcl-2 dependency for senescent cancer cell survival.

Due to the physiological nature of cytokine induced senescence the natural protein TNF related apoptosis inducing ligand (TRAIL) was tested for efficacy in apoptosis induction. Senescent β-cell tumour cells showed increased caspase 3 activation under treatment with TRAIL in comparison to non-senescent cancer cells, in a dose and time dependent manner (Figure 19).

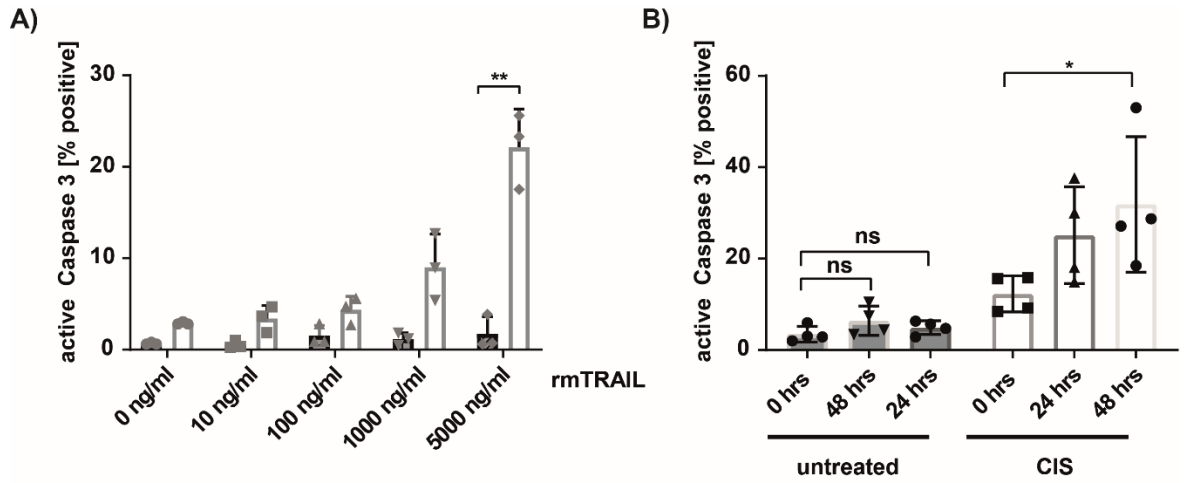

Figure 19: TRAIL treatment activates caspase 3 following CIS

Cancer cells after CIS (white bars) and untreated cancer cells (grey bars) were subjected to TRAIL treatment in varying concentrations for 24 hours. Active caspase 3 positive cells were determined (A). Unpaired t-test, two-tailed, ** p =0.0015; Mean ± SD of 3 cell lines. In B) senescent (CIS) and untreated cancer cells were subjected to TRAIL treatment [5 µg/ml] for 24 and 48 hours. Active caspase 3 positive cells were determined. Unpaired t-test, two-tailed, * p= 0.0215; Mean ± SD of 4 cell lines.

TRAIL is expressed in immune cells like macrophages and NK cells to mediate effective immune response and tissue homeostasis[116]. As TRAIL has proven to be effective in apoptosis induction predominantly in senescent cells, the efficacy of nitric oxide, another molecule released by classically activated macrophages after a type I immune response was investigated[117]. CIS and non-senescent cancer cells were treated with TRAIL, NO-Donor (NOC-18), combinatorial treatment of TRAIL and NOC-18, ABT263 or staurosporine. Non-senescent cancer cells showed no reduced viability to death inducers, except for broad-kinase inhibitor staurosporine. Senescent cancer cells, however, showed similar levels of reduced viability after TRAIL or pan-Bcl-2 inhibitor ABT263 treatment. Senescent cancer cells were responsive to NO-Donor, however viability varied between different primary cell lines. Combinatorial treatment of senescent cancer cells with TRAIL and NO-Donor had no synergistic effect in comparison to single treatment (Figure 20).

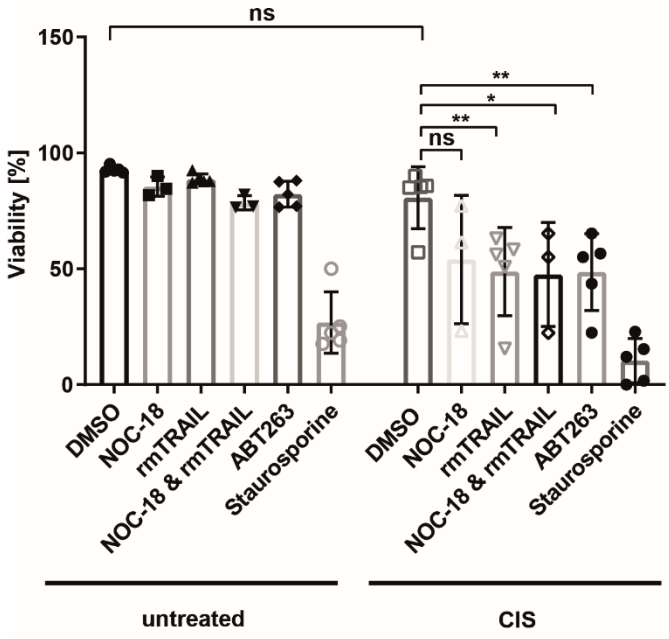

Figure 20: TRAIL induces cell death predominantly in tumour cells following CIS

Cell viability was assessed using Trypan Blue Exclusion Assay. CIS was induced for 96 hours before compound addition. Afterwards cells were incubated with NOC-18 [250 µM], TRAIL [5ug/ml], a combination of NOC-18 and TRAIL, ABT263 [0.1 µM] and staurosporine [0.1 µM] 48 hours. Ordinary one-way ANOVA, DMSO vs. rmTRAIL p=0.0047, DMSO vs. NOC-18&rmTRAIL p=0.0134, DMSO vs. ABT263 p=0.0044; Mean ± SD of 3 cell lines (NOC-18 & combination treatment with TRAIL), Mean ± SD of 5 cell lines (remaining treatments).

TRAIL, as a natural ligand, was able to reduce viability in senescent cancer cells to a similar extend as the designed compound ABT263, proving its effectiveness as a senolytic agent in β-cell tumour cells. This may be an explanation for senescent cancer clearance observed in occurrence with type I immune responses[42,86]. Further, CIS in mouse β-cell tumour cells is a prerequisite for regaining sensitivity to TRAIL induced apoptosis.

Interestingly, TRAIL seems to induce cell death in CIS via the mitochondrial pathway showed by loss of cytochrome c positive cells after TRAIL treatment (Figure 21C). Untreated β-cell-cancer cells showed slight increase of cytochrome c negative population. Following CIS, the cytochrome c negative population increased from 8,91% to 34,8 % after 48 hours of treatment with TRAIL.

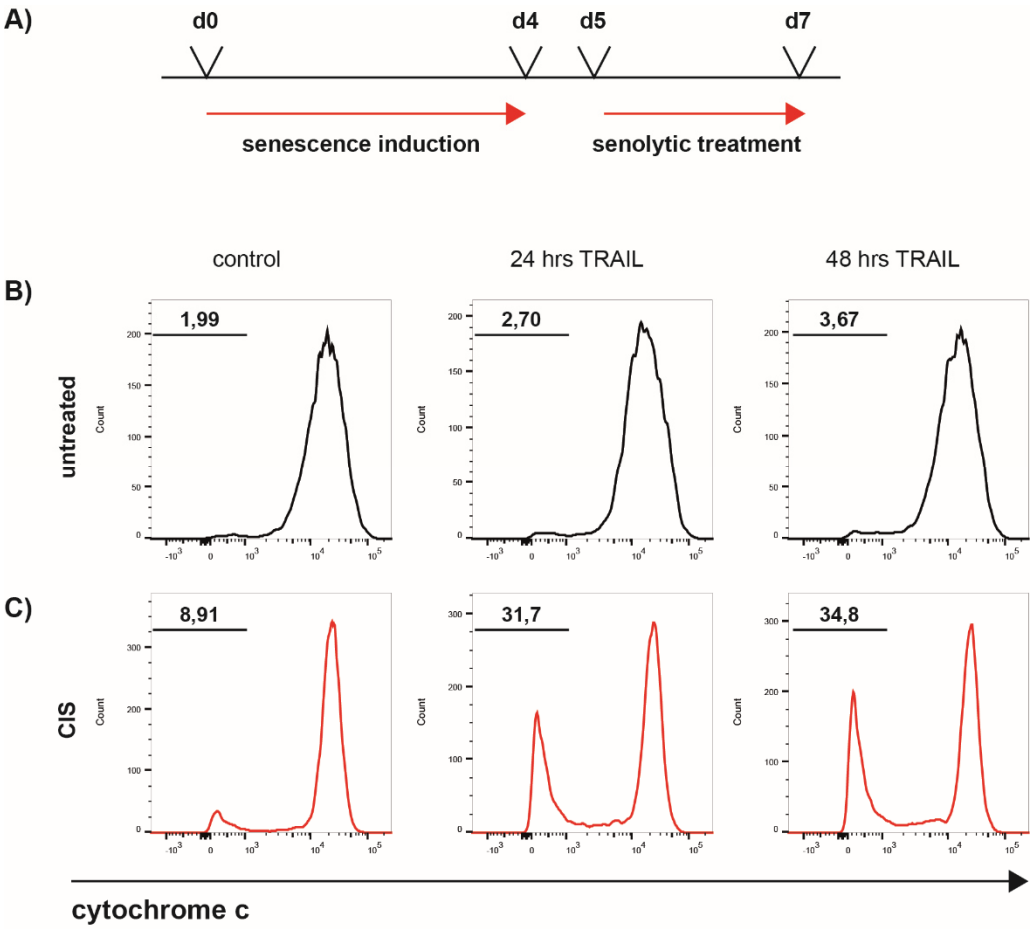

Figure 21: TRAIL induced cell death initiates cytochrome c release following CIS

TRAIL induces cell death preferentially in senescent cells. Here, cytochrome c staining of one exemplary cell line under TRAIL treatment is shown (A). TRAIL induces strong release of cytochrome c in cytokine induced senescence cells (C) in comparison to untreated cancer cells (B).

While all senescent primary cell cultures were responsive to TRAIL induced apoptosis, the amount of death induction varied. Therefore, receptor expression of Death Receptor 5 (DR5) and decoy TRAIL Receptor 1 (dcTRAIL R1) was analysed. Cell lines differed in DR5 expression under non-senescent conditions and showed no significant or uniform trend after senescence induction with IFN-γ and TNF (Figure 22A) The decoy receptor of TRAIL, however, without intracellular signalling capacity, was upregulated in cytokine induced senescence (Figure 22B).

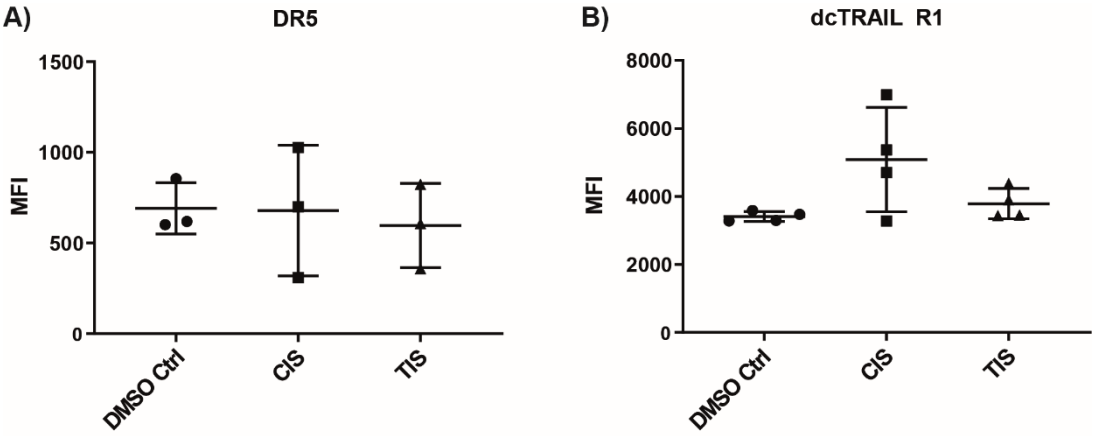

Figure 22: TRAIL receptor expression in senescence

FACS analysis of Death Receptor 5 after senescence induction (A). While the receptor is detectable in control treatment and senescence, no consistent regulation takes place in senescence. Analysis of the decoy Receptor of TRAIL shows no regulation after TIS in comparison to control but an increase after CIS (B) Mean ± SD of 3 cell lines for DR5 and 4 cell lines for dcTRAIL R1.

While the decoy receptor of TRAIL is upregulated, cell death can still be induced in senescent cancer cells with recombinant protein. The upregulation of dcTRAIL R1 without increased expression of DR5 may explain the relatively high amount of TRAIL needed to induce senolysis.

4.4 Cell death induction is necessary for immune mediated clearance of tumour cells

Senescent cancer cells accumulate stress factors and features associated with early apoptotic events yet manage to remain viable with a minority succumbing to cell death. To investigate whether the change undergone in senescence are sufficient to initiate clearance of senescent tumour cells by immune cells, senescent and non-senescent tumour cells were incubated with naïve primary bone-marrow derived macrophages. Naïve macrophages were able to phagocytose tumour cells; however, there was no significant difference in phagocytosis efficiency of macrophage if co-incubated with senescent or non-senescent tumour cells (Figure 23). Therefore, it was concluded that the changes undergone in senescence induction, like the increased exposure of

phosphatidylserine, are not enough to initiate clearance of senescent cancer cells by naïve macrophages.

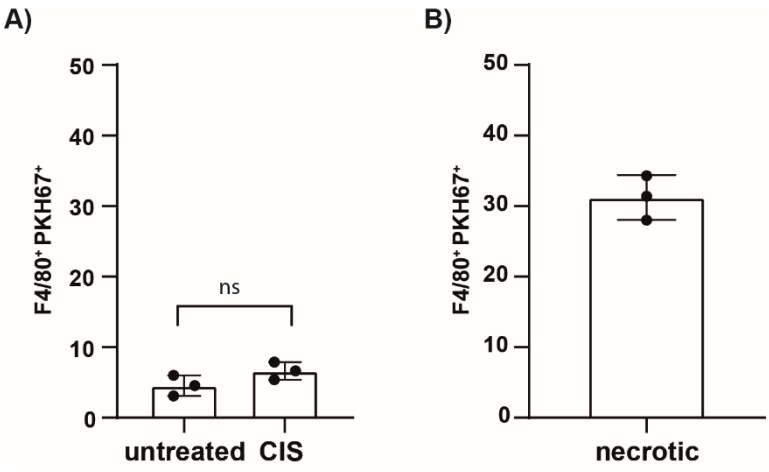

Figure 23: Uptake of senescent and non-senescent tumour cells by macrophages

Co-incubation assay of senescent and non-senescent cancer cells with naïve bone marrow derived macrophages. Cells were coincubated with naïve bone-marrow derived macrophages at an effector to target ratio of 5:1 for 24 hours. CIS and untreated tumour cells were phagocytosed in similar extend. In contrast, necrotic cancer cells were phagocytosed by unpolarised macrophages.

While senescence alone does not render tumour cell susceptible to immune cell clearance, senescence is accompanied by changes in the secretome, possibly influencing immune cells. Indeed, naïve macrophages showed increased migration towards the supernatant of cytokine induced senescent cells in comparison to non-senescent tumour cell supernatant (Figure 24A). This was not observed in TIS (Figure 24B).

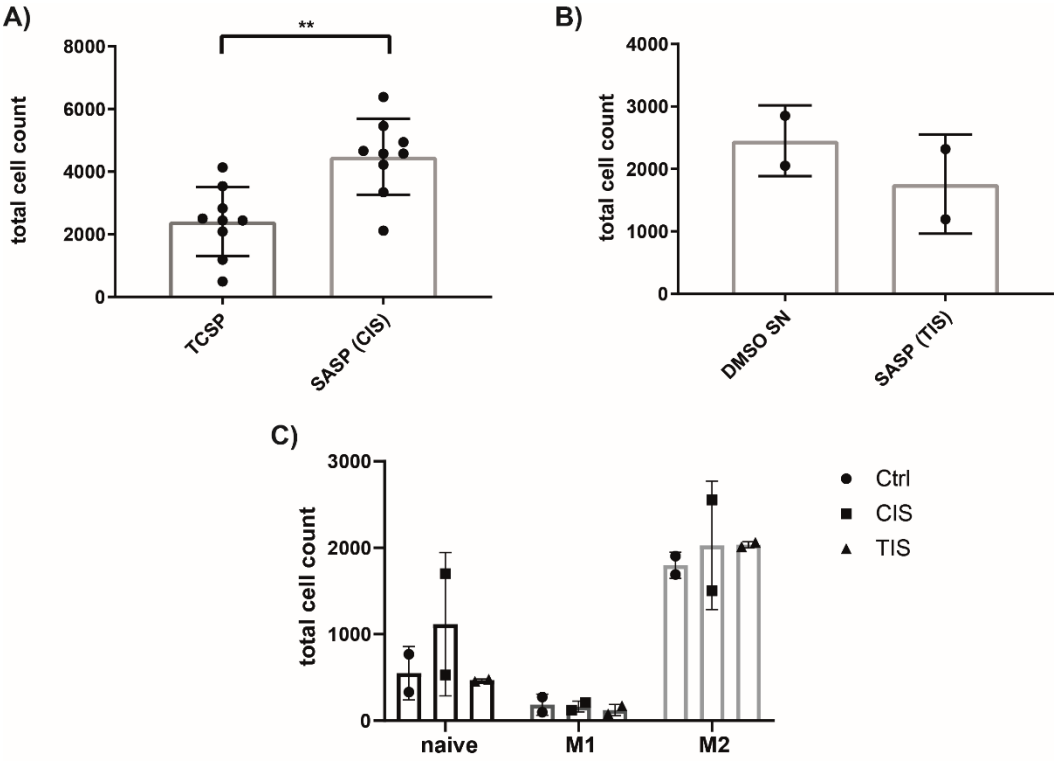

Figure 24: Migratory capacity of macrophages exposed to SASP of tumour cells after CIS or TIS

Supernatant of equal numbers of proliferating (tumour cell secretory phenotype – TCSP) and senescent tumour cells (senescence associated secretory phenotype – SASP) was collected 24 hours after complete senescence induction. Naïve bone marrow derived macrophages showed increased migration towards supernatant of senescent cells in a transwell assay (A). Unpaired t-test, two-tailed, ** p =0.0016. Mean ± SD of 8 supernatants from different cell cultures. B) Supernatant of cells treated with Palbociclib and DMSO control were generated as in A) No increase in migration was observed after exposure of macrophages to the SASP of TIS tumour cells. Mean ± SD of 2 supernatants from different cell lines. C) Bone marrow derived macrophages were classically (M1, using IFN-γ and LPS) or alternatively activated (M2, using IL-4) and migration observed after exposure to the SASP of tumour cells after CIS and TIS or tumour cell supernatant (Ctrl). Mean ± SD of 2 supernatants from different β-cell-tumour cell cultures.

After investigating the migration of macrophages SASP or non-senescent tumour cell supernatant, the phagocytic capacity of bone marrow derived macrophages to senescent and non-senescent tumour cells after TRAIL and ABT263 treatment was analysed. Coincubation of primary unpolarised bone marrow derived macrophages with senescent and non-senescent cancer cells does not lead to increased uptake of senescent cancer cells in comparison to non-senescent cancer cells (Figure 23).

Therefore, cells were challenged with TRAIL or ABT263 to induce apoptosis prior to coincubation with naïve macrophages and phagocytosis (Figure 25A). In non-senescent cancer cells the number macrophages that were positive for phagocytosis remained below 10 % on average (Figure 25B,C). In senescent cancer cells however, pre-treatment with senolytics lead to increased phagocytosis by macrophages up to 30 % after CIS (Figure 25D,E) and 20 % after TIS (Figure 25F,G) after 3 hours. Increased phagocytosis only occurred if cell death was inducible in cancer cells. Inhibition of apoptosis with pan-caspase inhibitor Z-VAD-FMK diminished uptake of cancer cells. Interestingly, the uptake fell below the level of DMSO control treated senescent cancer cells. This is in line with the observation of early apoptotic features and caspase 3 activation in senescence. It underlines the idea that some senescent cells may not be able to cope with senescence induction and subsequently initiate to cell death and allow for clearance by macrophages. However, another possible reason may be death induction by macrophages themselves that is not observed if incubated with pan-caspase inhibitor.

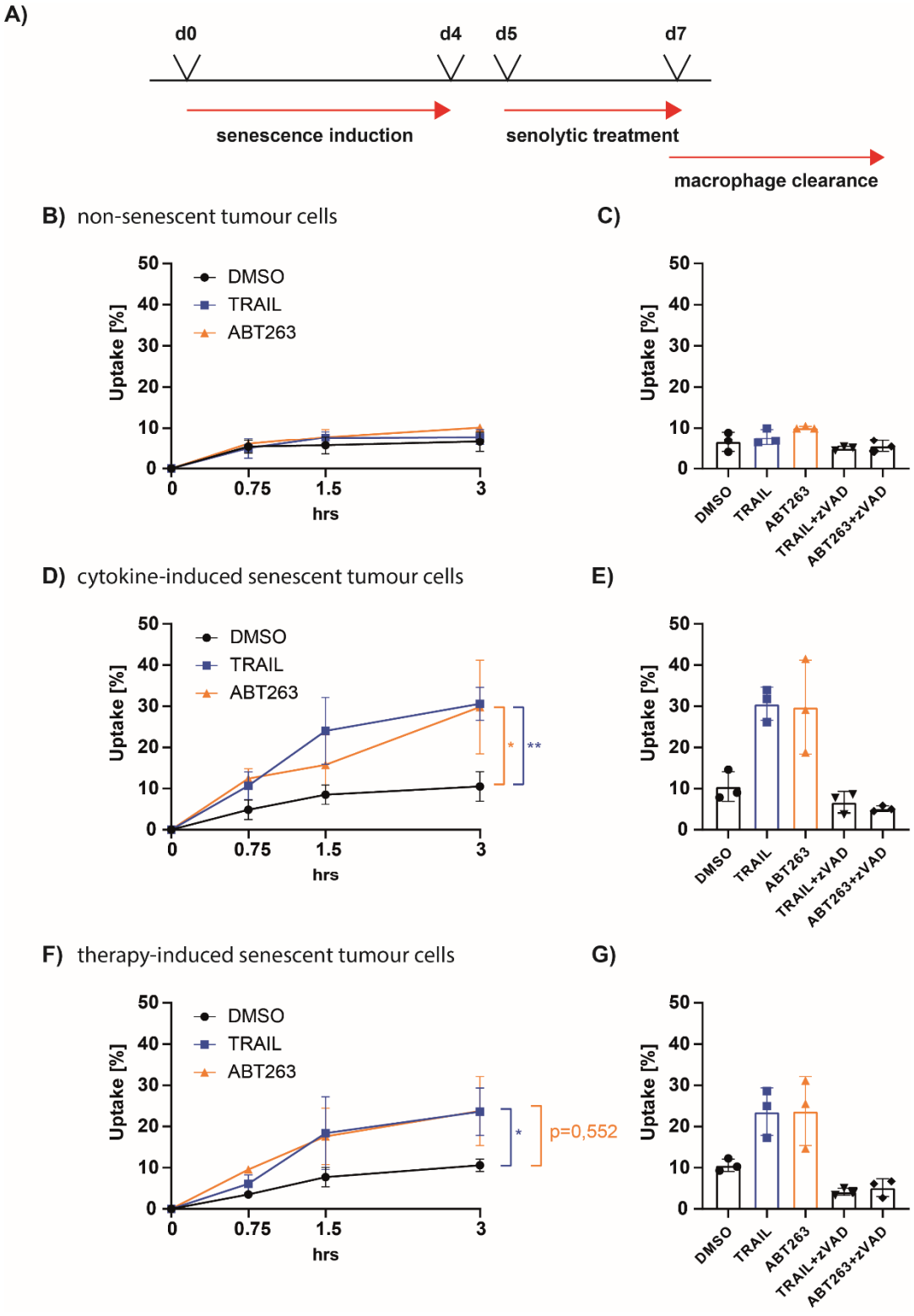

Figure 25: Clearance of senolytic cancer cells by macrophages

Co-incubation assay of senescent and non-senescent cancer cells with naïve bone marrow derived macrophages. After senescence induction for 96 hours and subsequent senolytic treatment as indicated in the figure for 48 hours, if applicable, cells were coincubated with macrophages at an effector to target

ratio of 5:1 for indicated time periods. Figure C,E,G depict the F4/80^{+},PKH67^{+} macrophage population after 3 hours of coincubation with tumour cells. In proliferating tumour cells (A,B), cytokine induced senescent (C,D) and therapy induced senescence tumour cells (E,F) phagocytosis by macrophages was detectable.

4.5 The phenotype of macrophages defines their senolytic and phagocytic capacity

To gain clarity on the relations of macrophages and tumour cells, bone marrow derived macrophages were polarized to an M1 (IFN-γ & LPS), M2 (IL-4) phenotype or left unpolarised before coincubation with proliferating and senescent cancer cells. Coincubation with unpolarised macrophages led to death induction in tumour cell independent of senescence status in non-senescent and CIS tumour cells (Figure 26). In TIS tumour cells incubation with unpolarised macrophages led to increased death induction that was not mathematically significant by statistical testing. There was no difference in death induction dependent on the polarization status of macrophages in non-senescent tumour cells. However, after CIS and TIS M1 polarized macrophages were able to increase cell death. This was also observed for M2 polarized macrophages after CIS and TIS (Figure 26C,D).

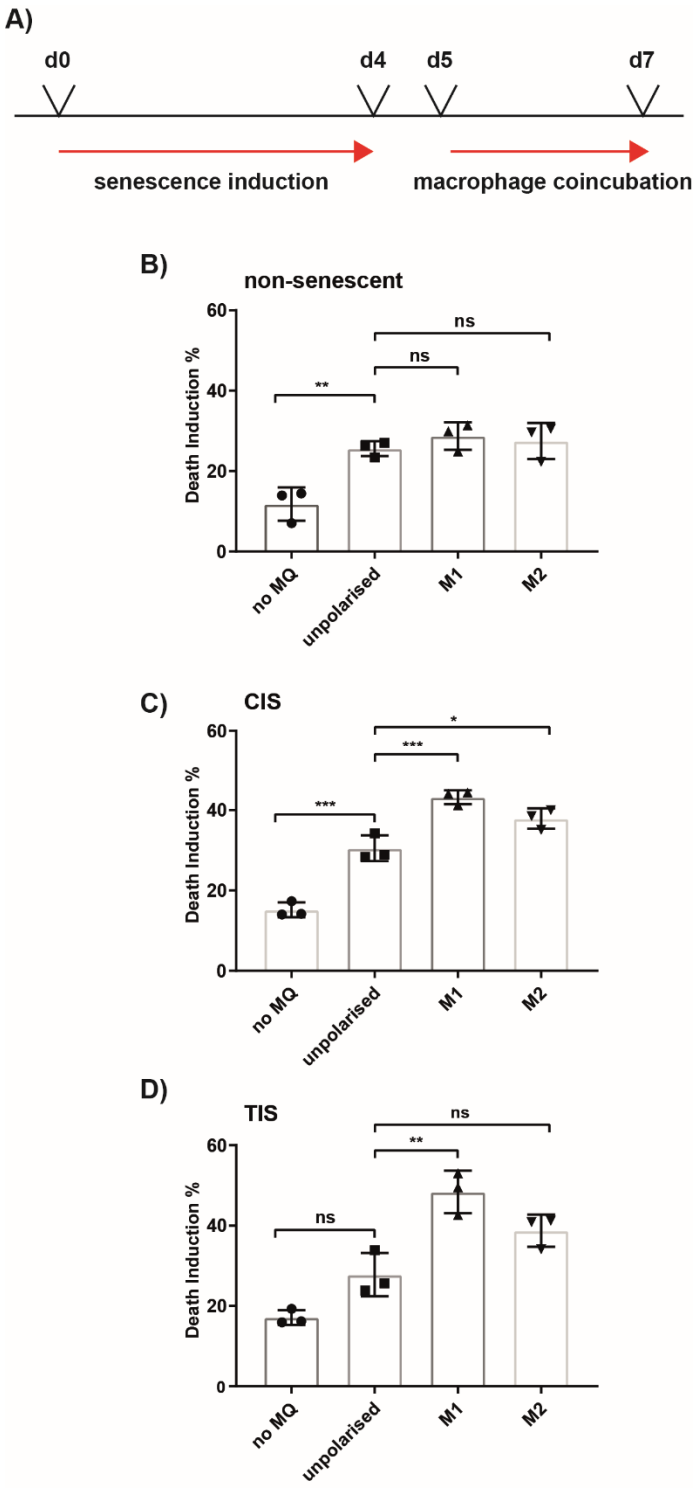

Figure 26: Macrophage phenotype influences death induction in senescence

Bone marrow derived macrophages were polarized to an M1 or M2 phenotype before coincubation with non-senescent tumour cells (B), of tumour cells after CIS (C) and TIS (D) cancer cells for 48 hours. Afterwards cell death in cancer cells was determined. Treatment scheme seen in A). Ordinary one-way ANOVA, B) no MQ (no macrophages) vs unpolarised p=0.0070; C) no MQ vs unpolarised p=0.0002, unpolarised vs M1 p=0.0009, unpolarised vs M2 p= 0.0231; D) no MQ vs unpolarised p=0.0678, unpolarised vs M1 p=0.0019, unpolarised vs M2 p=0.0606; Mean ± SD of 3 cell lines and 3 bone marrow derived macrophage isolations.

In part, this may be due to increased TRAIL expression on M1 macrophages, yet it is likely not the sole explanation (Figure 27). Further, the polarization status and therefore the phenotype of macrophages determine their migratory capacity. While M2 macrophages are migrating towards stimuli, M1 macrophages are less mobile than M2 macrophages (Figure 24). Therefore, direct contact is more likely to occur with

unpolarised or naïve macrophages or macrophages would have to obtain their polarisation status at the tumour margin.

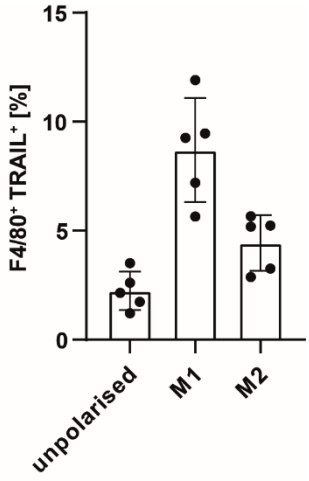

Figure 27: M1 macrophages express TRAIL

Analysis of TRAIL expression on bone marrow derived macrophages after polarization. Bone marrow derived macrophages were polarized to an M1 (IFN-γ & TNF) or M2 (IL-4) like phenotype or left unpolarised.

In conclusion the changes induced by senescence increased the vulnerabilities in tumour cells by rendering them susceptible to TRAIL or NO induced apoptosis. The heavy stress elicited under senescence induction alters cellular function, like proliferation and changes in the secretome. The secretome of β-cell tumour cells after CIS attracts macrophages, yet their interaction does not induce cell death in cancer cells. However, senolysis can be initiated by treatment with physiological ligand TRAIL which is expressed by macrophages, subsequently causing clearance of senescent tumour cells by macrophages. Senolysis in tumour cells can also be induced by macrophages themselves if pre-polarized to a TRAIL expressing phenotype (M1). Nonetheless, the efficacy of TRAIL mediated cell death in senescence and the possibility of immune mediated lysis of senescent cancer cells needs further and careful evaluation. The polarising effect of the SASP on immune cells may pose a tedious obstacle to overcome in establishing and investigating an immune mediated clearance of senescent cancer cells.

5 Discussion

In this thesis changes undergone by β-cell tumour cells after senescence induction were investigated. Therefore, primary mouse β-cell cancer cells were isolated and characterized for senescence response to two modes of senescence, namely cytokine induced senescence and therapy induced senescence. Senescent cell lines were examined for changes in mitochondrial status and various parameters associated with apoptosis. Interestingly, changes undergone to establish cytokine induced senescence are also found in early apoptotic cells. However, senescent β-cell tumour cells remained viable, probably due to the increase in Bcl-2 protein levels. Since senescence can be physiologically induced by immune cells, this work evaluated physiological death inducers that are enriched during type I immune responses. TRAIL and NO induced cell death preferentially in senescent cancer cells. The death induction was found to be necessary for the clearance of senescent cancer cells by macrophages. However, TRAIL and NO are also effector molecules of inflammatory M1 macrophages. Indeed, polarized macrophages induce cell death in senescent cancer cells more effectively than unpolarised macrophages.

5.1 Challenges in the definition of senescence in cancer cells

One defining feature of senescence is a permanent arrest in cell cycle with an inability to respond to mitotic stimuli, thereby distinguishing senescence from quiescence. While quiescent cells are G0 arrested, they can re-enter the cell cycle upon stimulation, removal of contact inhibition, or density dependent growth inhibition *in vitro*. Therefore, the majority of differentiated somatic cells are quiescent per definition. Prominent *in vivo* examples of the reversibility of quiescence are stem cells in the hair follicle[118] or proliferation stimulated by wound healing[47]. The effect of senescence induction on differentiation state of cancer cell lines or somatic cells remains elusive and is most likely cell type dependent. However, common pathways are shared between senescence induction and differentiation. Human keratinocytes, for example, readily enter replicative senescence *in vitro*. Differentiation into mature keratinocytes, however, was possible in senescent and non-senescent keratinocytes by increasing

the calcium concentration in culture media. Yet the time needed, to acquire a terminally differentiated state increased in senescent keratinocytes[119,120].

Senescence is predominantly attributed to aging with rising number of studies done in cancer cells. Therefore, biomarkers of senescence are common features also found in the aging phenotype. Consequently, research on senescence in aging led to the establishment of senescence associated β-galactosidase activity as a marker for senescence[7]. It was soon discovered that senescent-associated β-galactosidase positive cells may also occur as a stress response[30,121] or to other damaging signals[31,122], broadening the definition of senescence as a result.

In fact, the idea of senescence and SA-beta Gal as a marker exclusively associated with aging was further challenged when senescence-associated β-galactosidase was shown in murine embryogenesis, where SA-beta galactosidase positive cells were detected in the mesonephros and the endolymphatic sac[41,42]. SA-beta galactosidase positive cells can be found throughout development, from early embryonic stages into old age. Therefore, investigation of senescence on a local level, characterizing the senescent cells health status and its interactions with its environment may facilitate the understanding of basic features of senescence subtypes beyond restrictions of organismal age.

Moreover, the cellular state caused by cytokine induced senescence shows aspects of cellular stress and features associated with early apoptotic events. Yet, β-cell tumour cells treated with IFN-γ and TNF fulfil defining requirements of senescence, which are e.g. increased SA-beta galactosidase activity (Figure 7), alterations in secretome (Figure 9), and arrested proliferation (Figure 8). Upon induction of senescence a considerable part of the cell population dies, while the remaining cells become senescent. Therefore, our current methods of senescence induction select for a stress-resistant subpopulation of cells. This senescent subpopulation does not differ in β-cell markers compared to its non-senescent counterpart. Intriguingly, senescent cancer cells do not lose the proliferation marker Ki67 completely; rather exhibit a decreased expression (data not shown). This indicates that not all cells are growth arrested after induction of senescence with IFN-γ and TNF and possibly escape from senescence induction *in vitro*. Nevertheless, the dependency of Rip1-Tag2 tumour cells on Ki67 for

proliferation has not been shown. While Ki67 is generally believed to be essential for cell proliferation[123], recent studies challenge this view[124]. Therefore, to assess whether Ki67 positive cells are unable to become senescent or escaped senescence multi-staining with senescence biomarkers could answer these questions.

5.2 Senescence resembles a pro-apoptotic phenotype in β-cell tumour cells

The induction of senescence in β-cell tumour initiates changes in morphology and cellular status, likely leading to the acquirement of vulnerabilities. Consequently, the health status of these senescent cancer cells was investigated to characterize vulnerabilities after CIS and gain insight into possible exploitable phenotypes. While part of the cancer cells succumbs to cell death during senescence induction, the remaining senescent β-cells were able to avert cell death. Interestingly, one of the major anti-apoptotic proteins, Bcl-2 (Figure 17) is upregulated in CIS. Challenging senescent cancer cells with ABT263, a pan-Bcl2 inhibitor, showed induction of cell death preferentially in senescent cancer cells but not in non-senescent cancer cells (Figure 18). Hence, CIS cancer cells depended on anti-apoptotic Bcl-2 family members for survival. Thus, although senescent cells are viable, they do accumulate features associated with early apoptosis and poor overall health.

The RIP1-Tag2 model is one of the few murine models for pancreatic neuroendocrine tumours[125]. Expression of the oncogene SV40 Large T-antigen (Tag) under the rat insulin promotor (RIP1) initiates tumourigenesis in β-cells. Subsequently, the dysregulation of insulin secretion induces hypoglycaemia in tumour bearing mice (Figure 6)[96,97]. Primary β-cell function is the control of blood sugar levels by glucose sensing and regulation of blood sugar spikes by releasing insulin. In brief, glucose sensing by β-cells initiates glycogenesis under ATP depletion, initiating closure of ATP-sensitive potassium channels. Consequently, the intracellular accumulation of potassium ions depolarizes the plasma membrane and opens voltage-sensitive calcium channels. The influx of calcium ions along their concentration gradient stimulates the fusion of insulin vesicles with the plasma membrane[126]. In normal β-cell function mitochondrial activation is necessary for insulin secretion and replenishing depleted ATP stores. Interestingly, in diabetes, a disease characterized by the inability

of β-cells to control blood sugar levels mitochondrial dysfunction is a prevalent observation[127].

Cytokine induced senescent β-cell tumour cells exhibit reduced mitochondrial membrane potential (ΔΨm) (Figure 12), an important parameter of cellular health. In healthy cells ΔΨm is actively regulated by proton pumps and essential for energy delivery in oxidative phosphorylation. In basic cellular functions short-lived transient changes in ΔΨm are common. While transient membrane changes are necessary, sustained changes in ΔΨm of a high mitochondrial number may compromise the viability of the cell[128]. In senescence, increased numbers of depolarized mitochondria were observed, hinting towards a general dysfunction of mitochondria in senescence. Dysfunctional mitochondria are generally removed from the cell by mitophagy. Yet, no difference in mitochondrial mass was observed between senescent and non-senescent cancer cells (Figure 13). The method used for detection of mitochondrial mass, however, cannot distinguish between changes in total number of mitochondria or size. Therefore, it cannot be excluded yet, that increased number of mitochondria can compensate for dysfunction acquired by mitochondrial membrane depolarization in senescence.

Nevertheless, mitochondrial membrane potential regulation and stability is crucial for cellular energy metabolism and cell survival. Depolarization is also detected in mitochondria dependent apoptosis. After cytokine induced senescence induction cytochrome c levels are diminished, indicating a loss of cytochrome c from mitochondria (Figure 15). Coherently, changes in opening of the mitochondrial transition pore were found in senescent cells and increased caspase 3 activity was detected (Figure 16). Nevertheless, senescent cells remain viable suggesting coping mechanisms by upregulation of anti-apoptotic proteins like Bcl-2, XIAP and others.

All above discussed measurements were done directly after senescence induction and therefore it must be kept in mind that they merely provide a snapshot of cellular health status. To substantiate the hypothesis that mitochondria can recover in senescence and assume normal function further experiments are necessary. Investigation of the ATP production and respiratory chain efficiency are of special interest. Deficiency in respiratory chain may substantiate the senescent phenotype by lack of energy to

resume normal cellular function and resupply of energy therefore may be an exit strategy of senescence.

5.3 Senescence induced exploitable vulnerabilities in cancer cells opening a therapeutic window

The induction of CIS with physiological components of the immune system, as well as the acquired vulnerabilities, raised the question whether physiological death inducers that are released during type I immune response may preferentially kill senescent β-cancer cells. With the discovery of death receptors on the cell surface, capable to initiate apoptosis, new strategies were sought out for cancer treatment. Therefore, approaches have been made to target CD95, receptor to Fas or Death receptor 5, receptor to TRAIL. However clinical proof of concept is still missing. CD95 was hoped to be a promising target due to its potent death induction. Unfortunately systemic administration of CD95 antibody[129] or recombinant Fas[130] led to severe hepatotoxicity and death in mice. A further drawback was the elicited toxicity in non-cancerous cells. In contrast to Fas, TRAIL however was found to kill a variety of tumour cell lines without having an effect on non-cancerous cells[131–133]. Sadly, TRAIL failed to induce cell death in primary tumour cell culture. In the clinic, recombinant human TRAIL (dulanermin) was used in combination therapy with chemotherapeutic agents. A Phase1b study on dulanermin in combination with paclitaxel, carboplatin, and bevacizumab in non-small-cell lung cancer showed no adverse side effects of dulanermin[134]. Yet, advancing to phase II no improved outcome was found in patients treated with chemotherapeutics and dulanermin in comparison to control treatment[135]. Due to the lack of side effects *in vivo* but often observed *in vitro* potency TRAIL treatment or targeting its receptor may still be considered a valid strategy to pursue in cancer treatment.

Interestingly, senescence sensitizes β-cell tumour cells to TRAIL mediated killing (Figure 20). Senescent cancer cells activate caspase 3 in a time and dose dependent manner after TRAIL treatment in contrast to non-senescent cancer cells (Figure 19). However, concentrations of TRAIL needed to induce caspase 3 activation were unexpectedly high. Investigation of surface receptor levels revealed changes in DR5 presence in senescence, yet, not in a distinct manner. However, DcR1 presentation, a decoy receptor for TRAIL, lacking the intracellular domain, was increased after

cytokine induced senescence (Figure 22), possibly explaining the high concentrations of TRAIL needed to induce cell death in senescent cells, a process termed senolysis. Interestingly, increased presentation of DcR1 is not an exclusive feature of cytokine induced senescence as it has been described in replicative[82], DNA damage[136] and physiological senescence[81].

Furthermore, human cells express two functional death receptors, DR4 and DR5, in contrast to mouse cells only expressing DR5. This may be an additional explanation why studies conducted in human cell lines use TRAIL in nanomolecular concentrations. Further reasoning for the high concentrations of murine TRAIL needed to induce senolysis is the ligand-receptor interaction of TRAIL and DR5. For DR5 signalling three DR5 molecules bind a TRAIL homodimer. This complex structural set up inherently conveys a high specificity and functional regulation[137]. Therefore, to increase efficiency of TRAIL induced cell death pre-oligomerized TRAIL molecules have been developed. Nonetheless, increasing concentrations of recombinant TRAIL circumvent the capture by DcR1 and possible structural challenges, inducing caspase 3 dependent cell death preferentially in CIS cells.

5.4 Senescence and immune cell clearance

Macrophages, belonging to the group of myeloid immune cells, are involved in debris and dead cell clearance, as well as regulation of inflammatory processes. In CIS increased levels of phosphatidylserine (PS) were present on the cell membrane (Figure 10). Even though PS exposure is found on viable cells not undergoing apoptosis[91,93,104], it is also present on (pre-)apoptotic cells mediating phagocytic clearance[100,103,138]. Furthermore, CD47, a protein involved in immune evasion[109] was downregulated in senescent cancer cells (Figure 11). Therefore, it was investigated if increased PS exposure, in combination with reduced CD47 levels, was sufficient to trigger macrophage mediated clearance of senescent cancer cells. Interestingly, senescence was not sufficient to induce clearance of cancer cells by naïve bone-marrow derived macrophages (Figure 23). A slight increase in phagocytosis was, however, observed in co-culture of naïve macrophages with senescent cancer cells, likely due to increased baseline levels of active caspase 3 (Figure 19) in senescence

or death induction in a small number of tumour cells by naïve macrophages (Figure 26).

Conceivably, our data suggests that senescent induction is not sufficient to induce cancer cell clearance. On the contrary, it shows that senescent tumour cells are protected from clearance by macrophages. However, the acquired vulnerabilities in senescence allow the specific targeting of senescent tumour cells and senolysis induction using TRAIL (Figure 20). Indeed, treatment of senescent cancer cells with the senolytic agents TRAIL or ABT263 triggered apoptosis and phagocytic uptake by naïve bone-marrow derived macrophages in contrast to non-senescent cancer cells. Phagocytic uptake was reduced if pan-caspase inhibitor was present, reinforcing the finding that senolysis is needed for phagocytic clearance of senescent cancer cells (Figure 25).

TRAIL is expressed on the surface of a variety of immune cells of the innate and adaptive immune system[139]. Macrophages, for example, express TRAIL upon stimulation towards a pro-inflammatory M1 phenotype[139,140], whereas NK cells express TRAIL after activating stimuli[141,142]. Furthermore, constitutive expression of TRAIL has been found in NK cells of the liver *in vivo* upon chronic IFN-γ exposure[143]. In this thesis primary focus lies on macrophages, due to their possible dual function in death induction and phagocytosis.

Macrophages adapt different activation status in response to external stimuli. Traditionally, macrophage polarization is defined as classically activated M1 macrophages, achieved by polarization using LPS and IFN-γ, or as alternatively activated M2 macrophages, polarized by IL-4. M1 macrophages show a strong LPS induced pro-inflammatory phenotype, characterised by iNOS expression and NO production. M2 macrophages on the other hand are defined by an anti-inflammatory phenotype[144] This simplistic conceptual framework of macrophage polarization, however, does not do justice to the numerous functions and physiological activation states of macrophages. Nevertheless, it was used in this thesis for simplicity and proof of concept.

Bone-marrow derived macrophages increased TRAIL expression after activation with IFN-γ and LPS (M1). Interestingly activation with IL-4 (M2) also increased TRAIL

expression, albeit to a weaker extend than in M1 macrophages (Figure 27). In coculture studies, M1 and M2 macrophages were able to induce cell death in a larger fraction of senescent cancer cells in comparison to naïve macrophages. This is in line with their increased expression of TRAIL. However, naïve macrophages were able to kill cancer cells to some extend independent of their senescent status. While it was shown in this thesis, that TRAIL is a senolytic agent and M1 macrophages express TRAIL, it was not shown that TRAIL is the reason why M1 macrophages are able to induce cell death in senescent cancer cells. To proof this link TRAIL would either have to be removed or blocked by antibodies or tumour cells lacking DR5 need to be generated. Nonetheless, the increased capability of M1 macrophages to induce cell death in senescent cancer cells in comparison to non-senescent cancer cells, demonstrates an increased vulnerability of senescent tumour cells that can be therapeutically targeted.

Increasing the capacity of macrophages for therapeutic killing of cancer cells is an attractive, yet difficult strategy in cancer treatment. Macrophages are found in all tissues and macrophage pools can be replenished by monocyte differentiation; however, the flexible phenotype of macrophages poses a great challenge to overcome. For further investigation of macrophages as a potential effector cell in senolytic therapy fine tuning of macrophage polarization status could be more feasible using other, biologically inert Toll-like receptor (TLR) ligands other than LPS. TLR agonist that are under investigation in cancer immunotherapy, for example are targeting TLR9 (SD-101)[145], TLR3 (Hiltonol)[146,147] and TLR4 (GSK1795091)[148,149]. Studies have already shown enhanced TRAIL expression on immune cells after TLR2, TLR3 and TLR4 stimulation[150]. The efficacy of TLR ligands for polarization and TRAIL expression remains to be tested and follow up experiments for death induction in (non-)senescent cancer cells are yet to be done.

However, therapeutic modulation of the innate immune system has rarely been attempted. This may in part be due to the complexity of the innate immune system and the inability to separate its plethora of functions from each other. Involved in the fight of infections, wound healing, and tissue homeostasis its response pattern to TLR activation are evolutionary conserved an initiated in an all or nothing manner. This allows for a fast immune response without the need of a memory function. Even so,

first studies showed that the innate immune systems inflammatory response can be separated from its anti-infective response [151].

5.5 Bringing TRAIL back

Traditional chemotherapeutic agents generally induce cell death. One potential approach is the activation of the p53-mediated intrinsic apoptosis pathway, excluding tumours with mutated p53[152]. Thus, activating the extrinsic apoptosis pathway would extend the capacities in cancer therapy. Therefore, finding a strategy to reintroduce TRAIL into the clinic could have promising therapeutic effects. In this work, senescence induction is proposed as a promising step in cancer therapy to sensitize tumour cells to senolysis. The second stimulus, here TRAIL mediated apoptosis induction, exploits these vulnerabilities induced by senescence and allows for subsequent clearance of senescent cancer cells.

Unfortunately, cytokine induced senescence, using IFN-γ and TNF, would be a poor therapeutic option in human cancer treatment. Excess and sustained serum levels of TNF have been implicated in chronic inflammation, sepsis and subsequent vital organ dysfunction[153]. This limitation may be bypassed in the future by using autologous tumour specific $CD4^+$ T cell therapy. To ensure validity and transferability of this work and the proposed concept, therapy induced senescence (TIS) was investigated in comparison to CIS. Palbociclib, the compound used for TIS, is a CDK4/6 inhibitor clinically applied in Her2 negative mammacarcinoma in combination therapy with aromatase inhibitors[36]. Primary β-cell tumour cells were responsive to TIS, showing increased SA-beta-Gal activity, as well as arrested growth (Figure 6, Figure 7). As in CIS, TIS β-cell tumour cells show impaired health status. While mitochondrial depolarization (Figure 12), and increased pore flickering (Figure 14) was observed in TIS, subsequent cytochrome c release was not found (Figure 15). This suggests different mitochondrial dynamics after TIS and CIS. Nonetheless, β-cell tumour cells are susceptible to TRAIL induced senolysis after TIS and CIS. Bcl-2 levels were also increased after TIS (Figure 17) and phagocytic clearance was also only measurable after senolysis induction by TRAIL or ABT263 (Figure 25). An upregulation of DcR1 was not observed in TIS (Figure 22). Therefore, the underlying mechanisms why CIS and TIS are susceptible to TRAIL mediated killing likely differ.

Importantly, senolysis by TRAIL or ABT263 was needed for increased phagocytosis of senescent β-cancer cells (Figure 25). This consolidates the hypothesis of TRAIL as a senolytic agents and may allow to establish a system for investigating the clearance of senescent cancer cells in an immune mediated setting.

6 Conclusion

In cancer treatment senescence induction is a new therapeutic strategy that imposes benefits and risks that are currently under evaluation. Rejecting tumour removal for the benefit of growth arrested cancer cells is a viable option in non-resectable or difficult to resect tumours. The arrested growth of cancer cells may allow for increased patient survival but may also pose risks that are mediated by inflammatory SASP factors. This opens a therapeutic window, on the one hand, because treatment time is extended, on the other because senescence may introduce exploitable vulnerabilities to cancer cells. Senescence can be induced in β-cell tumour cells and other cancer cells using cytokines or therapeutics. This changes β-cell tumour cell physiology to a state resembling early apoptotic features. Profound dysregulation of mitochondrial function and survival associated proteins were found in senescent β-cell tumour cells in comparison to non-senescent β-cell tumour cells.

Whether or not it is of advantage to leave senescent cancer cells in the organism is currently under discussion. While a non-proliferating tumour cell is desirable over a proliferating one, the changes in secretome in senescent cancer could induce tumourigenesis in surrounding tissue or other tissue damage due to chronic inflammation. The senescent phenotype elicited in β-cell tumour cells raised vulnerabilities and sensitized these cells towards TRAIL and ABT263 (pan-Bcl2 inhibitor) mediated cell death. Furthermore, cell death induction in senescent cancer cells was necessary for immune mediated clearance *in vitro*.

Senescence induction therefore raises new vulnerabilities in cancer cells that can be exploited by secondary treatment with TRAIL or other apoptosis inducing compounds. The sensitivity of senescent cancer cells to TRAIL may lay the foundation for further investigations aiming at a dual immunotherapy in cancer treatment.

7 List of figures

8 List of tables

9 Acronyms

53BP1	p53-binding protein 1
7-AAD	7-Aminoactinomycin
ACK	Ammonium-Chloride-Potassium
ATM	ataxia-telangiectasia mutated
ATP	Adenosintriphosphate
ATR	Ataxia telangiectasia and Rad3 related
Bax	Bcl-2-associated X protein
BCL2	B-cell lymphoma 2
BID	BH3 interacting-domain death agonist
BIM	Bcl-2-interacting mediator of cell deat
BMDM	Bone marrow derived Macrophage
C12FDG	5-Dodecanoylaminofluorescein Di-β-D-Galactopyranosid
CaCl2	Calciumchloride
CCL2 (MCP-1)	CC-chemokine ligand 2
CCL5 (RANTES)	CC-chemokine ligand 5
CD	Cluster of Differentiation
CDK	Cyclin dependent kinase
CDKI	Cyclin dependent kinase inhibitors
cFLIP	cellular FLICE-like inhibitory protein
CIS	Cytokine induced senescence
CM-H2DCFDA	5-(and-6)-chloromethyl-2',7'-dichlorodihydrofluorescein diacetate, acetyl ester
CXCL10	CXC-Ligand 10
CXCL9	CXC-Ligand 9
DAPI	4′,6-diamidino-2-phenylindole
DCFDA	2',7' –dichlorofluorescin diacetate
DcR	Decoy Receptor
DDR	DNA damage respone
DISC	Death inducing signaling complex
DMSO	Dimethylsulfoxide
DNA	deoxyribonucleic acid
DR4/5	death receptor 4/5
EDTA	Ethylendiamintetraacetat

ELISA	Enzyme-linked Immunosorbent Assay
EMA	European Medicines Agency
ER	Endoplasmatic reticulum
FACS	fluorescence-activated cell sorting
FADD	Fas-associated protein with death domain
FCS	fetal calf serum
FLICE	Fas-associated death domain-like interleukin-1beta-converting enzyme
gmCSF	granulocyte macrophage colony-stimulating factor
H202	Hydrogen peroxide
HBSS/Ca	Hank's Balanced Salt Solution with Calcium
HEPES	4-(2-hydroxyethyl)-1-piperazineethanesulfonic acid
HP1	Heterochromatin Protein 1
IFN-γ	Interferon-γ
IGF-1	Insulin-like growth factor 1
IL	Interleukine
iPS	Induced pluripotent stem cells
JC-1	1H-Benzimidazolium, 5,6-dichloro-2-[3-(5,6-dichloro-1,3-diethyl-1,3-dihydro-2H-benzimidazol-2-ylidene)-1-propenyl]-1,3-diethyl-, iodide
JNK	c-Jun-N-terminalen Kinase
Klf4	Krüppel Like Factor 4
LPS	Lipopolysaccharid
MCP-1	monocyte chemotactic protein 1
mCSF	macrophage colony stimulating factor
MDC1	Mediator Of DNA Damage Checkpoint 1
MEF	Mouse Embryonic Fibroblasts
MFI	median fluorescent intensity
NaCl	Natriumchloride
NaOH	Natriumhydroxide
NBS1	Nijmegen breakage syndrome 1
NF1	Neurofibromin 1
NFKB	nuclear factor kappa-light-chain-enhancer of activated B cells
NK cell	Natural killer cell
NO	Nitric oxide

NRAS	Neuroblastoma Rat Sacroma
Oct4	Octamer binding transcription factor 4
OIS	Oncogene-induced senescence
PBS	phosphate buffered saline
PD-L1	Programmed Death Ligand 1
PI	Propidium iodide
PS	Phosphatidylserine
PTEN	Phosphatase and Tensin homolog
PUMA	p53 upregulated modulator of apoptosis
PVDF	Polyvinylidenfluorid
RANTES (CCL5)	Regulated upon Activation, Normal T Cell Expressed and Secreted
Ras	Rat sarcoma
Rb	retinoblastoma protein
ROS	Reactive Oxygen Species
SA-b Gal	Senescence-associated beta-galactosidase
SAGA	Senescence-associated growth arres
SAHF	Senescence-associated heterochromatin foci
SASP	senescence-associated secretory phenotype
SDS	Sodium Dodecyl Sulfate
shRNA	Small hairpin RNA
siRNA	Small interfering RNA
Sox2	SRY (sex determining region Y)-box 2
Suv39h1	Suppressor Of Variegation 3-9 Homolog 1
TBST	Tris-buffered saline with Tween20
TCSP	tumour cell secretory phenotype
TGFß	Transforming growth factor beta
Th cell	T helper cells
TIS	therapy induced senescence
TLR	toll-like receptor
TNF	tumour necrosis factor
TNFR1	tumour necrosis factor receptor 1
TRAIL	TNF-related apoptosis-inducing ligand
UV	ultraviolet
VEGF	Vascular Endothelial Growth Factor
VHL	Von Hippel–Lindau

X-Gal	5-Brom-4-chlor-3-indoxyl-β-D-galactopyranosid

10 References

1. Hayflick, L. The limited in vitro lifetime of human diploid cell strains. *Experimental Cell Research* **37,** 614–636; 10.1016/0014-4827(65)90211-9 (1965).

2. Hayflick, L. & Moorhead, P. S. The serial cultivation of human diploid cell strains. *Experimental Cell Research* **25,** 585–621; 10.1016/0014-4827(61)90192-6 (1961).

3. Harley, C. B., Futcher, A. B. & Greider, C. W. Telomeres shorten during ageing of human fibroblasts. *Nature* **345,** 458–460; 10.1038/345458a0 (1990).

4. Lundblad, V. & Szostak, J. W. A mutant with a defect in telomere elongation leads to senescence in yeast. *Cell* **57,** 633–643; 10.1016/0092-8674(89)90132-3 (1989).

5. Cooke, H. J. & Smith, B. A. Variability at the Telomeres of the Human X/Y Pseudoautosomal Region. *Cold Spring Harbor Symposia on Quantitative Biology* **51,** 213–219; 10.1101/SQB.1986.051.01.026 (1986).

6. Kuilman, T., Michaloglou, C., Mooi, W. J. & Peeper, D. S. The essence of senescence. *Genes Dev* **24,** 2463–2479; 10.1101/gad.1971610 (2010).

7. Dimri, G. P. *et al.* A biomarker that identifies senescent human cells in culture and in aging skin in vivo. *Proc Natl Acad Sci U S A* **92,** 9363–9367; 10.1073/pnas.92.20.9363 (1995).

8. Bhat, R. *et al.* Astrocyte senescence as a component of Alzheimer's disease. *PLOS ONE* **7,** e45069; 10.1371/journal.pone.0045069 (2012).

9. Di Fagagna, F. d.'A. *et al.* A DNA damage checkpoint response in telomere-initiated senescence. *Nature* **426,** 194–198; 10.1038/nature02118 (2003).

10. Webley, K. *et al.* Posttranslational Modifications of p53 in Replicative Senescence Overlapping but Distinct from Those Induced by DNA Damage. *Molecular and Cellular Biology* **20,** 2803; 10.1128/MCB.20.8.2803-2808.2000 (2000).

11. Fujita, K. *et al.* p53 isoforms Δ133p53 and p53β are endogenous regulators of replicative cellular senescence. *Nature Cell Biology* **11,** 1135 EP -; 10.1038/ncb1928 (2009).

12. Baerlocher, G. M., Mak, J., Röth, A., Rice, K. S. & Lansdorp, P. M. Telomere shortening in leukocyte subpopulations from baboons. *Journal of Leukocyte Biology* **73,** 289–296; 10.1189/jlb.0702361 (2003).

13. Herbig, U., Ferreira, M., Condel, L., Carey, D. & Sedivy, J. M. Cellular Senescence in Aging Primates. *Science* **311,** 1257; 10.1126/science.1122446 (2006).

14. Jeyapalan, J. C., Ferreira, M., Sedivy, J. M. & Herbig, U. Accumulation of senescent cells in mitotic tissue of aging primates. *Mechanisms of Ageing and Development* **128,** 36–44; 10.1016/j.mad.2006.11.008 (2007).

15. Serrano, M., Lin, A. W., McCurrach, M. E., Beach, D. & Lowe, S. W. Oncogenic ras Provokes Premature Cell Senescence Associated with Accumulation of p53 and p16INK4a. *Cell* **88,** 593–602; 10.1016/S0092-8674(00)81902-9 (1997).

16. Gorgoulis, V. G. & Halazonetis, T. D. Oncogene-induced senescence: the bright and dark side of the response. *Current opinion in cell biology* **22,** 816–827; 10.1016/j.ceb.2010.07.013 (2010).

17. Alimonti, A. *et al.* A novel type of cellular senescence that can be enhanced in mouse models and human tumor xenografts to suppress prostate tumorigenesis. *J Clin Invest* **120,** 681–693; 10.1172/JCI40535 (2010).

18. Chen, Z. *et al.* Crucial role of p53-dependent cellular senescence in suppression of Pten-deficient tumorigenesis. *Nature* **436,** 725–730; 10.1038/nature03918 (2005).

19. Bartkova, J. *et al.* Oncogene-induced senescence is part of the tumorigenesis barrier imposed by DNA damage checkpoints. *Nature* **444,** 633–637; 10.1038/nature05268 (2006).

20. Haferkamp, S. *et al.* Oncogene-induced senescence does not require the p16(INK4a) or p14ARF melanoma tumor suppressors. *The Journal of investigative dermatology* **129,** 1983–1991; 10.1038/jid.2009.5 (2009).

21. Kamijo, T. *et al.* Tumor Suppression at the Mouse INK4a Locus Mediated by the Alternative Reading Frame Product p19 ARF. *Cell* **91,** 649–659; 10.1016/S0092-8674(00)80452-3 (1997).

22. Braig, M. *et al.* Oncogene-induced senescence as an initial barrier in lymphoma development. *Nature* **436,** 660–665; 10.1038/nature03841 (2005).

23. Collado, M. *et al.* Senescence in premalignant tumours. *Nature* **436,** 642; 10.1038/436642a (2005).

24. Morton, J. P. *et al.* Mutant p53 drives metastasis and overcomes growth arrest/senescence in pancreatic cancer. *Proc Natl Acad Sci U S A* **107,** 246–251; 10.1073/pnas.0908428107 (2010).

25. Franza, B.R., Maruyama, K., Garrels, J. I. & Ruley, H.E. In vitro establishment is not a sufficient prerequisite for transformation by activated ras oncogenes. *Cell* **44,** 409–418; 10.1016/0092-8674(86)90462-9 (1986).

26. Leikam, C., Hufnagel, A., Schartl, M. & Meierjohann, S. Oncogene activation in melanocytes links reactive oxygen to multinucleated phenotype and senescence. *Oncogene* **27,** 7070–7082; 10.1038/onc.2008.323 (2008).

27. Ewald, J. A., Desotelle, J. A., Wilding, G. & Jarrard, D. F. Therapy-induced senescence in cancer. *J Natl Cancer Inst* **102,** 1536–1546; 10.1093/jnci/djq364 (2010).

28. Zheng, H. *et al.* Senescence Inducer Shikonin ROS-Dependently Suppressed Lung Cancer Progression. *Frontiers in Pharmacology* **9,** 519; 10.3389/fphar.2018.00519 (2018).

29. Prieur, A., Besnard, E., Babled, A. & Lemaitre, J.-M. p53 and p16INK4A independent induction of senescence by chromatin-dependent alteration of S-phase progression. *Nature Communications* **2,** 473; 10.1038/ncomms1473 (2011).

30. Velichko, A. K., Petrova, N. V., Razin, S. V. & Kantidze, O. L. Mechanism of heat stress-induced cellular senescence elucidates the exclusive vulnerability of early S-

phase cells to mild genotoxic stress. *Nucleic Acids Res* **43,** 6309–6320; 10.1093/nar/gkv573 (2015).

31. te Poele, R. H., Okorokov, A. L., Jardine, L., Cummings, J. & Joel, S. P. DNA Damage Is Able to Induce Senescence in Tumor Cells in Vitro and in Vivo. *Cancer Research* **62,** 1876 (2002).

32. Roberson, R. S., Kussick, S. J., Vallieres, E., Chen, S.-Y. J. & Wu, D. Y. Escape from Therapy-Induced Accelerated Cellular Senescence in p53-Null Lung Cancer Cells and in Human Lung Cancers. *Cancer Research* **65,** 2795; 10.1158/0008-5472.CAN-04-1270 (2005).

33. Chang, B.-D. *et al.* A Senescence-like Phenotype Distinguishes Tumor Cells That Undergo Terminal Proliferation Arrest after Exposure to Anticancer Agents. *Cancer Research* **59,** 3761 (1999).

34. Schmitt, C. A. *et al.* A Senescence Program Controlled by p53 and p16INK4a Contributes to the Outcome of Cancer Therapy. *Cell* **109,** 335–346; 10.1016/S0092-8674(02)00734-1 (2002).

35. Peter MacCallum Cancer Centre, Australia. Palbociclib, Letrozole & Venetoclax in ER and BCL-2 Positive Breast Cancer (PALVEN). Available at https://clinicaltrials.gov/ct2/show/NCT03900884?cond=NCT03900884&draw=2&rank=1 (2020).

36. European Medicines Agency. Ibrance. Available at https://www.ema.europa.eu/en/medicines/human/EPAR/ibrance (2019).

37. Braumüller, H. *et al.* T-helper-1-cell cytokines drive cancer into senescence. *Nature* **494,** 361 EP -; 10.1038/nature11824 (2013).

38. Cao, Z. A., Daniel, D. & Hanahan, D. Sub-lethal radiation enhances anti-tumor immunotherapy in a transgenic mouse model of pancreatic cancer. *BMC Cancer* **2,** 11; 10.1186/1471-2407-2-11 (2002).

39. Brenner, E. *et al.* Cancer immune control needs senescence induction by interferon-dependent cell cycle regulator pathways in tumours. *Nature Communications* **11,** 1335; 10.1038/s41467-020-14987-6 (2020).

40. European Medicines Agency. Ibrance. palbociclib.

41. Muñoz-Espín, D. *et al.* Programmed Cell Senescence during Mammalian Embryonic Development. *Cell* **155,** 1104–1118; 10.1016/j.cell.2013.10.019 (2013).

42. Storer, M. *et al.* Senescence Is a Developmental Mechanism that Contributes to Embryonic Growth and Patterning. *Cell* **155,** 1119–1130; 10.1016/j.cell.2013.10.041 (2013).

43. Nacher, V. *et al.* The quail mesonephros: a new model for renal senescence? *Journal of vascular research* **43,** 581–586; 10.1159/000096076 (2006).

44. Besancenot, R. *et al.* A senescence-like cell-cycle arrest occurs during megakaryocytic maturation: implications for physiological and pathological megakaryocytic proliferation. *PLoS Biol* **8**; 10.1371/journal.pbio.1000476 (2010).

45. Chuprin, A. *et al.* Cell fusion induced by ERVWE1 or measles virus causes cellular senescence. *Genes Dev* **27,** 2356–2366; 10.1101/gad.227512.113 (2013).

46. Bennett, D. C. Human melanocyte senescence and melanoma susceptibility genes. *Oncogene* **22,** 3063–3069; 10.1038/sj.onc.1206446 (2003).

47. Darby, I. A. & Hewitson, T. D. Fibroblast differentiation in wound healing and fibrosis. *International review of cytology* **257,** 143–179; 10.1016/S0074-7696(07)57004-X (2007).

48. Krizhanovsky, V. *et al.* Senescence of Activated Stellate Cells Limits Liver Fibrosis. *Cell* **134,** 657–667; 10.1016/j.cell.2008.06.049 (2008).

49. Sagiv, A. *et al.* Granule exocytosis mediates immune surveillance of senescent cells. *Oncogene* **32,** 1971–1977; 10.1038/onc.2012.206 (2013).

50. Kipling, D. & Cooke, H. J. Hypervariable ultra-long telomeres in mice. *Nature* **347,** 400–402; 10.1038/347400a0 (1990).

51. Evangelou, K. *et al.* The DNA damage checkpoint precedes activation of ARF in response to escalating oncogenic stress during tumorigenesis. *Cell Death & Differentiation* **20,** 1485–1497; 10.1038/cdd.2013.76 (2013).

52. Tavana, O. *et al.* Absence of p53-dependent apoptosis leads to UV radiation hypersensitivity, enhanced immunosuppression and cellular senescence. *Cell Cycle* **9,** 3348–3356; 10.4161/cc.9.16.12688 (2010).

53. Malaquin, N., Carrier-Leclerc, A., Dessureault, M. & Rodier, F. DDR-mediated crosstalk between DNA-damaged cells and their microenvironment. *Front Genet* **6,** 94; 10.3389/fgene.2015.00094 (2015).

54. Probin, V., Wang, Y., Bai, A. & Zhou, D. Busulfan Selectively Induces Cellular Senescence but Not Apoptosis in WI38 Fibroblasts via a p53-Independent but Extracellular Signal-Regulated Kinase-p38 Mitogen-Activated Protein Kinase-Dependent Mechanism. *Journal of Pharmacology and Experimental Therapeutics* **319,** 551; 10.1124/jpet.106.107771 (2006).

55. Spallarossa, P. *et al.* Doxorubicin induces senescence or apoptosis in rat neonatal cardiomyocytes by regulating the expression levels of the telomere binding factors 1 and 2. *American Journal of Physiology-Heart and Circulatory Physiology* **297,** H2169-H2181; 10.1152/ajpheart.00068.2009 (2009).

56. Marcotte, R., Lacelle, C. & Wang, E. Senescent fibroblasts resist apoptosis by downregulating caspase-3. *Mechanisms of Ageing and Development* **125,** 777–783; 10.1016/j.mad.2004.07.007 (2004).

57. Gong, T., Liu, L., Jiang, W. & Zhou, R. DAMP-sensing receptors in sterile inflammation and inflammatory diseases. *Nature Reviews Immunology* **20,** 95–112; 10.1038/s41577-019-0215-7 (2020).

58. Maderna, P. & Godson, C. Phagocytosis of apoptotic cells and the resolution of inflammation. *Biochimica et Biophysica Acta (BBA) - Molecular Basis of Disease* **1639,** 141–151; 10.1016/j.bbadis.2003.09.004 (2003).

59. Freund, A., Orjalo, A. V., Desprez, P.-Y. & Campisi, J. Inflammatory networks during cellular senescence: causes and consequences. *Trends Mol Med* **16,** 238–246; 10.1016/j.molmed.2010.03.003 (2010).

60. Wang, E. Senescent Human Fibroblasts Resist Programmed Cell Death, and Failure to Suppress bcl2 Is Involved. *Cancer Research* **55,** 2284 (1995).

61. Sasaki, M., Kumazaki, T., Takano, H., Nishiyama, M. & Mitsui, Y. Senescent cells are resistant to death despite low Bcl-2 level. *Mechanisms of Ageing and Development* **122,** 1695–1706; 10.1016/S0047-6374(01)00281-0 (2001).

62. Yosef, R. *et al.* Directed elimination of senescent cells by inhibition of BCL-W and BCL-XL. *Nature Communications* **7,** 11190 EP -; 10.1038/ncomms11190 (2016).

63. Chang, J. *et al.* Clearance of senescent cells by ABT263 rejuvenates aged hematopoietic stem cells in mice. *Nature Medicine* **22,** 78 EP -; 10.1038/nm.4010 (2015).

64. Palumbo, M. *et al.* Systemic cancer therapy: achievements and challenges that lie ahead. *Frontiers in Pharmacology* **4,** 57; 10.3389/fphar.2013.00057 (2013).

65. Yosef, R. *et al.* p21 maintains senescent cell viability under persistent DNA damage response by restraining JNK and caspase signaling. *EMBO J* **36,** 2280–2295; 10.15252/embj.201695553 (2017).

66. Dai, C. Y. & Enders, G. H. p16INK4a can initiate an autonomous senescence program. *Oncogene* **19,** 1613–1622; 10.1038/sj.onc.1203438 (2000).

67. Galanos, P. *et al.* Chronic p53-independent p21 expression causes genomic instability by deregulating replication licensing. *Nature Cell Biology* **18,** 777 EP -; 10.1038/ncb3378 (2016).

68. Loop, T. & Pahl, H. L. Activators and Target Genes of Rel/NF-κB Transcription Factors. In *Nuclear Factor κB,* edited by R. Beyaert (Springer Netherlands, Dordrecht, 2003), Vol. 279, pp. 1–48.

69. Filomeni, G., Zio, D. de & Cecconi, F. Oxidative stress and autophagy: the clash between damage and metabolic needs. *Cell Death And Differentiation* **22,** 377 EP -; 10.1038/cdd.2014.150 (2014).

70. Ogata, M. *et al.* Autophagy Is Activated for Cell Survival after Endoplasmic Reticulum Stress. *Molecular and Cellular Biology* **26,** 9220; 10.1128/MCB.01453-06 (2006).

71. Tai, H. *et al.* Autophagy impairment with lysosomal and mitochondrial dysfunction is an important characteristic of oxidative stress-induced senescence. *Autophagy* **13,** 99–113; 10.1080/15548627.2016.1247143 (2017).

72. Young, A. R.J. *et al.* Autophagy mediates the mitotic senescence transition. *Genes Dev* **23,** 798–803; 10.1101/gad.519709 (2009).

73. Patschan, S. *et al.* Lipid mediators of autophagy in stress-induced premature senescence of endothelial cells. *American Journal of Physiology-Heart and Circulatory Physiology* **294,** H1119-H1129; 10.1152/ajpheart.00713.2007 (2008).

74. Gosselin, K. *et al.* Senescent Keratinocytes Die by Autophagic Programmed Cell Death. *The American Journal of Pathology* **174,** 423–435; 10.2353/ajpath.2009.080332 (2009).

75. Pattingre, S. *et al.* Bcl-2 Antiapoptotic Proteins Inhibit Beclin 1-Dependent Autophagy. *Cell* **122,** 927–939; 10.1016/j.cell.2005.07.002 (2005).

76. Zhu, Y. *et al.* Identification of a novel senolytic agent, navitoclax, targeting the Bcl-2 family of anti-apoptotic factors. *Aging Cell* **15,** 428–435; 10.1111/acel.12445 (2016).

77. Baar, M. P. *et al.* Targeted Apoptosis of Senescent Cells Restores Tissue Homeostasis in Response to Chemotoxicity and Aging. *Cell* **169,** 132-147.e16; 10.1016/j.cell.2017.02.031 (2017).

78. Zhu, Y. *et al.* New agents that target senescent cells: the flavone, fisetin, and the BCL-X(L) inhibitors, A1331852 and A1155463. *Aging (Albany NY)* **9,** 955–963; 10.18632/aging.101202 (2017).

79. Stagni, V., Mingardi, M., Santini, S., Giaccari, D. & Barilà, D. ATM kinase activity modulates cFLIP protein levels: potential interplay between DNA damage signalling and TRAIL-induced apoptosis. *carcin* **31,** 1956–1963; 10.1093/carcin/bgq193 (2010).

80. Vjetrovic, J., Shankaranarayanan, P., Mendoza-Parra, M. A. & Gronemeyer, H. Senescence-secreted factors activate Myc and sensitize pretransformed cells to TRAIL-induced apoptosis. *Aging Cell* **13,** 487–496; 10.1111/acel.12197 (2014).

81. Madsen, S. D. *et al.* Decoy TRAIL receptor CD264: a cell surface marker of cellular aging for human bone marrow-derived mesenchymal stem cells. *Stem Cell Research & Therapy* **8,** 201; 10.1186/s13287-017-0649-4 (2017).

82. Wiley, C. D. *et al.* Analysis of individual cells identifies cell-to-cell variability following induction of cellular senescence. *Aging Cell* **16,** 1043–1050; 10.1111/acel.12632 (2017).

83. Morizot, A. *et al.* Chemotherapy overcomes TRAIL-R4-mediated TRAIL resistance at the DISC level. *Cell Death & Differentiation* **18,** 700–711; 10.1038/cdd.2010.144 (2011).

84. Xue, W. *et al.* Senescence and tumour clearance is triggered by p53 restoration in murine liver carcinomas. *Nature* **445,** 656–660; 10.1038/nature05529 (2007).

85. Sagiv, A. *et al.* NKG2D ligands mediate immunosurveillance of senescent cells. *Aging (Albany NY)* **8,** 328–344; 10.18632/aging.100897 (2016).

86. Kang, T.-W. *et al.* Senescence surveillance of pre-malignant hepatocytes limits liver cancer development. *Nature* **479,** 547 EP -; 10.1038/nature10599 (2011).

87. Amor, C. *et al.* Senolytic CAR T cells reverse senescence-associated pathologies. *Nature* **583,** 127–132; 10.1038/s41586-020-2403-9 (2020).

88. Del Rosso, M. *et al.* The urokinase receptor system, a key regulator at the intersection between inflammation, immunity, and coagulation. *Current pharmaceutical design* **17,** 1924–1943; 10.2174/138161211796718189 (2011).

89. Kim, K. M. *et al.* Identification of senescent cell surface targetable protein DPP4. *Genes Dev* **31,** 1529–1534; 10.1101/gad.302570.117 (2017).

90. Utsugi, T., Schroit, A. J., Connor, J., Bucana, C. D. & Fidler, I. J. Elevated Expression of Phosphatidylserine in the Outer Membrane Leaflet of Human Tumor Cells and Recognition by Activated Human Blood Monocytes. *Cancer Research* **51,** 3062 (1991).

91. Segawa, K., Suzuki, J. & Nagata, S. Constitutive exposure of phosphatidylserine on viable cells. *Proceedings of the National Academy of Sciences* **108,** 19246; 10.1073/pnas.1114799108 (2011).

92. Feng, Z. *et al.* A pathogenic picornavirus acquires an envelope by hijacking cellular membranes. *Nature* **496,** 367 EP -; 10.1038/nature12029 (2013).

93. Morizono, K., Chen, I. S. Y. & Doms, R. W. Role of Phosphatidylserine Receptors in Enveloped Virus Infection. *Journal of Virology* **88,** 4275; 10.1128/JVI.03287-13 (2014).

94. Lv, Z. *et al.* Loss of Cell Surface CD47 Clustering Formation and Binding Avidity to SIRPα Facilitate Apoptotic Cell Clearance by Macrophages. *The Journal of Immunology* **195,** 661; 10.4049/jimmunol.1401719 (2015).

95. Casey, S. C. *et al.* MYC regulates the antitumor immune response through CD47 and PD-L1. *Science* **352,** 227; 10.1126/science.aac9935 (2016).

96. Hanahan, D. Heritable formation of pancreatic beta-cell tumours in transgenic mice expressing recombinant insulin/simian virus 40 oncogenes. *Nature* **315,** 115–122; 10.1038/315115a0 (1985).

97. Hanahan, D. & Folkman, J. Patterns and emerging mechanisms of the angiogenic switch during tumorigenesis. *Cell* **86,** 353–364; 10.1016/s0092-8674(00)80108-7 (1996).

98. Hunter, K. E., Quick, M. L., Sadanandam, A., Hanahan, D. & Joyce, J. A. Identification and characterization of poorly differentiated invasive carcinomas in a

mouse model of pancreatic neuroendocrine tumorigenesis. *PLOS ONE* **8,** e64472; 10.1371/journal.pone.0064472 (2013).

99. Rescher, U. & Gerke, V. Annexins – unique membrane binding proteins with diverse functions. *Journal of Cell Science* **117,** 2631; 10.1242/jcs.01245 (2004).

100. Fadok, V. A. *et al.* Exposure of phosphatidylserine on the surface of apoptotic lymphocytes triggers specific recognition and removal by macrophages. *The Journal of Immunology* **148,** 2207 (1992).

101. Kaneko, N., Matsuda, R., Hosoda, S., Kajita, T. & Ohta, Y. Measurement of plasma annexin V by ELISA in the early detection of acute myocardial infarction. *Clinica Chimica Acta* **251,** 65–80; 10.1016/0009-8981(96)06294-8 (1996).

102. Masuda, J. *et al.* Levels of annexin IV and V in the plasma of pregnant and postpartum women. *Thromb Haemost* **91,** 1129–1136; 10.1160/TH03-12-0778 (2004).

103. Callahan, M. K. *et al.* Phosphatidylserine expression and phagocytosis of apoptotic thymocytes during differentiation of monocytic cells. *Journal of Leukocyte Biology* **74,** 846–856; 10.1189/jlb.0902433 (2003).

104. Elliott, J. I. *et al.* Membrane phosphatidylserine distribution as a non-apoptotic signalling mechanism in lymphocytes. *Nature Cell Biology* **7,** 808–816; 10.1038/ncb1279 (2005).

105. van den Eijnde, S. M. *et al.* Transient expression of phosphatidylserine at cell-cell contact areas is required for myotube formation. *Journal of Cell Science* **114,** 3631 (2001).

106. Ran, S. & Thorpe, P. E. Phosphatidylserine is a marker of tumor vasculature and a potential target for cancer imaging and therapy. *International Journal of Radiation Oncology*Biology*Physics* **54,** 1479–1484; 10.1016/S0360-3016(02)03928-7 (2002).

107. Vallabhapurapu, S. D. *et al.* Variation in human cancer cell external phosphatidylserine is regulated by flippase activity and intracellular calcium. *Oncotarget* **6,** 34375–34388; 10.18632/oncotarget.6045 (2015).

108. Chu, Z. *et al.* Targeting and cytotoxicity of SapC-DOPS nanovesicles in pancreatic cancer. *PLOS ONE* **8,** e75507-e75507; 10.1371/journal.pone.0075507 (2013).

109. Matlung, H. L., Szilagyi, K., Barclay, N. A. & van den Berg, T. K. The CD47-SIRPα signaling axis as an innate immune checkpoint in cancer. *Immunol Rev* **276,** 145–164; 10.1111/imr.12527 (2017).

110. Osellame, L. D., Blacker, T. S. & Duchen, M. R. Cellular and molecular mechanisms of mitochondrial function. *Best Pract Res Clin Endocrinol Metab* **26,** 711–723; 10.1016/j.beem.2012.05.003 (2012).

111. Doherty, E. & Perl, A. Measurement of Mitochondrial Mass by Flow Cytometry during Oxidative Stress. *React Oxyg Species (Apex)* **4,** 275–283; 10.20455/ros.2017.839 (2017).

112. Valentin-Vega, Y. A. *et al.* Mitochondrial dysfunction in ataxia-telangiectasia. *Blood* **119,** 1490–1500; 10.1182/blood-2011-08-373639 (2012).

113. Karch, J. & Molkentin, J. D. Identifying the components of the elusive mitochondrial permeability transition pore. *Proceedings of the National Academy of Sciences* **111,** 10396; 10.1073/pnas.1410104111 (2014).

114. Ichas, F. & Mazat, J.-P. From calcium signaling to cell death: two conformations for the mitochondrial permeability transition pore. Switching from low- to high-conductance state. *Biochimica et Biophysica Acta (BBA) - Bioenergetics* **1366,** 33–50; 10.1016/S0005-2728(98)00119-4 (1998).

115. Kale, J., Osterlund, E. J. & Andrews, D. W. BCL-2 family proteins: changing partners in the dance towards death. *Cell Death & Differentiation* **25,** 65–80; 10.1038/cdd.2017.186 (2018).

116. Sag, D., Ayyildiz, Z. O., Gunalp, S. & Wingender, G. The Role of TRAIL/DRs in the Modulation of Immune Cells and Responses. *Cancers (Basel)* **11,** 1469; 10.3390/cancers11101469 (2019).

117. van der Veen, R C, Dietlin, T. A., Pen, L., Gray, J. D. & Hofman, F. M. Antigen presentation to Th1 but not Th2 cells by macrophages results in nitric oxide production and inhibition of T cell proliferation: interferon-gamma is essential but insufficient. *Cellular immunology* **206,** 125–135; 10.1006/cimm.2000.1741 (2000).

118. Li, L. & Clevers, H. Coexistence of quiescent and active adult stem cells in mammals. *Science* **327,** 542–545; 10.1126/science.1180794 (2010).

119. Norsgaard, H., Clark, B. F. & Rattan, S. I. Distinction between differentiation and senescence and the absence of increased apoptosis in human keratinocytes undergoing cellular aging in vitro. *Experimental gerontology* **31,** 563–570; 10.1016/0531-5565(96)00011-3 (1996).

120. Jang, D. H. *et al.* A transcriptional roadmap to the senescence and differentiation of human oral keratinocytes. *The journals of gerontology. Series A, Biological sciences and medical sciences* **70,** 20–32; 10.1093/gerona/glt212 (2015).

121. Michelle A. Wood & Jane F. Cavender. Beta-Galactosidase Staining as a Marker of Cells Enduring Stress. *Bios* **75,** 139–146 (2004).

122. Rodier, F. *et al.* Persistent DNA damage signalling triggers senescence-associated inflammatory cytokine secretion. *Nature Cell Biology* **11,** 973–979; 10.1038/ncb1909 (2009).

123. Schlüter, C. *et al.* The cell proliferation-associated antigen of antibody Ki-67: a very large, ubiquitous nuclear protein with numerous repeated elements, representing a new kind of cell cycle-maintaining proteins. *The Journal of cell biology* **123,** 513–522; 10.1083/jcb.123.3.513 (1993).

124. Sobecki, M. *et al.* The cell proliferation antigen Ki-67 organises heterochromatin. *eLife* **5,** e13722; 10.7554/eLife.13722 (2016).

125. Babu, V., Paul, N. & Yu, R. Animal models and cell lines of pancreatic neuroendocrine tumors. *Pancreas* **42,** 912–923; 10.1097/MPA.0b013e31827ae993 (2013).

126. Fu, Z., Gilbert, E. R. & Liu, D. Regulation of insulin synthesis and secretion and pancreatic Beta-cell dysfunction in diabetes. *Curr Diabetes Rev* **9,** 25–53 (2013).

127. Sivitz, W. I. & Yorek, M. A. Mitochondrial dysfunction in diabetes: from molecular mechanisms to functional significance and therapeutic opportunities. *Antioxid Redox Signal* **12,** 537–577; 10.1089/ars.2009.2531 (2010).

128. Krippeit-Drews, P., Düfer, M. & Drews, G. Parallel Oscillations of Intracellular Calcium Activity and Mitochondrial Membrane Potential in Mouse Pancreatic B-Cells. *Biochemical and Biophysical Research Communications* **267,** 179–183; 10.1006/bbrc.1999.1921 (2000).

129. Ogasawara, J. *et al.* Lethal effect of the anti-Fas antibody in mice. *Nature* **364,** 806–809; 10.1038/364806a0 (1993).

130. Kondo, T., Suda, T., Fukuyama, H., Adachi, M. & Nagata, S. Essential roles of the Fas ligand in the development of hepatitis. *Nature Medicine* **3,** 409–413; 10.1038/nm0497-409 (1997).

131. Walczak, H. *et al.* Tumoricidal activity of tumor necrosis factor-related apoptosis-inducing ligand in vivo. *Nature Medicine* **5,** 157–163; 10.1038/5517 (1999).

132. Ashkenazi, A. *et al.* Safety and antitumor activity of recombinant soluble Apo2 ligand. *J Clin Invest* **104,** 155–162; 10.1172/JCI6926 (1999).

133. Ganten, T. M. *et al.* Proteasome inhibition sensitizes hepatocellular carcinoma cells, but not human hepatocytes, to TRAIL. *Hepatology (Baltimore, Md.)* **42,** 588–597; 10.1002/hep.20807 (2005).

134. Soria, J.-C. *et al.* Phase 1b Study of Dulanermin (recombinant human Apo2L/TRAIL) in Combination With Paclitaxel, Carboplatin, and Bevacizumab in

Patients With Advanced Non-Squamous Non–Small-Cell Lung Cancer. *Journal of Clinical Oncology* **28,** 1527–1533; 10.1200/JCO.2009.25.4847 (2010).

135. Soria, J.-C. *et al.* Randomized Phase II Study of Dulanermin in Combination With Paclitaxel, Carboplatin, and Bevacizumab in Advanced Non–Small-Cell Lung Cancer. *Journal of Clinical Oncology* **29,** 4442–4451; 10.1200/JCO.2011.37.2623 (2011).

136. Coppé, J.-P. *et al.* Senescence-associated secretory phenotypes reveal cell-nonautonomous functions of oncogenic RAS and the p53 tumor suppressor. *PLoS Biol* **6,** 2853–2868; 10.1371/journal.pbio.0060301 (2008).

137. Mongkolsapaya, J. *et al.* Structure of the TRAIL–DR5 complex reveals mechanisms conferring specificity in apoptotic initiation. *Nature Structural Biology* **6,** 1048–1053; 10.1038/14935 (1999).

138. Callahan, M. K., Williamson, P. & Schlegel, R. A. Surface expression of phosphatidylserine on macrophages is required for phagocytosis of apoptotic thymocytes. *Cell Death And Differentiation* **7,** 645–653; 10.1038/sj.cdd.4400690 (2000).

139. Ehrlich, S., Infante-Duarte, C., Seeger, B. & Zipp, F. Regulation of soluble and surface-bound TRAIL in human T cells, B cells, and monocytes. *Cytokine* **24,** 244–253; 10.1016/S1043-4666(03)00094-2 (2003).

140. Halaas, Vik, Ashkenazi & Espevik. Lipopolysaccharide Induces Expression of APO2 Ligand/TRAIL in Human Monocytes and Macrophages. *Scandinavian Journal of Immunology* **51,** 244–250; 10.1046/j.1365-3083.2000.00671.x (2000).

141. Sheard, M. A. *et al.* Membrane-bound TRAIL supplements natural killer cell cytotoxicity against neuroblastoma cells. *Journal of immunotherapy (Hagerstown, Md. : 1997)* **36,** 319–329; 10.1097/CJI.0b013e31829b4493 (2013).

142. Prager, I. *et al.* NK cells switch from granzyme B to death receptor-mediated cytotoxicity during serial killing. *The Journal of Experimental Medicine* **216,** 2113–2127; 10.1084/jem.20181454 (2019).

143. Smyth, M. J. *et al.* Tumor necrosis factor-related apoptosis-inducing ligand (TRAIL) contributes to interferon gamma-dependent natural killer cell protection from tumor metastasis. *The Journal of Experimental Medicine* **193,** 661–670; 10.1084/jem.193.6.661 (2001).

144. Mantovani, Alberto, Sica, Antonio & Locati, M. Macrophage Polarization Comes of Age. *Immunity* **23,** 344–346; 10.1016/j.immuni.2005.10.001 (2005).

145. National Cancer Institute. Clinical Trials Using TLR9 Agonist SD-101.

146. Saxena, M. *et al.* Poly-ICLC, a TLR3 Agonist, Induces Transient Innate Immune Responses in Patients With Treated HIV-Infection: A Randomized Double-Blinded Placebo Controlled Trial. *Front Immunol* **10,** 725; 10.3389/fimmu.2019.00725 (2019).

147. Sharma, S. *et al.* TLR3 agonists and proinflammatory antitumor activities. *Expert Opin Ther Targets* **17,** 481–483; 10.1517/14728222.2013.781585 (2013).

148. Hug, B. A. *et al.* Safety, Pharmacokinetics, and Pharmacodynamics of the TLR4 Agonist GSK1795091 in Healthy Individuals: Results from a Randomized, Double-blind, Placebo-controlled, Ascending Dose Study. *Clinical Therapeutics* **42,** 1519-1534.e33; 10.1016/j.clinthera.2020.05.022 (2020).

149. National Cancer Institute - Technology Transfer Center. Therapeutic Antitumor Combination Containing TLR4 Agonist HMGN1.

150. Diehl, G. E. *et al.* TRAIL-R as a Negative Regulator of Innate Immune Cell Responses. *Immunity* **21,** 877–889; 10.1016/j.immuni.2004.11.008 (2004).

151. Foster, S. L., Hargreaves, D. C. & Medzhitov, R. Gene-specific control of inflammation by TLR-induced chromatin modifications. *Nature* **447,** 972–978; 10.1038/nature05836 (2007).

152. Hientz, K., Mohr, A., Bhakta-Guha, D. & Efferth, T. The role of p53 in cancer drug resistance and targeted chemotherapy. *Oncotarget* **8,** 8921–8946; 10.18632/oncotarget.13475 (2017).

153. Panacek, E. A. & Kaul, M. IL-6 as a Marker of Excessive TNF-α Activity in Sepsis. *Sepsis* **3,** 65–73; 10.1023/A:1009878726176 (1999).